NTNU
Det skapende universitet

Bruk av MPC for MPD

Johannes Møgster

Master i teknisk kybernetikk (2 årig)
Innlevert: Juni 2013
Hovedveileder: Lars Imsland, ITK
Medveileder: John-Morten Godhavn, Statoil
Gerhard Nygaard, IRIS

Norges teknisk-naturvitenskapelige universitet
Institutt for teknisk kybernetikk

Problem Description

Background
As production on the Norwegian shelf enters tail production, drilling wells with vanishing pressure windows becomes more attractive. This motivates use of automatic control systems for controlling downhole pressure using Managed Pressure Drilling (MPD) techniques. PID SISO control solutions for MPD are by now relatively standard, and well understood. The task in this project is to examine the potential of using a multivariable MPC solution to control the pressure throughout the open wellbore (that is, several controlled variables) using choke and possibly pumps as manipulated variables.

Work description
Develop an MPC solution to control pressure in an open wellbore to stay between given boundaries (pore and fracture pressures). Pressure at at least three locations should be controlled, e.g. casing shoe, TD, and a narrow spot. Discuss necessary instrumentation/-calculations/estimation to obtain these values. Discuss control objectives and the use of prioritization and weighting in the MPC optimization to obtain these objectives. For example, tune MPC with low weight on set point and high weight on constraints (pore and frac pressures). Choke usage should also be weighted. Start with single input (choke) with main pump and back pressure pumps and drillpipe position as measured disturbances (DVs). Extend to multivariable input using pumps as MVs. Cases to test:
I. Normal drilling
II. Connection
III. Tripping
IV. Power loss
The solution should be tested using the Wemod drilling simulator as process. Statoil's MPC tool SEPTIC should be used for modelling/identification and control.

Start date: January 14$^{\text{th}}$, 2013

Summary

Downhole pressure control is the deciding factor when it comes to safety during search and production of hydrocarbons. If the pressure becomes too high or too low, it can result in environmentally unfriendly drilling mud being spilled or an uncontrolled ”kick”. The consequences are potentially fatal and environmentally hazardous. Pressure control can be improved by utilizing new downhole tools, such as wired drill pipe, to measure the pressure itself at multiple downhole locations. Applying an advanced MIMO controller, such as MPC, can contribute to increased pressure control, as well as allowing further automation of the process by including automatic control of mud pumps in addition to the conventional choke valve (MPD). This addition of manipulated variables allows an ability to automatically control the pressure profile downhole, not just the pressure at one spot.

To utilize the addition of wired drill pipe a method for calculating the pressure at a specific spot downhole is presented. The ability to control the downhole pressure gradient is shown to be possible when using linear control. This has previously been illustrated using non-linear control theory. A comparison of linear and non-linear MPC is presented to offer some insight to the advantages of using the simpler linear controller. Linear MPC is presented in depth and is used in the simulations of different drilling scenarios using a commercial well simulator. The simulations shows some of the potential to further automate the drilling process by letting the MPC take control of more of the drilling equipment. The pressure control shows promising results.

Samandrag

Nedihols trykkregulering er den avgjerande faktoren når det kjem til tryggleik under søk og utvinning av hydrokarbonar. Viss trykket blir for høgt eller for lågt, kan det resultere i at miljøfarleg borevæske blir sølt eller at det oppstår eit ukontrollert "brønnspark". Konsekvensane er potensiellt livsfarlege og miljøfarlege. Trykkregulering kan forbetrast ved å nyttiggjere nye nediholsverktøy, som til dømes borerøyr med elektronikk, for å måle sjølve trykket fleire stadar nedihol. Ved å tilføre ein avansert MIMO (fleire inngangar, fleire utgangar) regulator, slik som MPC (modell predikativ regulator), kan ein bidra til auka trykkhandtering, så vel som å tillate vidare automasjon av prosessen ved å inkludere automatisk styring av pumper i tillegg til den konvensjonelle strupeventilen (MPD). Denne tilføyinga av manipulerte variablar tillet ein evne til å automatisk styre trykkprofilen nedihol, ikkje berre trykket på ein stad.

For å benytte tilføringa av elektronisk borerøyr har det blit laga ein metode for å kalkulere trykket på bestemte stadar nedihols. Evna til å regulere nedihols trykk-gradienten er vist mogleg ved bruk av lineær regulering. Dette har tidlegare blitt illustrert ved bruk av ulineær reguleringsteknikk. Ei samanlikning av lineær og ulineær MPC er presentert for å kunne gi eit innblikk i fordelane ved å bruke den enklare lineære regulatoren. Lineær MPC er presentert i djupna og er brukt i simuleringar av forskjellige bore-scenario vha. ein kommersiell brønnsimulator. Simuleringane viser noko av potensialet for vidare automatisering av boreprosessen ved å la MPCen ta styring over meir av boreutstyret. Trykkreguleringa viser lovande resultat.

Preface

This master thesis was written in my 4th and final semester at NTNU for the MSc. degree in Engineering Cybernetics. It was carried out in the period from January to June, 2013. I was accepted into this master's program based on my BSc. degree in Electronics from Sogn og Fjordane University College, from 2011.

The main advisor for this thesis has been prof. Lars Imsland of NTNU, with co-advisors prof. John-Morten Godhavn of Statoil and prof. Gerhard Nygård from IRIS. Statoil, IRIS and NTNU have provided the software and licenses needed for the simulations regarding this thesis.

I would like to thank all my advisor's for their contributions, which I value greatly. Also, I would like to thank Morten Fredriksen at Statoil for his user support regarding SEPTIC and for sharing his practical MPC knowledge with me. Thank you.

Trondheim, June 2013

Johannes Møgster

Abbreviations

ABP	Annular Back Pressure
BHA	Bottom Hole Assembly
CCS	Continuous Circulation System
Cvr	Controlled Variable
DHP	Down Hole Pressure
Dvr	Disturbance Variable
ECD	Equivalent Circulation Density
EOC	End of Casing
IRIS	International Research Institute of Stavanger
KKT	Karush-Kuhn-Tucker (Optimality conditions)
LWD	Logging While Drilling
MIMO	Multiple Input Multiple Output
MISO	Multiple Input Single Output
MPC	Model Predictive Control
MPD	Managed Pressure Drilling
MPT	Mud Pulse Telemetry
Mvr	Manipulated Variable
MW	Mud Weight
NMPC	Non-linear Model Predictive Controller
NPT	Non-Productive Time
NRV	Non-Return Valve
OBD	Over Balanced Drilling
PID	Proportional Integral Derivative
QP	Quadratic Problem
ROP	Rate Of Penetration
RPM	Revolutions Per Minute
SEPTIC	Statoil's Estimation and Prediction Tool for Identification and Control
SG	Specific Gravity
SISO	Single Input Single Output
WDP	Wired Drill Pipe

Contents

1 Introduction **1**

2 Drilling **5**
2.1 Pore and Fracture pressure 5
2.2 Managed Pressure Drilling 6
2.2.1 Hydraulic Model 9
2.3 Instrumentation 16
2.3.1 Calculating pressure at a static spot 17

3 Model Predictive Control (MPC) **23**
3.1 (L)MPC vs. NMPC 25
3.2 First order step response models 28
3.3 Priority hierarchy 32
3.4 Control hierarchy 34

4 Controller Design **37**
4.1 Step responses (MPC) 37
4.2 Tuning 38
4.2.1 Weighting 38
4.2.2 Mvr blocking and Cvr evaluation points 39
4.2.3 Constraints 40
4.2.4 Set-point/range 42
4.2.5 Filtering 43
4.2.6 Procedure 46
4.3 Coordinating flow and choke 47

5 Simulation and Results **53**
5.1 SEPTIC, OPC and WeMod 53
5.2 Well Description 54
5.2.1 Effect of pump rate on DHP profile 56
5.3 Simulation Cases 59
5.3.1 Normal Drilling 59
5.3.2 Connection 65
5.3.3 Tripping 73
5.3.4 Power Loss 75
5.3.5 Reference Tracking 79

6 Discussion **83**

7 Conclusions and Future Work **87**

A Example of SEPTIC .mdf file **90**

B P,PI,PID Control **91**

C Adding Tripping to the Simulator **92**

D Figures **95**

1 Introduction

Drilling on the Norwegian Shelf

In 1962 a private company offered the Norwegian government a monthly USD 160 000 for the de facto rights to all of the Norwegian shelf in terms of searching for hydrocarbons[1]. This was motivated by a recent discovery of gas outside Holland. This was rejected, and for comparison, the (Norwegian) Government Pension Fund (also known as the Norwegian Oil Fund) is now (2013) over USD 700 000 000 000 and expected to pass USD 1 trillion (10^{12}) by the end of 2019. Less than half of the predicted oil and gas reserves on the Norwegian shelf have been produced and sold by today (2013)[2]. Needless to say, drilling on the Norwegian shelf is big business, and there is still a lot of profit to be made. The technology connected to drilling for hydrocarbons has naturally evolved over the years. Most of the focus has been connected to health, safety and environment (HSE), and not so much connected to control theory in a historical perspective, nor has there been a high demand for it. That is, production wells have been fairly easy to drill till date. The upcoming drilling challenges though, are something that motivates advanced control theory. When drilling in an area close to an already depleted well, it is likely that occurring pressure windows will be considerably smaller as a result, which sets higher demands to control and inherently acquiring good data from downhole. Also, with better control and other aspects of drilling technology, we will be able to drill deeper into higher temperatures and higher pressures while still maintaining control and ensuring the safety of the deckhands and the environment. In other words, the term ”undrillable well” will have to be reconsidered as the worlds research society further evolves the technology connected to drilling. Another aspect of the evolving technology, is further automation. That is, removing humans from hazardous working environments and into a control room, where they can monitor the, potentially, fully automated process of drilling. Three key terms has stood out the last few years in regards to the technology of drilling. First, Managed Pressure Drilling (MPD), which is a specific drilling technology. Second, Wired Drill Pipe (WDP), which offers a tremendous amount of continuous data from downhole. Third, Model Predictive Control (MPC), which is a specific type of advanced control theory.

MPC for MPD

Using model predictive control for managed pressure drilling is a control engineering subject that has been discussed in the oil industry for some time. Three main points differentiates most of the studies in regards to model predictive control. First, whether communication downhole is done using mud pulse telemetry, using estimation or using wired drill pipe. Second, the choice between linear and non-linear model predictive control, and lastly, the number of controlled variables vs. manipulated variables. In regards of managed pressure drilling, two specific types have been in focus. Namely, applied back pressure and dual gra-

[1] http://www.regjeringen.no/nb/dep/oed/tema/olje_ og_ gass/norsk oljehistorie pa 5 minutter.html?id=440538

[2] http://en.wikipedia.org/wiki/The_ Government_ Pension_ Fund_ of_ Norway

dient drilling.

A small study of linear model predictive control with measured bottom hole pressure as the only controlled variable and the choke in an applied backpressure managed pressure drilling set up as the only manipulated variable, can be found in [Breyholtz, 2007].

A master thesis exploring the use of non-linear model predictive control with a combination of mud pulse telemetry and estimation for acquiring readings of the bottom hole pressure as the only controlled variable, and the choke in an applied backpressure managed pressure drilling set up as the only manipulated variable, can be found in [Breyholtz, 2008].

A Ph.D thesis including a study of linear model predictive control for both applied backpressure managed pressure drilling and dual gradient drilling can be found in [Breyholtz, 2011]. Different controlled variables are considered, but the focus is on the bottom hole pressure. For the applied backpressure managed pressure drilling set up, the considered manipulated variables are main mud pump, backpressure pump, choke and block position. For the dual gradient drilling set up, the considered manipulated variables are rig pump, mud level and block position. In these two cases, there are more manipulated variables than controlled variables, and hence, ideal resting values for some of the manipulated variables are considered. Also, both cases are simulated assuming the bottom hole pressure is measured, but several alternatives, including mud pulse telemetry, are considered.

In [Breyholtz et al., 2009] controlling a down hole pressure profile is specifically considered, as opposed to only controlling the pressure at the bottom. A non-linear model predictive controller is used in a dual gradient set up. The main pump and a sub sea pump is used as manipulated variables and both the bottom hole pressure and the pressure at the end of the last casing is used as controlled variables. Both pressures are assumed measured using wired pipe.

In this master thesis, applied backpressure managed pressure drilling will be the choice of set up in combination with linear model predictive control. Downhole measurements are assumed to be attained using wired drill pipe with sensors at the end of the drillstring and in intervals up through the well. The manipulated variables will be the main mud pump, choke, back pressure pump and, for the case of tripping, drill string velocity. The controlled variables will be three downhole pressures, one more than what has been considered before. The three pressures will be the conventional bottomhole pressure, the pressure at the end of the last casing and the pressure at a narrow spot in the pre-calculated pressure profile. The pressure profiles for pore- and fracture-pressure will be used as constraints for the three pressures. A priority hierarchy will be implemented in such a way that the pore- and fracture-pressures for the three controlled variables will be a high priority, the bottom hole pressure set point will have the next priority, the pressure set point for the narrow spot after that, and finally the pressure set point for the end of casing pressure will have a low priority. This

effectively means that two pressures are controlled, but all three are monitored and ensured to be within its respective limits. As mentioned above, controlling the downhole pressure profile has been done before, with non-linear model predictive control. To the author's knowledge, it has not previously been done using linear model predictive control.

Research Focus

At first, the focus seemed to be to offer an alternative to the well known PI control of the downhole pressure. The already implemented PI control automatically controlled the downhole pressure by taking control of the choke, leaving the operator more room to handle other variables such as flow and density. Non-linear model predictive control was proposed to do the exact same thing, which could be viewed as a bit of an over-kill. Gain scheduled PI control on the other hand[Godhavn, 2009], was received better as it offered an improvement on the already accepted controller. Specifically, gain scheduling handled most of the non-linear characteristics of the choke valve, which gives a large improvement when the choke is operating nearly closed. The results from the NMPC studies have been taken further, where the goal has shifted to focus more on offering a higher degree of automation. Model predictive control offers two main strengths; handling of constraints and handling several inputs and outputs at once. This allows a higher degree of automation since i.e. pumps can be included in the controller. Furthermore, hardware limitations can be included as constraints. In fact, every task of the operator can be left to an MPC application, potentially rendering the process autonomous. This is not realistic with PI control.

Thesis Outline

The outline of this thesis is as follows. Section 2 is devoted to drilling in general and applied back pressure managed pressure drilling. Section 3 introduces model predictive control, modelling by step response, priority hierarchy and the general control hierarchy. Section 4 presents the key aspects of designing the model predictive controller used in Section 5. Subsection 4.3 presents the potential for controlling the downhole pressure profile with linear control by utilizing the choke and main mud pump. Simulation cases, set up and results are presented in section 5. Based on the results from simulation, the general performance is discussed in Section 6. Conclusions regarding the results of this thesis and recommendations for future work is presented in Section 7. Additional figures from simulation results are collected in the Figures appendix D, and only the most descriptive figures are used within the main text itself.

First, an introduction to the process of drilling will be presented.

2 Drilling

This section will elaborate to some extent the aspects of drilling which directly influences the use of a downhole pressure regulator. More information can be found in [Skalle, 2012], [Breyholtz, 2008], [Kaasa et al., 2012], [Birkeland, 2009].

2.1 Pore and Fracture pressure

One of the main goals for a downhole pressure regulator is to keep the downhole pressure within the pressure boundaries formed by what is called the Pore pressure and the Fracture pressure.

$$p_{pore} < p_{dh} < p_{frac} \tag{1}$$

This is to keep the open wellbore from fracturing, which could lead to a loss[3], and to avoid unwanted influx[4], which could lead to a kick[5]. In both cases, time is likely to be lost, but the consequences can also be fatal.

Beyond these boundaries are the so called collapse pressure and the overburden pressure.

$$p_{collapse} < p_{pore} < p_{dh} < p_{fracture} < p_{overburden} \tag{2}$$

The collapse pressure indicates a lower pressure boundary at which the well can collapse on it self, which can cause the drill string to get stuck[6]. If the formations are very porous, the collapse pressure can be higher than the pore pressure. Lastly, "Overburden pressure is the combined weight of formation materials and fluids in the geological formations above any particular depth of interest in the earth." [Skalle, 2012]

$$\max\left(p_{collapse}, p_{pore}\right) < p_{dh} < p_{fracture} < p_{overburden} \tag{3}$$

A downhole pressure regulator needs to stay within its given limit at all times (t) at all locations along the wellbore (x).

$$\max\left(p_{collapse}(t,x), p_{pore}(t,x)\right) < DHP(t,x) < p_{fracture}(t,x) \tag{4}$$

When a well is ready for production, its quality will to some degree depend on what pressure the formations have been exposed to in the open well bore where hydrocarbons are to be collected. If this section of the well has been exposed to a relatively highly pressurized mud, the formations can be somewhat clogged by the mud/cuttings, making the production

[3]Drilling mud leaking out of the well and into the formations is called a loss or loss of mud. The mud is both valuable and restricted by environmental laws.

[4]Influx is only desired during production. That is, influx of valuable hydrocarbons.

[5]If gas enters the well at the bottom, it will expand as it rises to the surface. This can result in a dangerous increase of pressure, often called a kick, and can result in a blow out.

[6]This scenario is often called "stuck pipe".

slower. Therefore, it is desirable to stay closer to the lower boundaries of the down hole pressure, rather than the higher boundaries. When this is of a high importance, the collapse pressure is safe and influx is manageable, UBD[7] can be used.

Pore and fracture pressures are predicted before drilling, and verified along the way. This sets high demands to the geologist. In this thesis, pore and fracture pressure predictions will be assumed to be known in all simulations.

One way of illustrating the pore and fracture pressures is to display them as lines on a 2-dimensional plot of pressure versus true vertical depth (TVD) like the example in Figure 1.

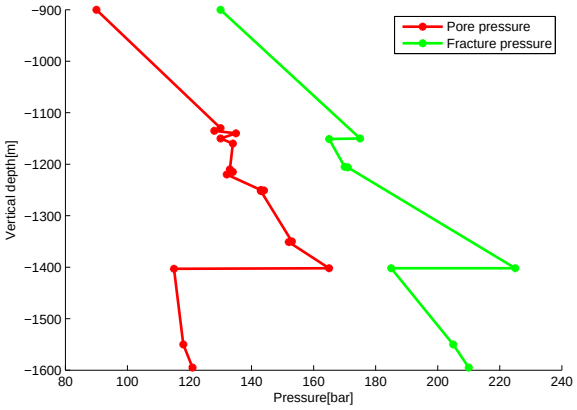

Figure 1: Example of Pore and fracture pressures at given depths. Inspired by a lecture at NTNU [Kaasa, 2012]. Throughout the open wellbore, the downhole pressure must lie within pore and frac. pressure at each point of depth.

TVD can be known from the measured depth (MD) and certain angles, i.e. Inclination and Azimuth angles, by using calculations such as the Tangential method, Balanced Tangential method, Average Angle method, Radius of Curvature method or Minimum Curvature method[8]. The latter is by far the most suited for computations[9].

One specific method for controlling the downhole pressures, is managed pressure drilling.

2.2 Managed Pressure Drilling

MPD falls in the catagory of Over Balanced Drilling (OBD), meaning the downhole pressure is balanced above the pore pressure. In a practical sense, MPD stands out in the way that

[7]UBD, Under balanced drilling, is a type of drilling that keeps the down hole pressure below the pore pressure.

[8]Example of use: http://www.drillingahead.com/profiles/blogs/minimum-curvature-method

[9]Quick introduction: http://petrowiki.org/Calculation_ methods_ for_ directional_ survey

it can be viewed as a closed system.

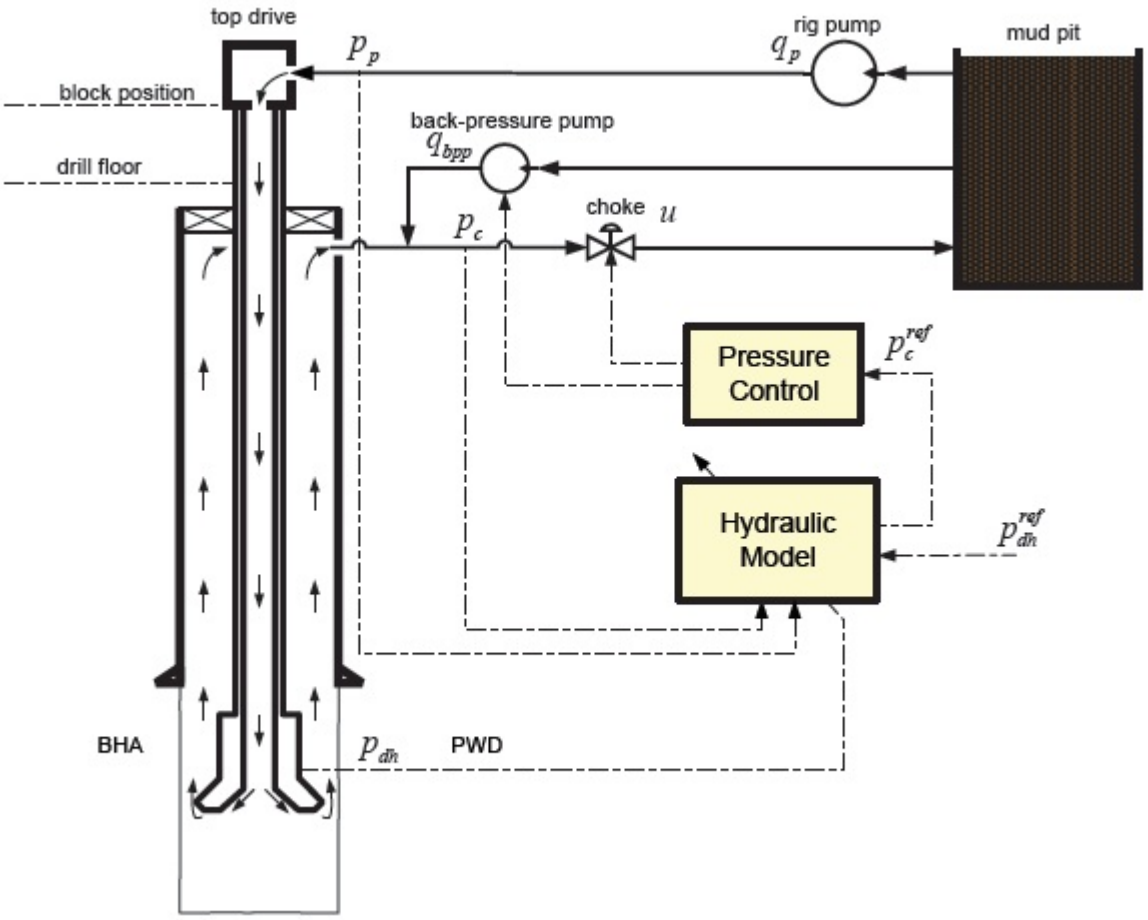

Figure 2: Schematic of an automated ABP-MPD system. Copied from [Kaasa et al., 2012]

The top of the annulus is closed off and routed through a choke valve by what is called a rotating control device, allowing the operator to manage the downhole pressure relatively fast by opening and closing the choke valve.

Figure 2 shows a typical automated ABP-MPD system. A rig pump pumps mud from a mud pit, down the drill string. The drill string is rotated by the top drive, which together with the flow of the mud rotates the drill bit, connected to the end of the drill string, for drilling. Furthermore, the weight on the bit (WOB) sets the final Rate Of Penetration (ROP) given the current rock formations, that is, the rate of which the drill bit penetrates the specific rock formation. The WOB can be manipulated to a large extent by adjusting the block position. This is connected to what is called the ”draw works”, which simply put is a pulley system to

adjust the weight on top of the drillstring[10]. The WOB is a deciding factor for the lifetime of the bit. When a bit is worn out, the entire drillstring must be pulled out in order to replace it.

Steel casings are cemented around the drill string. When the pressure profiles (pore and frac.) of the open wellbore become too challenging, a new casing is inserted. The operator wishes to drill as long as possible before having to insert a new casing, in order to save time. Casings are inserted with decreasing diameter.

Given that the downhole pressure is between the pore and fracture pressures of the open wellbore, the mud returns up through the annulus. Flow rate and density must, in combination, be high enough to lift any cuttings from the bottom of the well to the top. This is referred to as hole-cleaning, which is very important.

In Figure 2, an additional pump is placed before the annulus choke valve. This is called a back-pressure pump. It is used primarily when the rig pump is off, to maintain the downhole pressure without having to close the choke valve completely, but can also be used with the same aim as for the choke valve. Use of the back pressure pump is minimized to reduce its wear.

Pump rates, mud density and ROP are normally pre-determined. To then maintain a desired downhole pressure, only the choke is manipulated. This can be done using a simple SISO PID controller, where the choke input is decided from the error defined as the difference between the measured and desired downhole pressure at one point, normally at the bit.

Figure 2 suggests a controller scheme using a hydraulic model of the system to calculate a reference value for the choke pressure based on pressure readings and a reference value for the down hole pressure. This choke pressure reference is then suggested to be used in an inner controller for the choke position and the back pressure pump flow. Such controllers have been researched to some extent. The main possible advantage is that the non-linearity of the choke can be controlled by the inner controller. One specific choke pressure controller can be found in [Godhavn et al., 2011].

In this thesis, the main mud pump will also be available for control. The set points for pump flows and choke position will be calculated using a linear model of the system based on step responses. Such a set up gives a further potential for automation.

This thesis is aimed at exploring the possibilities when using multiple inputs and multiple outputs (MIMO). Specifically, using Model Predictive Control (MPC) to manage pressures throughout the open wellbore, not just at one point, by the means of both choke and pumps.

Any essay on MPD needs to include the definition as per IADC Underbalanced Operations

[10] An alternative to this pulley system does exist. Pulleys delay the response of adjusting the weight.

and Managed Pressure Committee:

"Managed Pressure Drilling (MPD) is an adaptive drilling process used to precisely control the annular pressure profile throughout the wellbore. The objectives are to ascertain the downhole pressure environment limits and to manage the annular hydraulic pressure profile accordingly."

2.2.1 Hydraulic Model

In any regulation problem, it is paramount to get an understanding of the system at hand. Mathematically, a hydraulic model wrt. Figure 2 can be formed as [Kaasa et al., 2012] :

$$\frac{V_d}{\beta_d}\frac{dp_p}{dt} = q_p(u_p) - q$$

$$\frac{V_a}{\beta_a}\frac{dp_c}{dt} = q + q_{bpp}(u_{bpp}) - q_c(p_c, z_c) - \dot{V}_a \tag{5}$$

$$M\frac{dq}{dt} = \begin{cases} p_p - p_c - f_d(q) - f_a(q) + (\rho_d - \rho_a)gh & \text{if } q > 0 \\ 0 & \text{if } q = 0 \end{cases}$$

$$p_{dh} = p_c + f_a(q) + \rho_a gh \tag{6}$$

where

- V_d: Drill string volume
- V_a: Annulus volume
- β_d: Effective bulk-modulus for drill string
- β_a: Effective bulk-modulus for annulus
- p_p: Rig pump pressure
- p_c: Annulus choke pressure
- p_{dh}: Downhole pressure
- q_p: Rig pump flow
- q_c: Annulus choke flow
- q: Flow at bit
- q_{bpp}: Back-pressure pump flow
- g: Acceleration of gravity

- h: True vertical depth
- ρ_d: Density in drill string
- ρ_a: Density in annulus
- M: Integrated density per cross section over the flow path
- f_a: Frictional pressure drop in annulus
- f_d: Frictional pressure drop in drill string

From eq. (6), one can observe that the downhole pressure is a direct result of Mud Weight (MW) and indirectly of the choke and pumps. In this respect, the downhole pressure can clearly be controlled by the means of manipulating the flow, mud density and choke valve.

For deducting the hydraulic model above, two control volumes[Çengel and Cimbala, 2010] were used. One leading from the main mud pump and down the drill string. The second running from the bottom of the well and up the annulus to the choke. This, together with several other simplifications, captures the most important dynamics of the system. Such a model has been proven to fit purposefully in controller design, where feedback can compensate for the slower dynamics. When designing a simulator on the other hand, a more complex model is desired.

A simulator does not have the same requirements to computational speed as a controller. It is desired to be as advanced as possible to offer a realistic environment for simulation. This can be achieved by not performing the simplifications needed to form the model in (6) and (5), and in addition create several control volumes. This way, the slow varying dynamics are included and the effect of different parameters can be different throughout the well. Furthermore, other relevant dynamics can be included in a simulator. Examples of all this can be;

- The effect of temperature on the DHP when the flow is stagnant
- The effect of the roughness, bends and width at different spots in the well
- Swirl
- Mud gelling
- Pump dynamics
- ROP dynamics
- WOB dynamics
- Cuttings

- Bit wear
- Loss of mud to the formations
- Influx
- General rock formation characteristics

An example of a well simulator that incorporates parts of this list is the WeMod simulator from IRIS [Nygård et al.] which is used for the simulations in this thesis. The specifics of this commercial software is not publicly available.

Some specific simplifications used to deduct the hydraulic model in (6) and (5) from [Kaasa et al., 2012] are; first, constant fluid density throughout the well which cancels most of the density terms. Second, neglecting the effects of temperature on density. Third, 1-D flow along the main flow path (through pipe and annulus). Fourth, radially homogeneous flow, meaning the properties of the flow can be averaged over the cross section of the flow. Fourth, the change in drillstring volume, V_d, is only current when connecting additional pipe and therefore removed. Other simplifications occur, but these are the main ones.

To illustrate the use of the simplifications, a simple and direct approach to deduct the same model is presented next. Lets start with the simple first principle of mass balance, that is, mass does not disappear or appear in the the control volume other than the difference between mass coming in and out from inlet/outlet.

$$\dot{m} = \omega_{in} - \omega_{out} \tag{7}$$

Mass can be expressed by density $[kg/m^3]$ and volume $[m^3]$, $m = \rho V$, giving

$$\frac{d}{dt}(\rho V) = \omega_{in} - \omega_{out} \tag{8}$$

Expanding using the product rule of derivation

$$\frac{d}{dt}(\rho V) = \dot{\rho} V + \rho \dot{V} \tag{9}$$

Mass coming in and out, or mass flow rate $[kg/s]$, can be described by the flow $[m^3/s]$ and density, that is $\omega = \rho q$, giving

$$\dot{\rho} V + \rho \dot{V} = \rho_{in} q_{in} - \rho_{out} q_{out} \tag{10}$$

Rearranging

$$\dot{\rho} V = -\rho \dot{V} + \rho_{in} q_{in} - \rho_{out} q_{out} \tag{11}$$

or

$$\frac{d\rho}{dt} V = -\rho \dot{V} + \rho_{in} q_{in} - \rho_{out} q_{out} \tag{12}$$

The density of a compressible fluid can be expressed as function of temperature and pressure. A decrease of pressure will let the fluid expand (decreased density), and an increase of temperature will also decrease the density. This can be expressed empirically as

$$\rho = \rho(p, T) = \rho_0 + \frac{\rho_0}{\beta}(p - p_0) - p_0\alpha(T - T_0) \tag{13}$$

Taking the partial derivative of (13) wrt. pressure gives

$$\frac{\partial \rho}{\partial p} = \frac{\rho_0}{\beta} \tag{14}$$

By neglecting temperature effects, pressure becomes the only variable and hence

$$\frac{d\rho}{dp} = \frac{\rho_0}{\beta} \tag{15}$$

Rearranging

$$d\rho = \frac{\rho_0}{\beta} dp \tag{16}$$

Inserting eq. (16) into eq. (12)

$$\rho_0 \frac{V}{\beta} \frac{dp}{dt} = -\rho \dot{V} + \rho_{in} q_{in} - \rho_{out} q_{out} \tag{17}$$

By applying the simplification of constant density, that is $\rho = \rho_0 = \rho_{in} = \rho_{out}$, we are left with the basis for the first two equations in (5)

$$\frac{V}{\beta} \frac{dp}{dt} = q_{in} - q_{out} - \dot{V} \tag{18}$$

For the first control volume (see Figure 3), from main mud pump to the end of the drill string we have

$$\frac{V_d}{\beta_d} \frac{dp_p}{dt} = q_p - q \tag{19}$$

since the change in drillstring volume, $\dot{V}_d$, only occurs when connecting additional lengths of pipe.

For the second control volume (see Figure 3), from the end of the drillstring to the choke we have

$$\frac{V_a}{\beta_a} \frac{dp_c}{dt} = (q + q_{bpp}) - q_c - \dot{V}_a \tag{20}$$

Where both the flow out of the drill string q and the flow from the back pressure pump q_{bpp} are the inlets, while the choke is the only outlet. The change in the annular volume $\dot{V}_a$ occurs from movement of the drill string. Such movement will be caused by mainly three

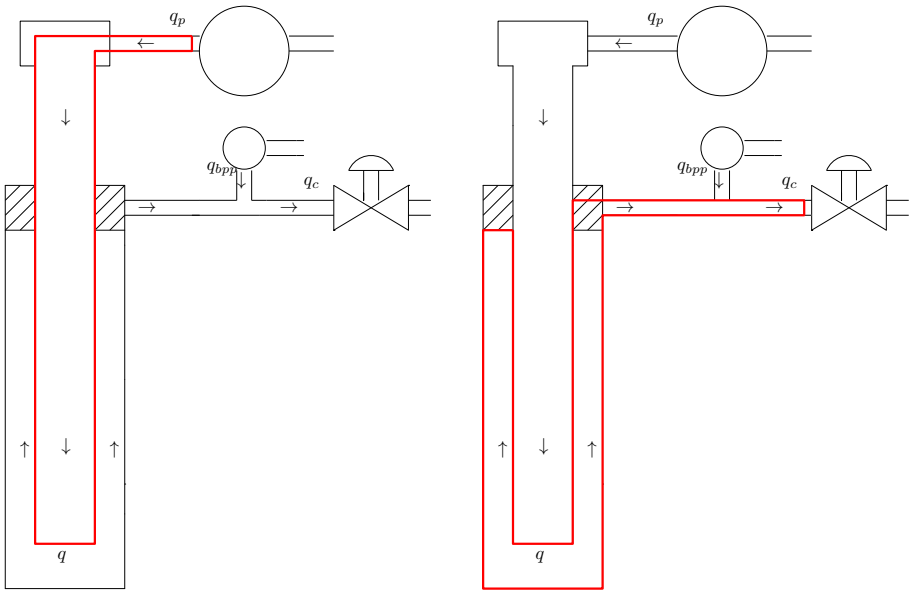

Figure 3: Illustration of the two control volumes (red) for the drillstring and the annulus.

things. One, tripping[11], that is, pulling the drillstring out or inserting in. Second, drilling. Third, heave motions if the drilling rig is floating and effected by oceanic waves. The change in pressure caused by such movements are often called surge and swab effects.

The output equation (6) for the BHP can be simply illustrated as the pressure at the choke plus the pressure caused by the weight of the column of mud from the bottom of the well to the choke, and viscous pressure caused by the flow and friction in the annulus.

The friction in the well, $f(q)$, needs to be expressed in some way. The simplest way is to assume laminar flow in the annulus, and turbulent flow in the drillstring. This can be expressed empirically as $f(q) = f_a q + f_d q^2$.

To derive the one remaining equation in (5), the laws of momentum balance[12] can be used. Given a new, smaller, control volume that surrounds only the area near the end of the drillstring, such that the inlet is the flow from the end of the drillstring and the outlet is the flow starting up the annulus. See Figure 4. The moment balance can be expressed from Newton's second law[sir. Isaac Newton, 1687] as

$$\sum F = ma = \frac{d}{dt}(mv) \tag{21}$$

[11]Tripping is described in depth in Appendix C.
[12]Norwegian: Impulsbalanse. Units are in Newton, not Newton meters as in torque balance.

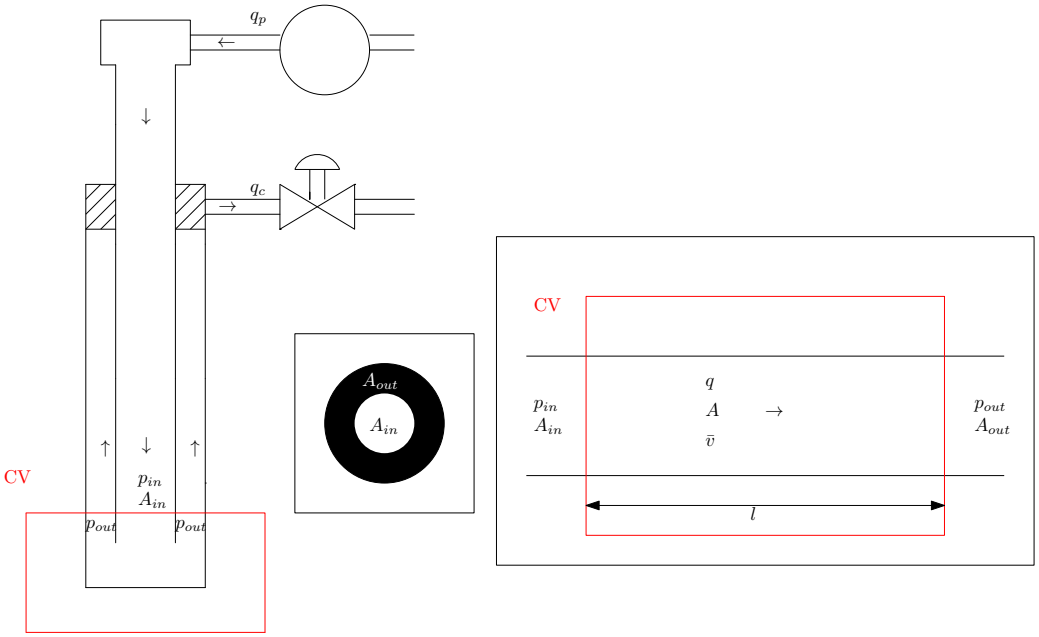

Figure 4: Illustration of the small control volume (CV) used for the moment balance at the bottom of the well. The box in the middle illustrates the cross-sectional areas A_{in} and A_{out} of the drillstring and annulus, respectively. The box to the right is a "stretched out" version of the CV.

Keeping in mind that $Force[N] = Pressure[N/m^2]\ Area[m^2]$, two forces are acting on the control volume that are of specific interest

$$p_{in}A_{in} - p_{out}A_{out} = \frac{d}{dt}(mv) \tag{22}$$

By simplifying to 1-D flow in the flow direction, and using an average velocity of the entire flow path as $\bar{v}$, we have that $\frac{d}{dt}(mv) = \frac{d}{dt}(m\bar{v})$. Lets rewrite the average velocity $[m/s]$ as a term of average flow q $[m^3/s]$ and area A $[m^2]$, and further expand using equations for mass m

$$\frac{d}{dt}(m\frac{q}{A}) = \frac{d}{dt}(\rho V\frac{q}{A}) = \frac{d}{dt}(\rho Al\frac{q}{A}) = \frac{d}{dt}(\rho lq) \tag{23}$$

By simplifying the density in the control volume to be independent of time, and the length also, we have

$$\frac{d}{dt}(\rho lq) = \rho l\frac{dq}{dt} \tag{24}$$

This gives

$$\rho l\frac{dq}{dt} = p_{in}A_{in} - p_{out}A_{out} \tag{25}$$

Simplify the cross-sectional areas to be equal, as A

$$\frac{\rho}{A} l \, \frac{dq}{dt} = p_{in} - p_{out} \tag{26}$$

Lump together $\frac{\rho}{A} l$ as M

$$M \, \frac{dq}{dt} = p_{in} - p_{out} \tag{27}$$

Equation (27) expresses the small control volume at the bottom. The pressures working on it, p_{in} and p_{out} can be described similar to the BHP in (6), and the derivation mentioned earlier, that is

$$M \, \frac{dq}{dt} = (p_p - f_d(q) + \rho_d g h) - (p_c + f_a(q) + \rho_a g h) \tag{28}$$

Eq. (28) can be expanded to match eq. (5) with the addition of a non-return valve (NRV) at the end of the drill string which insures non-negative flow q, that is

$$M \frac{dq}{dt} = \begin{cases} p_p - p_c - f_d(q) - f_a(q) + (\rho_d - \rho_a) g h & \text{if } q > 0 \\ 0 & \text{if } q = 0 \end{cases} \tag{29}$$

As a final note, prof. Kaasa expresses the parameter M as the "Integrated density per cross section over the flow path", where the flow is 1-D in the x direction, that is

$$M(l_1, l_2) = \int_{l_1}^{l_2} \frac{\rho(x)}{A(x)} \, dx \tag{30}$$

If one simplifies ρ and A to be constant, we are left with an integral of 1 wrt. the flow direction x. Which is l, giving $M = \frac{\rho}{A} l$.

For a more advanced deduction, the reader is referred to the source of the "Kaasa model" i.e. [Kaasa et al., 2012].

A simplified model such as (6) and (5) has proven to fit purposefully as a NMPC system model[Breyholtz, 2008] in specific simulation cases. A model based controller inherits the complexity of its model, and hence a simple model is desired. If one where to construct a simulator on the other hand, a more complex model can be desired and several control volumes spread out from main mud pump to choke. In a simulator, this works since the flow in and out of each control volume is more or less set by the creator. A hydraulic model that captures as much as possible of the dynamics of the system, but is not so complex that it cripples the model based controller, is what a control engineer desires. In [Landet et al., 2012] the number of control volumes is argued and it is demonstrated that "It is shown by simulations that significantly reduced order models obtained by applying the method of frequency-weighted balanced model reduction to large models outperform those obtain by simply reducing the number of control volumes". This suggest that in the more difficult drilling scenarios/simulations, a better hydraulic model can be constructed without compromising the model based controller wrt. computation time.

In conventional MPD, only pressure readings[13] are available down hole and normally only at the bit. This poses a challenge if one would like to use more than two control volumes as to capture more of the complex dynamics in a real well. One would need more and better available data continuously from down hole. Any controller will perform better with better measurement tools.

With this practical and mathematical elaboration of drilling, it can be interesting to see what can actually be measured with modern instrumentation. This is part of the following subsection.

2.3 Instrumentation

As seen in the previous sections, there are a few components that stand out in a drilling process, such as pumps, chokes and sensors. For a more complete list, and elaboration, see [Skalle, 2012].

Mud pumps are made to offer a large flow rate. Up to 6000 l/min[14]. The ability to deliver such a flow rate is dependant on the resistance the pump meets. Pump dynamics are not considered in this thesis, and is not included in the commercial well simulator. The chokes used are heavy duty hydraulic chokes. Such chokes can go from fully opened to fully closed, and vice versa, in around 30 seconds[15]. This can be translated to a max/min choke rate of change of $\pm 3.3\frac{\%}{s}$, where the opening is in the range 0-100%.

Sensors for the DHP are naturally the most important sensors for controlling this pressure. It is then somewhat unlucky, that these sensor readings have been, by far, the most difficult to ascertain. The conventional method for transmitting the sensor readings from the bottom of the well to the surface has been mud-pulse-telemetry (MPT). By this method, signals from downhole to surface are formed as pressure changes in the mud. This allows a bit-rate of maybe 10bps[Cayeux, 2009], which for the controller could mean, practically, around 2 measurements per minute. Much work has been done to provide estimators instead of, or in combination with[Breyholtz, 2008], the DHP measurement. A minimum of flow is required to transmit signals through the mud.

Wired pipe is an alternative to mud-pulse telemetry and estimation. Wrt. to Figure 5, this concept hides a coaxial data cable inside the drill string pipe, allowing both measurements and commands to travel electronically back and forth between downhole and surface with a bit-rate in the range of 1Mbps[Cayeux, 2009]. This allows the measurements to be used in real time.

[13]WDP offers continuous pressure and temperature readings down hole.

[14]Large pump example: http://www.whitestarpump.com/docs/anatomy.pdf

[15]Choke example: http://www.uztel.ro/index.php/en/products/bop-system-and-manifolds/hydraulic-operated-drilling-chokes

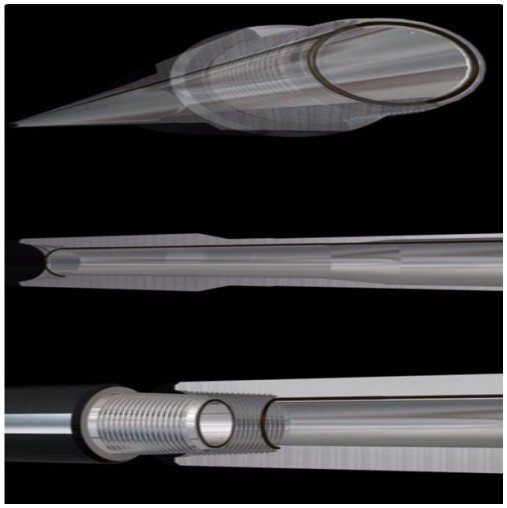

Figure 5: Wired pipe. The coaxial data cable (black) is hidden within the pipe.

In addition, logging while drilling (LWD) can be done online topside, instead of saving data in the BHA and having to wait until the next time the BHA is tripped out.

National Oilwell Varco post the following claim on their website[NOV, 2013]
"NOV™ IntelliServ® provides the oil and gas industry with the only high-speed, high-volume, high-definition, bi-directional broadband data transmission system that enables downhole conditions to be measured, evaluated, monitored and actuated in real time."

This might be a somewhat overzealous statement by their marketing division, but to this date (spring, 2013) there is no published material on any alternative technology, to the author's knowledge.

An electrical generator can be placed in the BHA to supply electricity from the mud flow[16]. This then allows power to be supplied to the measurement tools, drillbit and more. The electrical signals (measurements/data) has to be transmitted a considerable distance through the coaxial cable. As with any electrical conductor, there will be a voltage drop[17]. For coaxial cables of normal quality and a data signal of medium bandwith, the maximum length of the cable is in the magnitude of 100's of meters. A well is likely to be in the magnitude of 1000's meters. This is why signal repeaters are placed in intervals along the pipe together with additional sensors. Signal repeaters are essentially amplifiers, which not only amplifies the desired signal, but also the noise. The severity of this noise is not considered in this thesis.

Wired Drill Pipe (WDP) can be implemented with pressure sensors in intervals, e.g. 450m apart. If given a pressure profile, pore and frac., that clearly shows a difficult section at a specific depth which lies between the casing and the bit, one would then like to have a reading at that point at all times. Since the drill string moves when drilling, this is not the case. However, it can be estimated as shown next.

2.3.1 Calculating pressure at a static spot

In this subsection, a simple way of calculating the pressure at a static spot in the open well bore, using the nearest pressure sensor, will be presented. An example will be used, were pressure readings are provided by a WeMod simulator[18].

[16]This can offer a flow measurement as a bonus.
[17]Optical cables is the alternative.
[18]The WeMod simulator is presented in Section 5

The result is *not* used in the simulations in the following chapters, but it does illustrate the concept which offers measurements of a down hole pressure at a chosen tight spot[19] on the pressure profile.

To calculate the pressure at a specific spot in the open well bore the following can be done; Locate the sensor closest to the TVD in question, call this pressure reading p_y, subtract or add the appropriate MW and viscous pressure. Find the pressure at the difficult depth, called p_x.

Example

$$p_x = p_y - \rho g(TVD_y - TVD_x) - \frac{f_a}{MD_{est}}(MD_y - MD_x)q \tag{31}$$

In this example, f_a is calculated beforehand using an empirical friction model assuming laminar flow in the annulus and eq. (6). A dataset with alternating flow[20] was used. The identification procedure for this is not elaborated further.

The case now would be to control both p_x in addition to p_{dh}. This calls for a multi-variable approach to the controller design.

To illustrate the possible use of eq. (31), two test scenarios are constructed from the well simulator in Section 5. One scenario with constant choke and the other with constant pump flow. The pressures at casing and a chosen spot at 1650m TVD is calculated using eq. (31) with the measured BHP as p_y and the pump flow q_p as q. The results are compared to the measurements provided by the WeMod simulator[21].

The chosen measure of error is the maximum error $\|e\|_\infty$ (infinity-norm) and the error norm $\|e\|_2$ (2-norm). The initial result of using eq. (31) and the simple friction estimation can be seen in Figure 7 and 6.

The discrepancy between the measured and calculated pressure in Figure 6 and 7 is considerably high, as can be seen. Possible sources of this error in eq. (31) is the parameters ρ, g, f_a or the friction model as a whole. The equation does however capture the general dynamics.

The density ρ was found by measuring the ECD at zero flow. An alternative to this could be to use the value given in the well simulator description [Nygård et al.], which is slightly lower.

[19] The desired pressures are already available in the simulator, and does not need to be calculated.

[20] This is to accomplish sufficient excitation of the system as to reveal the best parameter fit. See "Persistent Excitation" in e.g. [Ioannou and Sun, 2003].

[21] WeMod is presented in Section 5

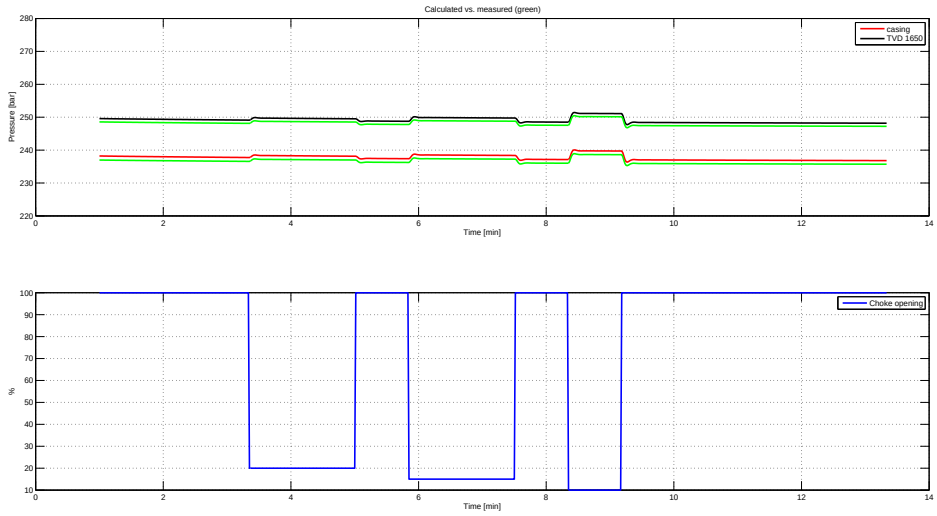

Figure 6: Comparison of Wemod simulated pressure, called measured, against eq. (31). The annulus friction parameter f_a was estimated before hand. Constant flow. Maximum error for casing was 1.2 bar and error norm 31.0 bar. Maximum error for the spot at 1650m TVD was 1.0 bar and error norm 26.4 bar.

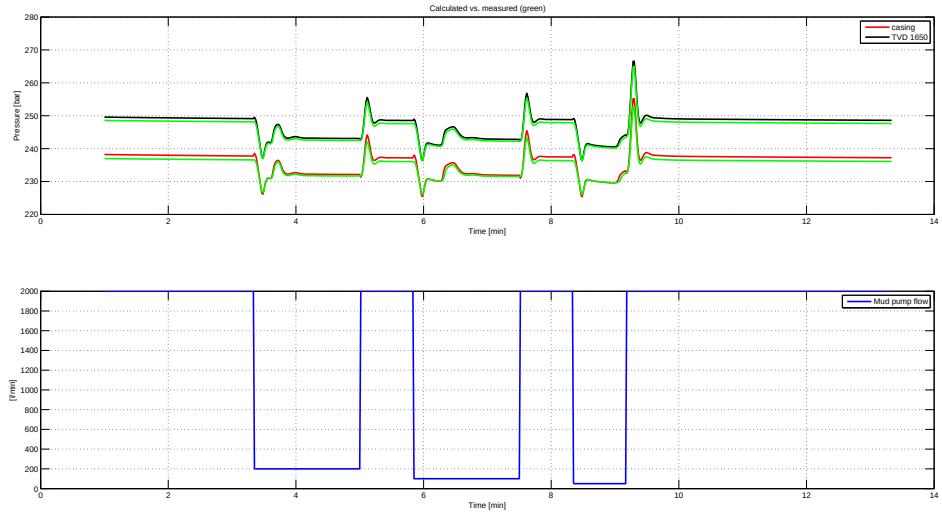

Figure 7: Comparison of Wemod simulated pressure, called measured, against eq. (31). The annulus friction parameter f_a was estimated before hand. Constant choke. Maximum error for casing was 2.4 bar and error norm 28.4 bar. Maximum error for the spot at 1650m TVD was 1.6 bar and error norm 24.2 bar.

The gravitational acceleration g is nearly constant across the planet at reasonable depths.

It is however, possible to express g as a function of latitude, such as:

$$g = G45 - (Gpoles - Gequator) * cos(\frac{2\pi * latitude}{180}) \tag{32}$$

in addition, the height above, or depth below, sea level comes into play. All measurements of g on planet earth can be found to be $9.8\frac{m}{s^2}$ when using one decimal, which in the context of the pressure measurements can be assumed as a fair constant for g.

The friction parameter f_a, which should capture the friction in the annulus, was estimated for the entire annulus, and then divided in equal parts of the MD. That is, $\frac{f_a}{MD_{est}}$. This would state that the friction is equal at all places in the annulus. This is not true. The casings has a friction coefficient connected to their steel surface, while the open wellbore has a friction coefficient connected to formations at each point. Also, from surface to bottom, the width of the annulus is decreasing. Furthermore, the wellbore is likely to contain bends and varying drillstring girth caused by the BHA and more, which would indicate that the friction varies throughout the entire annulus.

After tuning the friction parameter f_a, by no other means than trial and error, the results seen in Figure 9 and 8 was achieved.

Tuning the friction parameter f_a gave some improvement overall. At its best, the pressure at 1650m TVD was calculated to within a maximum error of 1.5 bars compared to the simulator pressure. The simple friction model works considerably better when the flow is constant. This is due to the fact that the viscous pressure is a term of flow and friction, and therefore constant flow will give a nearly constant error depending on f_a. For the scenario with constant flow, the maximum error was 0.3 bar for the pressure calculation at 1650m TVD. Calculating pressures closer to the BHP is more accurate, which suggests that the distance from the nearest sensor can not be excessive, and therefore, several sensors in intervals is desirable. For exact replication, the friction model could be altered to match that of the simulator.

The process of estimating the friction parameter f_a in the example above, shows some of the difficulties connected to system identification. When NMPC is used, several parameters (including friction) have to be estimated to get an accurate model of the system to use for control. This can be a considerable challenge in a practical sense, since the excitation to the system needed to identify all the parameters can cause a considerable amount of NPT. However, there are possibilities to identify parameters while operations are current.

With more than one DHP available by the procedure above, a MIMO controller can be desirable. Such a controller can potentially take control of more than one input and steer more than one output. In the following section, MPC will be presented. MPC has some considerable strengths when it comes to MIMO systems.

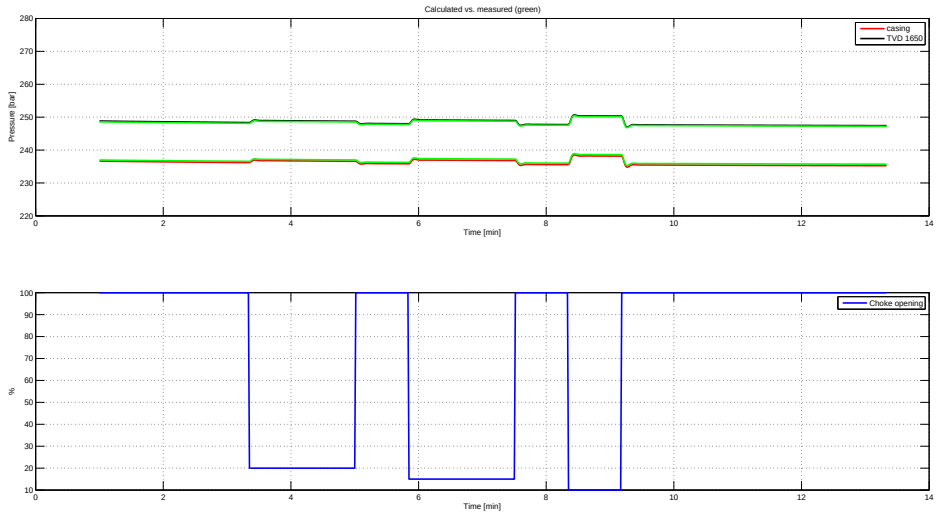

Figure 8: Comparison of Wemod simulated pressure, called measured, against eq. (31). The annulus friction parameter f_a was estimated before hand, and then tuned. Constant flow. Maximum error for casing was 0.6 bar and error norm 11.7 bar. Maximum error for the spot at 1650m TVD was 0.3 bar and error norm 5.8 bar.

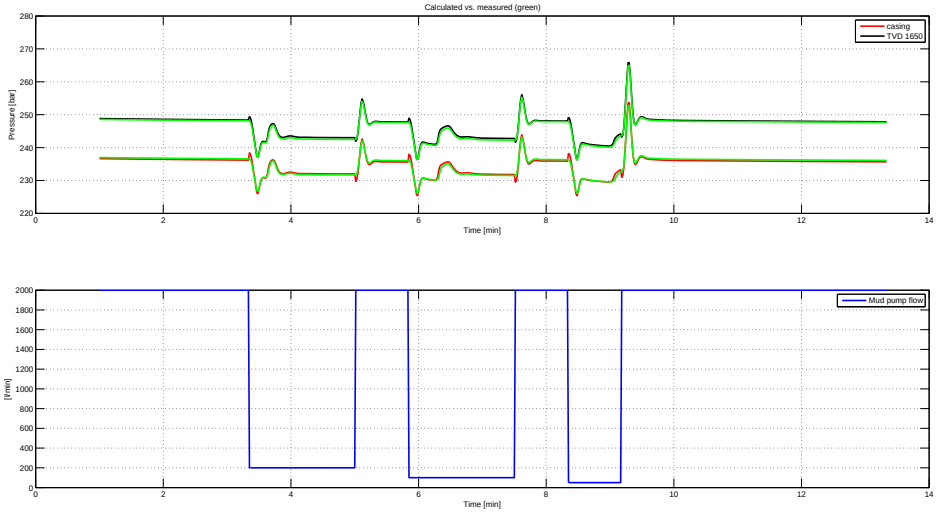

Figure 9: Comparison of Wemod simulated pressure, called measured, against eq. (31). The annulus friction parameter f_a was estimated before hand, and then tuned. Constant choke. Maximum error for casing was 2.1 bar and error norm 13.3 bar. Maximum error for the spot at 1650m TVD was 1.5 bar and error norm 10.9 bar.

3 Model Predictive Control (MPC)

"This type of controller has become *the* advanced process control technology in chemical process industry, and usage is spreading to other application areas." [Imsland, 2007].

In 2013, MPC is an accepted, high performing tool in process industry. It solves an optimization problem at each instant in time to find the next optimal input. Hardware limitations for such computations are decreasing. In addition, process industry is dominated by slow varying dynamics, which leaves seconds or even minutes available.

MPD under normal operating conditions also offer more than enough time for computations. However, certain events do occur that requires a faster update of the input set points. In such a case, linear models can be preferred for their ease of computation.

The optimization problem, a QP [Strand et al., 2003]

$$\begin{aligned} \underset{\Delta u}{\text{minimize}} \quad & y_{dev}^T Q_y y_{dev} + u_{dev}^T Q_u u_{dev} + \Delta u^T P \Delta u \\ \text{subject to} \quad & u_{min} < u < u_{max} \\ & \Delta u_{min} < \Delta u < \Delta u_{max} \\ & y_{min} < y < y_{max} \\ & y = M(y, u, d, v) \end{aligned} \tag{33}$$

Where y is the vector of outputs, u is the vector of inputs, Q_y, Q_u and P are weight matrices, y_{dev} and u_{dev} are output deviation and input ideal-value deviation and Δu is the vector of input rate of change. d are measured disturbances and v are unmeasured disturbances.

In the more capable words of Stig Strand [Strand et al., 2003]: **"The quadratic program of equations** (33) **is solved each control sample to find the optimal control actions."**
"The quadratic objective function penalizes CV (y) deviations from set point, MV (u) deviations from ideal values, and MV moves. The constraints are: MV high and low limits; MV rate of change limits; and CV high and low limits. The dynamic model predicts the CV response from past and future CV and MV values as well as past DV (d) values and estimated and optionally predicted unmeasured disturbances v."

It can be of value to point out, that the cited quadratic program (QP) in (33) does not include an explicit time horizon. That is, the cost function should include the sum of costs

over the entire prediction horizon $Npred$[22] i.e.:

$$\sum_{k=1}^{Npred} (y_k - y^{sp})^T Q_y (y_k - y^{sp}) + (u_k - u^{iv})^T Q_u (u_k - u^{iv}) + \Delta u_k^T P \Delta u_k \tag{34}$$

And the constraints must be upheld over the entire horizon.

The optimal solution to problem (33) over a specified time horizon is the input sequence that minimizes output and input deviations, as well as input rate of change, without breaking the constraints in the predicted future based on the model M. Only the first entry of the optimal input sequence is used, then a new measurement y_0 is done and the computations are repeated. By performing these calculations with the new measurement of y_0 and only using the first entry of u, feedback is achieved. The feedback can used to identify measurement off-set. The simplest way is to estimate it as a constant defined as the difference between measured and modelled output. That is $d_k = y_k - \hat{y}_k$. Integral action can be achieved by a small alteration to the optimization problem 33 as in [Imsland, 2007], by e.g. including d_k in the cost function and augmenting the model M. Furthermore, by using diagonal weight matrices (Q, P), all the states can be decoupled to some extent. The implicit prediction and control horizon in (33) is the length of the vectors y_{dev} and u_{dev}, respectively.

By balancing the penalty for state deviance and input usage, steady state error can be weighted. Weighting the input usage can give a dampening effect, similar to the derivative effect in a PID regulator. The difference between measured and predicted value for a Cvr is used to handle the steady state error in general, to the point were a change in input is not worth the predicted (weighted) improvement in state deviation.

Cvr constraints are often posed as soft in (33). This can be done by setting a slack variable which determines the maximum amount that a constraint can be broken. The slack variable is then included in the cost function as e.g. a linear or quadratic term. The weighting of this term determines how hard[23] or soft the constraint is. Input constraints are often hardware limitations an are therefore absolute.

Multiple inputs and outputs (MIMO) fits naturally into the MPC problem.

Model predictive controllers are generally divided in two specific types, linear and non-linear. Both with its own strengths and weaknesses and degrees of complexity. If a simple controller achieves the same objective as an advanced controller, the simple controller should always be preferred. To give an impression of the difference between (L)MPC and NMPC a mostly theoretical comparison will be presented next.

[22] The control horizon can be set equal to the prediction horizon for simplicity.
[23] No slack gives what can be called a hard constraint.

3.1 (L)MPC vs. NMPC

Performance of an MPC controller falls on mainly two things, namely tuning and modelling. The model, $y = M(y, u, d, v)$, can be given as e.g. a set of equations as in (5), or from step response models.

Since a model based on (5) will be highly non-linear, it will take longer to compute the next optimal input. This can be illustrated by comparing the complexity of simulating (5) using i.e. an ODE solver to predict the effect of Mvr changes, and the simplicity of multiplying a step-response model by the changes in the Mvr to predict the same effect. However, the result is expected to be superior when using a model such as (5). An MPC scheme with a non-linear model is called non-linear MPC (NMPC). If fluid properties, friction parameters and other quantities depending on the chosen model of the system, are estimated and updated frequently enough, the model will represent the true system very well and allow the regulator to predict future system behaviour accurately. One specific advantage of using such a complex model is that the resulting regulator can be invariant to the pressure set point range. For instance, the effect of adjusting a choke valve will be considerably different if the pressure on the valve, and consequently the BHP, is high or low. In [Breyholtz, 2008] this is illustrated with a BHP reference tracking scenario where the range of pressure does not fade the performance of his NMPC. A PI regulator is used for comparison. This scenario is replicated in *this* thesis in Section 5.3.5 for the PI regulator as to further compare to linear MPC.

Linear MPC use linear models for M in (33). These will be somewhat different for high and low pressure ranges. If one chooses to use only one set of linear models, it is preferable to use models created in the range where the transients are fast. This will give the most conservative and robust models, with the possible drawback of slower response. When the system is manipulated towards an operating range where the linear models are a poor fit, some help can be found in increasing the controller update frequency. This is a probable aid, since linear models are fast to compute, as mentioned earlier.

When using linear models with a MIMO system, one delicate simplification can sometimes be applied. If one models each input to all outputs, one input at a time, and as a result use a sum of all the models when predicting future behaviour of the system, superposition has been applied. The superposition principle [Chen, 2009] is only valid for linear systems. As mentioned earlier, MPD is a non-linear process. An input that in theory is the next optimal input based on linear model of a non-linear system, is not necessarily the true optimal input.

Both non-linear and linear models require the MPD operator to move around the different inputs and log the resulting outputs in order to have enough data to identify the parameters needed to create the respective models. In addition, it might be required to perform laboratory testing of mud properties. For linear models it can be very simple to create models from step responses. For non-linear models, it can be laborious, time consuming and all in

all difficult to identify the correct parameters for the model of the system. However, some parameters in a NMPC model can be posed as adaptive, which is a great advantage, i.e. observers can be implemented to update friction parameters, measured depth etc. on the go.

To find the next optimal input with (L)MPC or NMPC, an optimization algorithm must be applied. An example of a QP solver for linear MPC is the *Active-Set Method for Convex QP*. Such an algorithm essentially starts with an initial guess of optimal set of active constraints, called the working set. All the inequality constraints in the current working set is posed as equality constraints, and an equality constrained QP is solved to find a step towards the optimal solution. This is repeated until the optimal active set is found and the KKT conditions fulfilled. An example of an Active-Set Method for Convex QP from [Nocedal and Wright, 2006] is presented in Algorithm 1. This algorithm tries to solve the inequality (and equality) constrained quadratic example problem given in (35), by solving a subset of equality constrained quadratic programs in the form in (36) to find the next step p towards the optimal solution x^*.

$$\begin{aligned} \underset{x}{\text{minimize}} \quad & \frac{1}{2}x^T G x + x^T c \\ \text{subject to} \quad & a_i^T x = b_i, \ i \in \mathcal{E} \\ & a_i^T x \geq b_i, \ i \in \mathcal{I} \end{aligned} \tag{35}$$

(With the set of inequality indexes $\mathcal{I}$ and equality indexes $\mathcal{E}$.)

$p = x - x_k$, $g_k = Gx_k + c$

$$\begin{aligned} \underset{p}{\text{minimize}} \quad & \frac{1}{2}p^T G p + g_k^T p \\ \text{subject to} \quad & a_i^T p = 0, \ i \in \mathcal{W}_k \end{aligned} \tag{36}$$

If the step p is to large, it is shorten by a factor α such that the step does not violate any constraints.

Compute a feasible starting point x_0;
Set $\mathcal{W}_0$ to be a subset of the active constraints at x_0;
for $k = 0, 1, 2...$ **do**
  Solve (36) to find p_k ;
  if $p_k = 0$ **then**
    Compute Lagrange multipliers that satisfy $\sum_{i \in \mathcal{W}_k} a_i \hat{\lambda}_i = G\hat{x} + c$;
    if $\hat{\lambda}_i \geq 0 \ \forall \ i \in \mathcal{W}_k \cap \mathcal{I}$ **then**
      stop with solution $x^* = x_k$;
    else
      $j \leftarrow \arg\min_{j \in \mathcal{W} \cap \mathcal{I}} \hat{\lambda}_j$;
      $x_{k+1} \leftarrow x_k$;
      $\mathcal{W}_{k+1} \leftarrow \mathcal{W} \setminus \{j\}$;
    end
  else $p_k \neq 0$
    Compute $\alpha_k \triangleq \left(1, \min_{(i \ni \mathcal{W}_k, \ a_i^T p_k < 0)} \ \frac{b_i - a_i^T x_k}{a_i^T p_k}\right)$;
    $x_{k+1} \leftarrow x_k + \alpha_k p_k$;
    if *there are blocking constraints* **then**
      Obtain $\mathcal{W}_{k+1}$ by adding one of the blocking constraints to $\mathcal{W}_k$;
    else
      $\mathcal{W}_{k+1} \leftarrow \mathcal{W}_k$
    end
  end
end

Algorithm 1: Active-Set Method for Convex QP[Nocedal and Wright, 2006].

Algorithm 1 is fairly intricate, but for comparison, consider the following Algorithm 2. This is an example of a sequential QP (SQP) which can be used to solve non-linear problems (NLP). A NMPC application will have a non-linear model as equality constraint, but other than that, it is likely to be the same as linear MPC wrt. the optimization problem. SQP can be used to find the next optimal input for NMPC. Algorithm 2 solves a series of QPs comparable to Algorithm 1. This is a clear example of why NMPC is more complex and needs more time to compute the next optimal input given the same horizon as for a linear MPC.

To clarify the procedure of Algorithm 2, consider the NLP on the form

$$\begin{aligned} \underset{x}{\text{minimize}} \quad & f(x) \\ \text{subject to} \quad & c_i(x) = 0, \ i \in \mathcal{E} \\ & c_i(x) \geq 0, \ i \in \mathcal{I} \end{aligned} \tag{37}$$

and its linearisation

$$\begin{aligned} \underset{p}{\text{minimize}} \quad & f_k + \nabla f_k^t p + \frac{1}{2} p^T \nabla_{xx}^2 \mathcal{L}_k p \\ \text{subject to} \quad & \nabla c_i(x_k)^T p + c_i(k_k) = 0, \ i \in \mathcal{E} \\ & \nabla c_i(x_k)^T p + c_i(k_k) \geq 0, \ i \in \mathcal{I} \end{aligned} \tag{38}$$

The linearised problem in (38) is comparable to the QP in (35). In linear MPC, a problem of such complexity is solved once to find the next optimal input. In NMPC such a problem is solved several times, making NMPC more complex.

Choose initial pair (x_0, λ_0) ;
Set $k \leftarrow 0$;
repeat
  Evaluate f_k, ∇f_k, $\nabla_{xx}^2 \mathcal{L}_k$, c_k and ∇c_k ;
  Solve (38) ;
  Set $x_{k+1} \leftarrow x_k + p_k$ and $\lambda_{k+1} \leftarrow l_k$;
until *convergence test is satisfied*;

Algorithm 2: Local SQP Algorithm for solving (37)[Nocedal and Wright, 2006].

It should be noted that the SQP example in Algorithm 2 is simplified, e.g. no line search algorithm or merit function is used.

The Hessian of the Lagrangian $\nabla_{xx}^2 \mathcal{L}_k$ is time consuming to compute (and also needs to be inverted) in the SQP algorithm, which further adds to the complexity of NMPC.

Convex QP's can be solved in polynomial time. Using big O notation, one example[Christodoulos A. Floudas, 2009] of an Interior Point (IP) algorithm exhibits a time complexity of $O(\sqrt{m}L)$ iterations, with each iteration requiring $O(m^3)$ arithmetic operations on integers each of which has at most $O(L)$ digits. Where the Hessian of the cost function has m^2 entries, L denotes the length of input data, that is the total number of digits to write (G, c, a_i, b_i) in (35). NLP's like NMPC on the other hand, is NP-hard.

Table 2 sums up a simple comparison of linear and non-linear MPC, with focus on MPD.

In this thesis, linear MPC will be used for MPD. The linear models will be deducted from step responses. First order step responses will be presented briefly and a specific case of modelling by step response will be presented next.

3.2 First order step response models

Step response models can be used for $y = M(y, u, d, v)$ in eq. (33) to predict future behaviour of the system. These can either be deducted from actual step responses or e.g. modelled as

Table 2: (L)MPC vs. NMPC. Key aspects for comparison.

(L)MPC	NMPC
Convex QP	Non-Convex NLP
Uses fast QP solvers	Uses slower solvers, e.g, SQP
P	NP-Hard
Mostly offline model calibration	Online model calibration
Simple	Complex
No choke characteristics	Includes choke characteristics

first order step response models.

First order systems without zeros can be modelled in the Laplace domain as

$$\frac{Y(s)}{U(s)} = \frac{K}{\tau s + 1} \tag{39}$$

Where Y is the output, U is the input, s is the laplace operator, $-1/\tau$ is the only pole, τ is the time constant of the system and K is the steady state gain.

One simple equation to calculate, approximately, the time constant τ from a step response is

$$\tau = \frac{T_s}{4} \tag{40}$$

Where T_s is the settling time, that is the time from the step is made to the response is within 2% of its final value [Nise, 2008].

To identify the parameters K and τ from a step response, e.g. a step of 500 l/min on the main pump with the BHP as the output wrt. MPD, the following can be done.

while *Process not stable* **do**
 | Get stable;
end
a=U.Measured;
b=Y.Measured;
U.set(a+step);
regulators.state = off;
while *Process not settled* **do**
 | log measurements;
end
H=(Y.log-b)/(U.log-b);

Algorithm 3: MPD step response modelling

Algorithm 3 can be used to model the response in BHP from changing the flow as follows; Have the system at a steady state. Note the measurements of BHP and pump flow before the step. Do the step on the flow. Wait for the BHP to settle. Subtract the noted values from all the respective readings. Divide output by input, that is BHP by pump flow, or Cvr by Mvr equivalently.

This example of step response modelling was carried out on a well simulated in WeMod[24]. The results are presented in Figure 10.

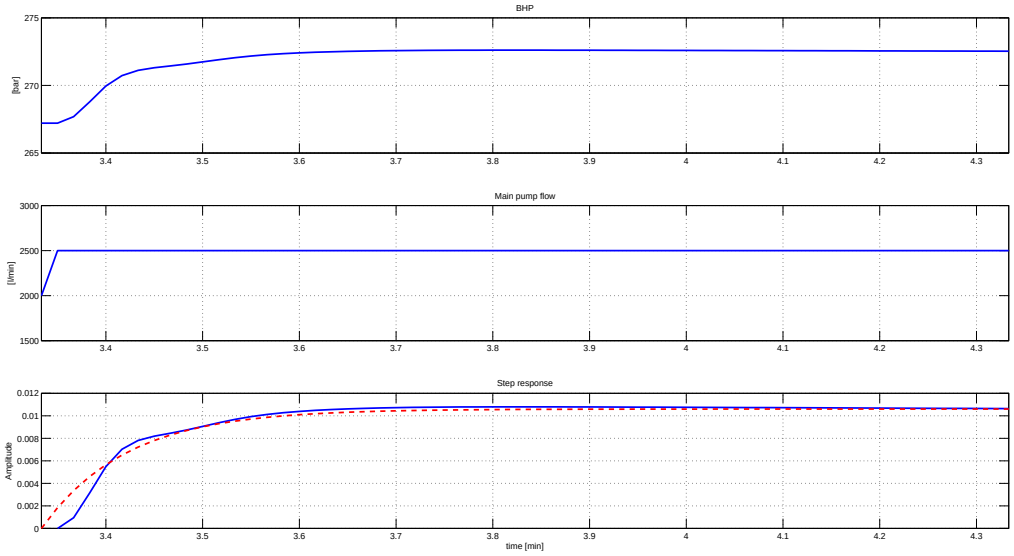

Figure 10: A step of 500 l/min is performed on the main pump (middle) resulting in an increase of pressure at the bottom of the well (top). The resulting transfer function is plotted at the bottom (blue). The parameter K can be found as the final steady state value as approx. $K = 0.0106$. An approximate time for the response to settle within 2% of its final value can be found as $T_s = 21$ seconds. A step response from a first order model based on this settling time and steady state gain is also plotted (red dash).

Figure 10 illustrates the ease of modelling with step response models in MPC. In Statoil's MPC tool SEPTIC[25], a pre-determined number of points on the step response curve can be stored in a .mdf file. The step response curve itself can be deducted or constructed as elaborated above. An example of such a file, which correlates to Figure 10, can be found in Appendix A.

[24] The well simulator WeMod is presented in Section 5

[25] Also presented in Section 5

The way these models are used to predict future behaviour of the outputs is simple. The stored step response is scaled with the change in input and that is the predicted output. At the next time instant, if there is no new change in input, the predicted output is still the same, only one step further on the scaled step response curve. If there is a new change of input, the stored step response will again be scaled with the change in input and added to predicted future behaviour. The same applies for MIMO systems. All input changes are scaled through the stored step response models and added to the predicted behaviour of the outputs. The error between measured and predicted output, which is updated before each calculation of the next input, is used to account for the final output deviation from desired value.

Scaling the step response in Figure 10 with the change of input, the 500 l/min step on the mud pump, gives the predicted future behaviour of the BHP. This prediction has the form of the step response curve and a final pressure increase of K times the step size, that is $0.0106 * 500 = 5.3bar$. This is, of course, an exact prediction since it is merely a reverse engineering of step response model itself.

This simple concept of step response modelling does come with a drawback. For example, the response in BHP would not have the same form as in Figure 10 if the pump flow was moved from 500 to 1000 l/min. Similar, the gain K in a step response from choke to BHP would be dramatically different if the choke step was from 2% to 1% or 52% to 51%. The latter is an example of the non linear choke characteristics that linear models does not include. This means that a compromise must be done when choosing which step response models to be used, where the normal operating area would be the deciding factor.

When the models need updating, one could of course make new step responses, or use historical data to find a better gain and time constant. MPD is a process that is not always on, like e.g an oil refinery, so simple system identification steps are likely to be allowed during NPT. The time needed to perform these steps is dependant on the dynamics of the MPD system. The example of the mud pump step in Figure 10 had a time scale of minutes. From this, a very rough estimate for the time needed to do steps from all the Mvr's in MPD, is 5 minutes times the number of Mvr's.

Gain scheduling and feed forward offers great possible improvements in PID controllers for MPD as shown in [Breyholtz, 2007]. Similar concepts can be added to step response models. The models themselves can be altered during operations. If one chooses to model the step responses using first order models, one can alter K and τ to adapt to the current pressure range. As a simpler alternative, one can store several step response models for different pressure ranges and switch between them. Also, tuning parameters can be posed as adaptive, which can increase the performance without altering the models. Feed forward is achieved by modelling the disturbances. A Dvr can be described as an Mvr that is not manipulated by the controller, but it is measured. The obvious problem then is to perform a step on the

Dvr, which may not be possible depending on the variable.

After the modelling is done, MPC offers to prioritize different properties of the Cvr's and Mvr's. This can be posed as a priority hierarchy, which is presented next.

3.3 Priority hierarchy

MPC tools for linear MPC often incorporates a priority hierarchy, which offers added flexibility for controlling the process and helps ensure that the QP in (33) does not become infeasible[26]. This problem especially arises when the degrees of freedom (DOF) are low, which makes solving the problem in (33) difficult.

$$DOF = N_{Mvr} - N_{Cvr} \tag{41}$$

When using WDP with multiple down hole sensors the DOF is likely to become negative, meaning there are more Cvr's than Mvr's. This means that reaching all Mvr's and Cvr's set points is improbable. This is where a priority hierarchy comes into play.

Priority hierarchy example from SEPTIC[Strand et al., 2003]

(I) Mvr rate of change limits

(II) Mvr high and low limits

(III) Cvr hard constraints

(IV) Cvr set point, Cvr high and low limit and Mvr ideal value with priority level 1

(V) Cvr set point, Cvr high and low limit and Mvr ideal value with priority level n

(VI) Cvr set point, Cvr high and low limit and Mvr ideal value with priority level 99

The way the priority hierarchy example above is structured allows the Mvr rate of change limits to always be respected, as are the Mvr limits unless they come in conflict with the rate of change limits. This is the highest priority since these are most often hardware limitations. A sequence of steady-state QP's is solved to respect the remaining priorities, $iii - vi$. Each stage in the solution sequence respects the achievements from the previous stages. If some priorities are equal, weighting will play a role. "When the achievable steady-state targets have been calculated, the control specifications are adjusted accordingly for the dynamic optimization problem"[Strand et al., 2003].

With negative DOF it is likely that the QP in (33) becomes impossible to solve. One would then successively drop the least important priority and try to solve it again and again until

[26]If the problem becomes infeasible, the next control input can not be found and the previous input will be used.

a solution can be found.

Such a priority hierarchy can be used to always respect the hardware limitations of the pumps and choke, and there after the pore- and fracture-pressure constraint at each DHP. Following this, the different DHP set points can be prioritized, since most likely not all of them can be reached at once. This allows the engineer to tune the controller to first ensure that the pore- and fracture-pressure is respected (hard constraints) before trying to reach the specific set points.

In many cases, the Cvr set points are reached first, and after this, the Mvr's are balanced to reach their prioritized ideal values, without compromising the already accomplished Cvr set points. In [Breyholtz, 2011] several scenarios were simulated where the DOF was positive. This was due to that only one DHP was controlled. It was illustrated that this allowed a number of Mvr's, equal to the positive number of DOF, to reach its ideal value.

Ideal value rate of change can also be set for the Mvr's. This is specifically useful if the engineer needs to control the rate of change when the Mvr is far away from its ideal value and consequently the rate of change is being dominated by the ideal value deviation penalty. The Mvr's reaction to changes in the Cvr's is limited by the max up and max down limits of the Mvr's. The ideal rate of change is separated from this, which means that for Cvr changes, the Mvr changes are limited by the Mvr bounds. While for Mvr ideal value changes, the Mvr changes are limited by the ideal value rate of change. Ideal value rate of change is prioritized together with ideal value set point.

The priorities can be altered on line. This means that if the main mud pump needs to be shut down, its ideal value can be set to 0 and its corresponding priority set to 1. This will be utilized in the connection simulations.

A priority hierarchy can be seen as something that decides set points for the MPC. This can be illustrated at the top of a different hierarchy, often called a control hierarchy. This is presented next.

3.4 Control hierarchy

A control hierarchy constitutes the relationships between the layers of control, from the process itself to the geologists planning the pressure profiles.

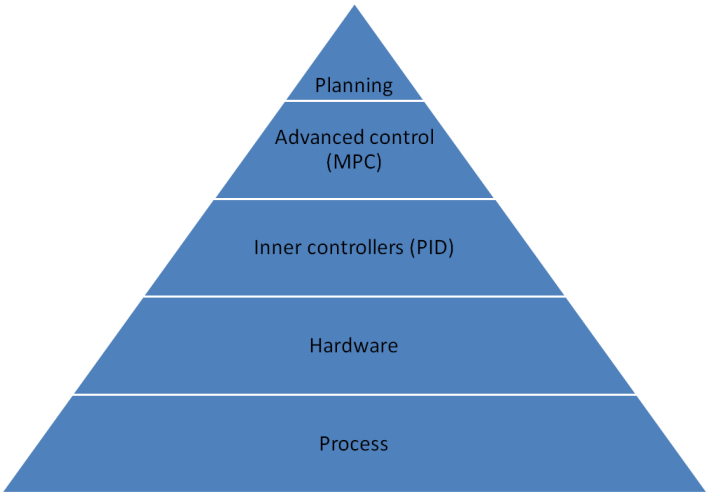

Figure 11: Example of control hierarchy in process control.

With respects to Figure (11) the process of drilling for hydrocarbons can be considered the base of the pyramid. A lot of hardware is connected to this, such as sensors, transmitters, pipes, pumps, valves etc.

A choke valve can be assumed to be fast in comparison with the time constants of the process. However it can often be somewhat unreliable wrt. choke opening set points, as these can be greatly affected/disturbed by the pressure/flow going through the valve. This is often mended by applying a basic control layer, or inner controllers. Simple PID controllers are excellent for controlling such valves. The set points for the PID are then given by the advanced control layer e.g. an MPC application or another set of PID controllers. Dividing the control in two parts simplifies the design of the MPC for MPD.

At the top of the pyramid is the geologist and the operator. These people estimate the down hole environment and plans the set points and constraints for the down hole pressures, as well as mud density and so forth. It should be noted, that an advanced control layer is capable of replacing the operator completely, but this has not yet been implemented.

In todays drilling the operator is normally present at all times from the ”drillers cabin”, see Figure 12. This is a specially built chair that allows the operator to monitor the process and adjust the flow, choke etc. MPD has been implemented in such a manual control, as well as a more autonomous version where PID control is used to control the BHP automatically by using the choke as input. More advanced control theory, such as MPC, has not been accepted, yet.

An advanced control layer, which would replace the operator, needs to set off alarms for the observer to register. The accuracy of such alarms is crucial, as the human observer can get tired of false alarms and consequently disregard correct alarms when it matters the most.

The priority hierarchy from the previous section can be included in the planning phase or as an intermediate level. Priorities can be seen as set points for the MPC layer.

Figure 12: A MPD operator adjusts the set-points for the BHP, flow and choke etc. from his/hers special operators chair.

This then concludes most of the theoretical deductions and elaboration of MPD and MPC in this thesis. From the process itself to the MPD operator and geologist. Section 4 elaborates how the linear MPC used in Section 5 is formed and tuned in a more practical manner. Also, Section 4.3 elaborates how automatic control of the main mud pump in coordination with the the choke, can be used to control more than one DHP while using linear control. Both linear PID and linear MPC can do this. A mathematical elaboration will explain how the linear MPC is able to do this by adding a certain extra Cvr. Section 5 includes all the simulation cases from the problem description, and an elaboration of the software set up used to achieve the results.

4 Controller Design

This section presents how the MPC controllers for the following simulations are constructed. The linear MPC uses step response models. The step responses from a specific example will be presented. Tuning is a key aspect of MPC that requires a great deal of experience given the large number of tuning parameters. The most influential tuning parameters, and how they are used in the subsequent simulations, are elaborated in this chapter.

A simple mathematical derivation and a subsequent simulation will illustrate the ability to control two DHPs while using linear control.

4.1 Step responses (MPC)

Figure 13 shows examples of step responses[27] when, initally, the main mud pump is running at 2000 l/min, the choke is set at 4%, the back pressure pump is off and drilling is not active. The steps are +500 l/min for the main mud pump, -2% for the choke, +500 l/min for the back pressure pump and for the MD a length of 1m is drilled at a rate of 25 m/h with the RPM set to 120.

From the step response matrix in Figure 13 it can be seen that manipulating the choke during normal flow has a large response on the DHPs, while the flow has a lower impact. The disturbance resulting from drilling, which has been bundled in the MD variable, provides a moderate disturbance.

What is not evident here, is that the choke has little to no effect in the area from 15 to 100%. This might suggest that the choke valve is very large. The case is the same with a flow of 5000 l/min.

The flow impacts the DHPs differently. That is, it creates a greater pressure increase at the bottom than further up the annulus. This can be utilized as shown in Subsection 4.3.

To use the step responses in Figure 13 as models for the MPC, the procedure described in Algorithm 3 is used. The models are then used to predict future behaviour of the Cvr's based on change in the Mvr's and Dvr's. If the bias between modelled and measured Cvr increases, some models need updating. This can be due to changes in the set up, e.g. the well has been drilled longer or equipment has started to wear out or pumps have been replaced with new ones. In a MIMO application, it is not necessarily clear from the Cvr which of the Mvr's needs a model calibration. A procedure for model calibrating, other than repeating the step response modelling, is to go through historical data and calculate the appropriate gains and time constants. Such parameters needs to be manually updated when it is "clear" that the models are a poor fit.

[27] A description of the simulated well used to create the steps responses can be found in Section 5.2

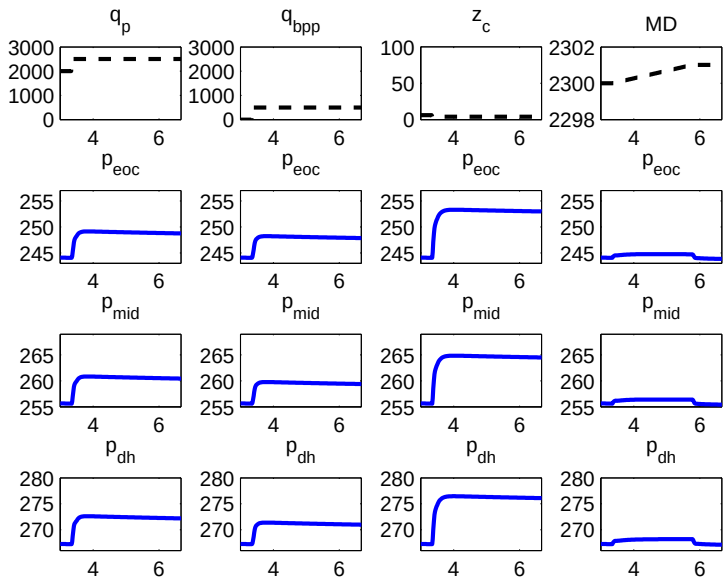

Figure 13: Step responses from different Mvr to Cvr. The top row shows the Mvr step. The three plots following beneath each Mvr is the response in pressure readings from the end of casing (p_{eoc}), a chosen spot in the middle between EOC and BHP (p_{mid}) and the BHP (p_{dh}), respectively. Each Mvr step was simulated exclusively, meaning one simulation was performed for each of the four columns.

After modelling the effect on the Cvr's from all the Mvr's, and as many Dvr's as possible, it is time to tune the MPC application.

4.2 Tuning

This subsection covers the main ideas used when tuning the MPC for each of the simulations in Section 5. There are variables common in MPC that is not mentioned here. Also, there is a large number of software specific variables not mentioned here. However, the ones that are included in this section are the ones that perhaps are the most important, and the most often tuned. Weights in the cost function for example, are frequently tuned to achieve the desired response.

4.2.1 Weighting

Key tuning parameters for an MPC application wrt. (33) are the weight matrices Q_y, Q_u and P. These penalize state deviation for Cvr, ideal value deviation for Mvr and Mvr usage, respectively.

Consider the following SISO example where the only Cvr is a DHP and the only Mvr is a choke valve. We would like to adjust the weight matrices as expressions reflecting the resolution of the sensor/valve and the specific penalty.

By choosing the scalars[28] $Q_y = (\frac{Fulf}{Span})^2$, $Q_u = (\frac{Fulf}{Span})^2$ and $P = (\frac{MovePnlty}{Span})^2$, the cost function can be expressed by

$$\Big(\frac{Fulf(prediction - setpoint)}{Span}\Big)^2 + \Big(\frac{Fulf(prediction - idealvalue)}{Span}\Big)^2 + \Big(\frac{MovePnlty\ \Delta u}{Span}\Big)^2 \tag{42}$$

In eq. (42) $Span$, $Fulf$ and $MovePnlty$ is unique for each Cvr and Mvr. $Span$ represents the resolution. The choke valve input is posed as 0-100% and expected to be accurate within 1%, and therefore $Span$ can be set to 1 for the Mvr. For the DHP Cvr the sensor is accurate and the allowable deviation is 1 bar, its $Span$ variable can therefore also be set to 1. The $Fulf$ variables now represent the specific penalties for the Cvr and Mvr deviation, and can be tuned under the same premiss as any other MPC application[29]. The same applies for $MovePnlty$, which is now the specific penalty for Mvr usage.

Some measurements are larger than others in terms of digits. This will lead to large, dominating deviation terms from those variables. This is avoided by also viewing $Span$ as a scaling variable.

The nomenclature used in the example above corresponds to SEPTIC, which is presented as the chosen MPC software for this thesis in Section 5.

4.2.2 Mvr blocking and Cvr evaluation points

Mvr blocking, or input blocking, is essential in MPC. It allows the user to divide the control horizon into blocks of constant inputs, such that a lower number of inputs have to be calculated during prediction. This can drastically reduce the time needed to calculate the next optimal input as it simplifies the problem. However, the quality of the next input will be reduced to some extent. Finding a balance to this problem is part of the MPC tuning.

Input blocking is unique for each Mvr. Normally, the blocks are of increasing length. The blocks cover the entire prediction horizon. It can be a good idea to place the starting point of the last block at the predicted settling time of the response. This would then effectively state the control horizon, and the rest of the prediction horizon is given the last, constant, input. For non-minimum phase systems, it is likely that there will be a ”dip” in the start

[28] Since there is only one Mvr and one Cvr the matrices are scalar in the example.

[29] Since the DOF in the example is 0, the ideal value can be dropped since it is likely to not be achieved without compromising the Cvr set point.

of the response. It is then desirable to have more frequent changes of the input near the beginning of the prediction horizon, and less frequent later[Maciejowski, 2002].

As an example, consider again the response of pump flow on a DHP in Figure 10. Consider a sampling frequency and input update frequency of 1Hz, and prediction horizon of 100 samples. The settling time is approx. 21 seconds, therefore the last block can start close to sample number 21 on the prediction horizon. By choosing the number of blocks to be 5, an example of input blocks can be

$$Blocking = \begin{bmatrix} 1 & 3 & 7 & 11 \end{bmatrix} \tag{43}$$

where the blocks are of increasing length to try and account for "dips"[30], and each index is the number of samples in the block. The last block starts at sample number 1+3+7+11 = 22 and covers the remaining prediction horizon. This simplifies the optimization problem to calculate a sequence of 5 inputs. For comparison, without input blocking the example would require calculation of 100 potentially unique inputs. Only the first input is used at the next input update, before the calculations are repeated with the resulting new measurements as initial values, which is the fundamental principle of MPC.

To test the choice of input blocking, a set point step can be set on a Cvr that the Mvr influences. After a time equal to the prediction horizon has passed, the initial Mvr prediction should resemble the real history of inputs. An example is presented in Figure 14.

Cvr evaluation points are specific future time samples where the MPC is evaluating the optimization criterion. Setting the number and placement of Cvr evaluation points is done so that critical dynamics from Mvr movements may be observed. Also, setting evaluation points during possible "dead time" or "inverse response" (i.e. non-minimum phase effect) periods should be avoided[Hauger, 2012]. As with Mvr blocking, setting the number of Cvr evaluation points will reduce the optimization problem. One way of handling this is to specify the placements of the evaluation points, as with the blocking. Another approach is to specify a number of evaluation points, which will be of equal distance over the prediction horizon, and a number of samples to ignore in the beginning of the prediction horizon. Neval and EvalDT in SEPTIC, respectively. An example is presented in Figure 15.

4.2.3 Constraints

Optimal handling of constraints is the key advantage of MPC. Other regulators such as PID and LQG does not explicitly incorporate this strength, which in most cases is why MPC is considered as the choice of regulator.

[30]Non-minimum phase effect is not evident in the example response, but it is likely appear in a MIMO setting.

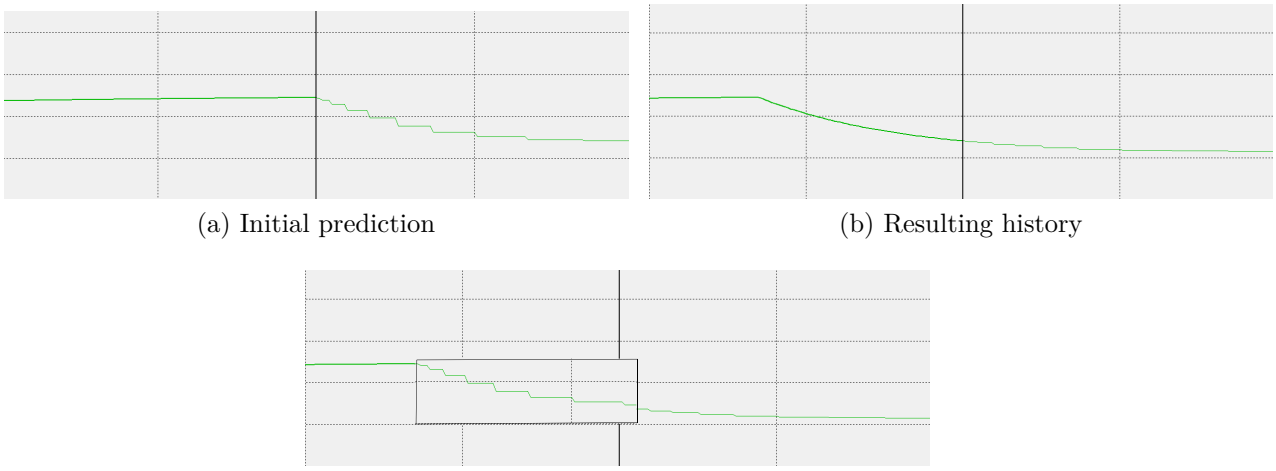

(a) Initial prediction

(b) Resulting history

(c) Comparison

Figure 14: The three figures above shows prediction and history for an Mvr with blocking. The middle solid line divides future and past. Figure (c) is the same as Figure (b), with a cut out from Figure (a) indicated by the black rectangle. Since Figure (c) resembles Figure(b), it can be seen that the prediction resembles the later history, which suggests that the chosen blocking is sound.

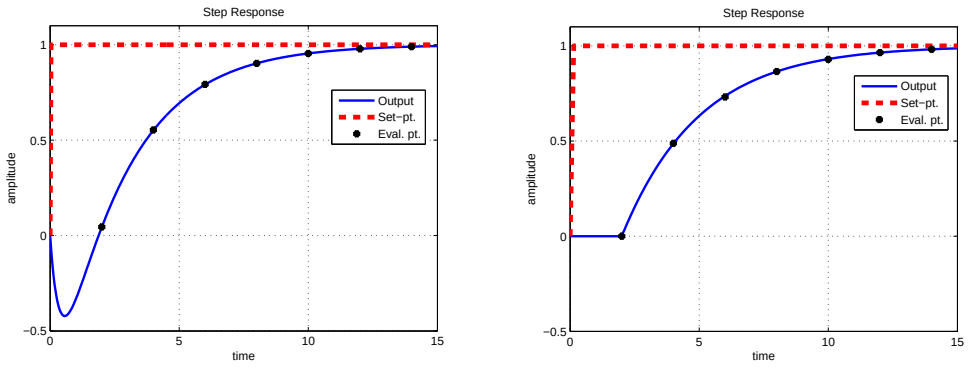

(a) Inverse response

(b) Dead zone (delay)

Figure 15: Illustration of evaluation points for a non-minimum phase system: $\frac{-2s+1}{s^2+3s+1}$ (zero in +0.5) and a system with dead zone: $e^{-2s}\frac{1}{3s+1}$ (delay). If the initial "dip" or delay is not wanted to influence the MPC, the placement of evaluation points can be done like this. The evaluation points are placed with equal distance with the first point after the initial inverse response or delay.

Mvr constraints often reflect hardware limitations, e.g. a choke valve can not be more than 100% open or less than closed at 0%. Furthermore, it is likely that there is a quantifiable measure on how fast an Mvr can be manipulated, e.g. a choke can go from 100% to 0% in 30 seconds suggesting a maximum rate of change at 3.3%/s. A different, but maybe equally important Mvr constraint which is not a hardware limitation, is to maintain minimum flow

rate for sufficient hole cleaning. This should dictate the lower constraint on the main mud pump when this is used as an Mvr.

Cvr constraints can be posed as hard or soft. A hard constraint, as for Mvr, is not allowed to be broken and is therefore absolute[31]. For the DHP's, the hard constraints are the pore and fracture pressures at the depth of the sensor.

An alternative to these hard constraints, is to define a set of more conservative constraints, such as allowable set point error, and define the distance from these constraints to the hard constraints as the maximum allowable limit that the soft constraints can be broken. As an example, consider ϵ as the amount the upper constraint on a DHP has been broken. That is

$$\epsilon = \max(0, DHP - High) \tag{44}$$

where High is the upper conservative constraint on the DHP. The new variable ϵ can then be included in the cost function in (33) as e.g. a quadratic term with its own penalty as $(HighPnlty\ \epsilon)^2$. The upper limit on ϵ can then be the distance between the conservative and the hard constraint (fracture pressure), but it can also be set as infinity with the goal of insuring that the problem does not become infeasible.

$$0 \leq \epsilon \leq HighLimit \tag{45}$$

$$DHP \leq High + \epsilon \tag{46}$$

The nomenclature used in this example of soft/hard constraints corresponds to SEPTIC, which is presented as the chosen MPC software for this thesis in Section 5.

4.2.4 Set-point/range

There are two ways to view the placing of set-points for Cvr's. The typical way is a normal set-point. If the Cvr is away from it, it is penalized. The alternative, is to not have a set-point, but more of a set-range. That is, a defined max/min limit instead of a point. If the Cvr approaches one of the limits, it is penalized. The latter can allow the Cvr to move around a bit without being penalized, but only a defined amount. Examples are shown in Figure 16 (a) and (b). The difference between constraints, and what here is called set-range, is that a set-range would be closer to the desired Cvr value and softer.
The profit of letting the Cvr move around, is lower use of the Mvr's. This however, can also be done by weighting the Mvr usage.

In all simulations regarding this thesis, there will be low weights on Cvr set-points and high weights on Cvr constraints (pore and fracture pressure). An illustration of the resulting penalties for the Cvr's is shown in Figure 16 (c). Furthermore, high weights will be placed on the Mvr usage to make them more conservative. There will not be a set-range.

[31] Again, hard Cvr constraints can make it impossible to calculate a new allowable input.

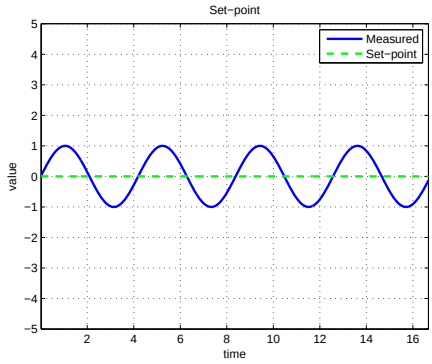

(a) Set-point

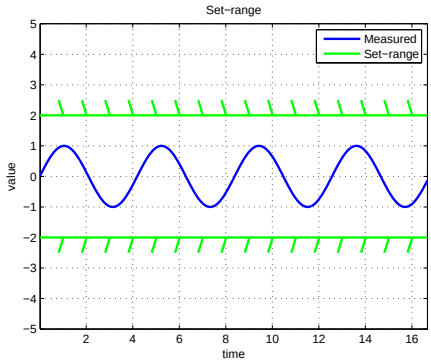

(b) Set-range

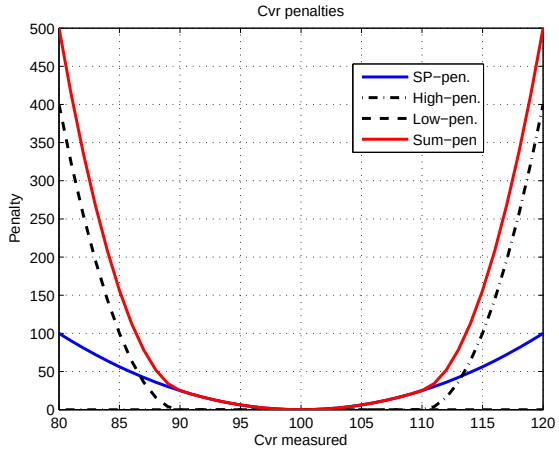

(c) Set-point and constraints penalties

Figure 16: Illustration of the two concepts for Cvr deviation, (a) Set-point and (b) Set-range. Subfigure (c) shows penalties for a Cvr with set-point (at 100) weighting and soft constraints.

4.2.5 Filtering

Measurements are likely to be noise inflicted. High frequency noise, e.g. white noise, can propagate to the Mvr, causing excessive hardware wear and tear. It is then preferable to low-pass filter the measurements. This way, the MPC will not try to regulate the noisy signal, and consequently the Mvr's will be smoother.

Measurement noise can be handled by employing a low-pass filter on the Cvr's model-error update with a recommended[32] time constant equal to 2-10 times the sample frequency. The drawback is a longer response time. With a sample frequency of 1Hz, a filter constant of 2 seconds will double the response time, meaning a slower response. The benefit with regards to removing noise on the Mvr's has to be weighed against this one clear drawback. An

[32] As per the SEPTIC users manual.

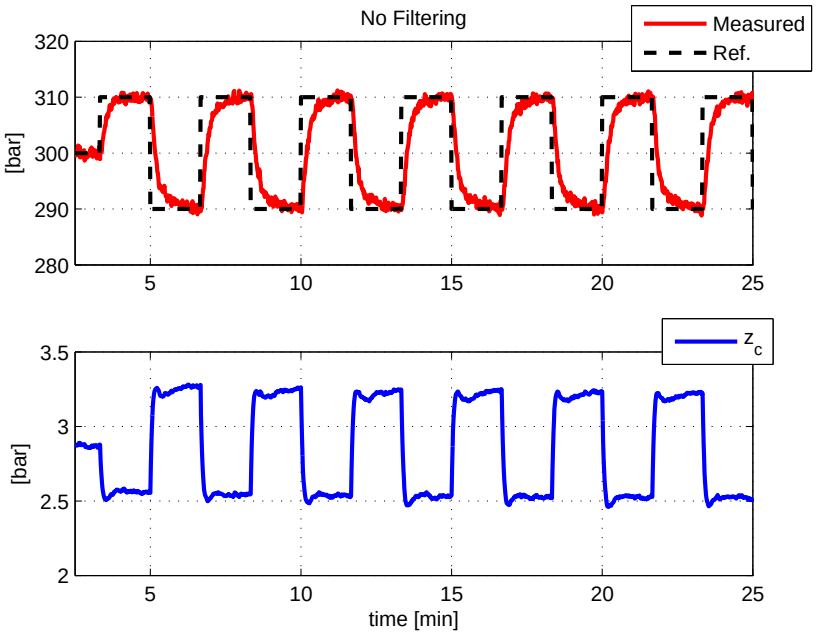

Figure 17: No filtering. The noise from the BHP measurement is transferred to the choke.

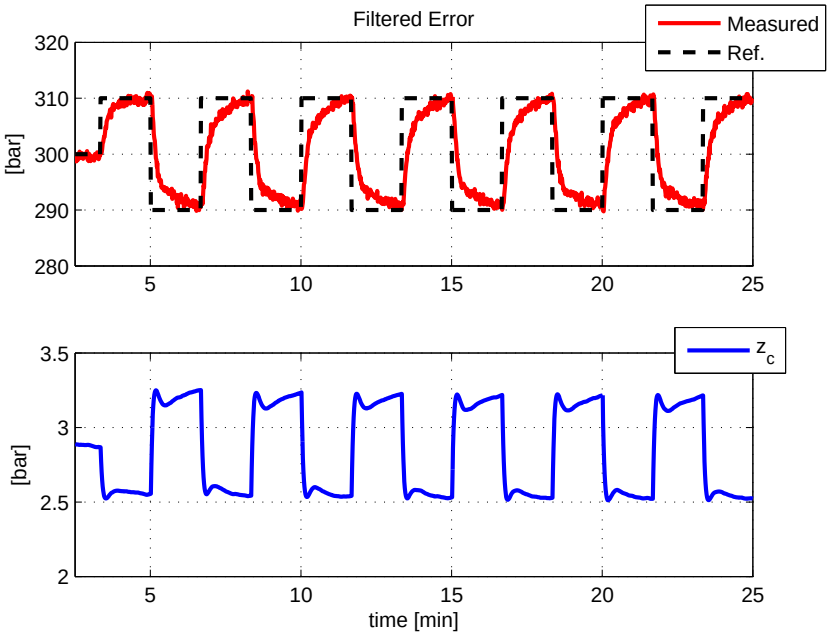

Figure 18: BiasTfilt set to 0.2 [min]. The choke is now relatively noise free, but the response is slower.

example is presented in Figure 18 and 17 where the noise[33] from a BHP measurement is

[33]White noise with zero mean and 0.25 variance.

transferred to the choke. By filtering the error, the noise is removed from the choke, but the response is slower. As an alternative, one could filter the input signal itself, or e.g. employ a step choke[34] to smooth the Mvr's. With regards to MPC, this can be considered as "cheating". Such alternatives are, presumably, outside of the MPC view, which means that the MPC looses control, and hence, this can be considered a bad idea. By filtering the Cvr's model-error update, the MPC still has a full view over the Cvr's and Mvr's, but the error can be filtered smooth. In the chosen MPC software for this thesis, SEPTIC, all Cvr's have an individual, tunable model-error update low-pass filter constant called BiasTfilt with units in minutes.

It is worth mentioning, that creating step-responses from noisy measurements will give noisy models. This should be avoided and is easily handled by adjusting/filtering the response model, or e.g. replicate the response without noise by fitting K and τ in eq. (39).

[34] A step choke limits the size and frequency of allowable choke set-point changes.

4.2.6 Procedure

Tuning an MPC application is a matter of experience. The (short) flowchart in Figure 19 suggests a specific tuning procedure. This procedure incorporates many of the elements described earlier. Deciding horizons, blocking, constraint limits etc. should be reasoned before hand and should not be subject to as much tuning as the parameters in Figure 19. Furthermore, the variables in Figure 19 are all typically possible to tune online. However, Span should be reasoned first and not receive as much focus as a tunable variable.

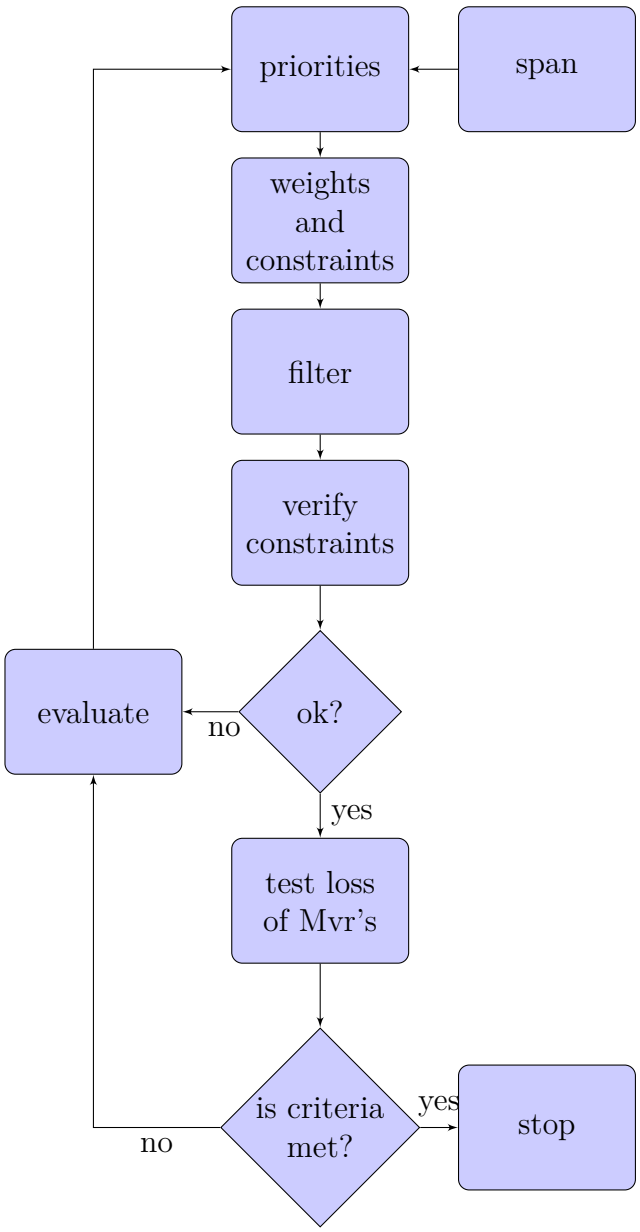

Figure 19: Flowchart illustrating a simple tuning procedure.

The procedure suggested in Figure 19 is to; Choose Span wrt. scaling and allowable Cvr deviance. Set priorities between all Cvr's (SP,high,low) and Mvr's (IV). Tune Cvr Fulf, HighPnlty, LowPnlty, and Mvr Fulf, MovePnlty, rate limits (MaxUp,MaxDown). Tune BiasTfilt. Push all limits to verify constraints. Test loss of Mvr's. Repeat items 2-6 until performance criteria is met.

An example of testing a lost Mvr is the power loss simulation in Section 5.3.4. This simulates the loss of power to both the main mud pump and back pressure pump. In this specific case though, the power loss is detected and the pumps redefined as Dvr's since the control is lost.

4.3 Coordinating flow and choke

By coordinating the flow and choke it is possible to manipulate the gradient of the pressure profile while keeping the BHP relatively constant.

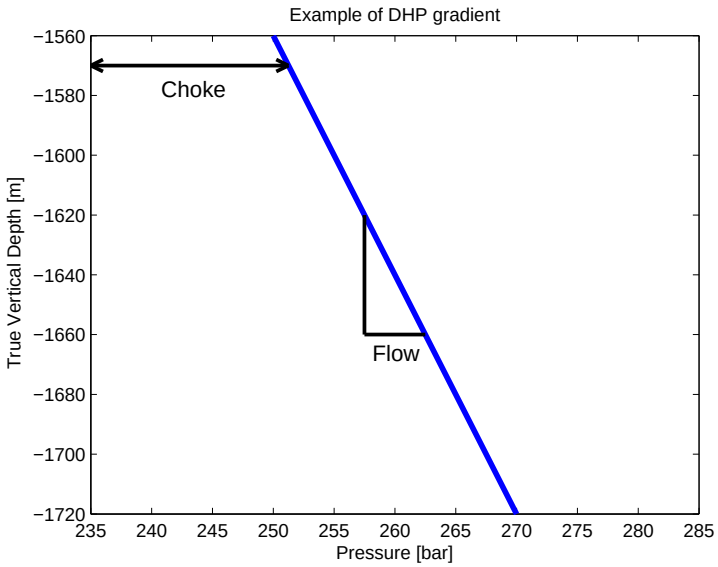

Figure 20: Simplified illustration of choke and flow effect on a down hole pressure profile.

One simple way this can be accomplished, is by controlling the BHP from the choke, and an additional point further up the well, i.e. p_{mid}, by using the mud pump. This way, two points are controlled, which is enough to the get the desired pressure profile as illustrated in Figure 20.

By restating equation (6), one can formulate the BHP as

$$p_{dh} = p_c + f_a(q) + \rho_a g h$$

and in turn from eq. (31) one can formulate the pressure p_{mid} as

$$p_{mid} = p_{dh} - \rho g(TVD - TVD_{mid}) - \frac{f_a}{MD_{est}}(MD - MD_{mid})q \tag{47}$$

From these two equations it is clear that the BHP is affected by both the choke and the flow and the same, in turn, applies for p_{mid}. This means that controlling one pressure with one input, affects the other pressure. To clearly express how one can manipulate the gradient of the pressure profile, consider the difference between the two pressures.

$$p_{diff} = p_{dh} - p_{mid} = \rho g(TVD - TVD_{mid}) + \frac{f_a}{MD_{est}}(MD - MD_{mid})q \tag{48}$$

Controlling two points on the pressure profile, can be done by controlling the difference between them. From equation (48) it is clear that this can be done by means of the flow. This effect will be larger if the friction is large and if the open wellbore is long. That is, if the distance between p_{dh} and p_{mid} is large then the term $(MD - MD_{mid})$ will be large.

For PID control it is simple enough to create two regulators and accomplish the desired gradient. That is, SISO control of BHP/choke and p_{mid}/pump. For a linear MPC with step response models, it can be preferable to add p_{diff} as a controlled variable.

Since the step response from mud pump to all the DHP's are similar, it can be difficult for the QP solver to distinguish the effect on each of them. Consider the cost function in (34), with all desired values as zero, that is

$$\sum_{k=1}^{N_{pred}} y_k^T Q_y y_k + u_k^T Q_u u_k + \Delta u_k^T P \Delta u_k \tag{49}$$

This can be formulated in matrix form as

$$zHz^T \tag{50}$$

With $z = \begin{bmatrix} y_1,\ ...,\ y_{N_{pred}},\ u_0,\ ...,\ u_{N_{pred}-1},\ ,\ \Delta u_1,\ ...,\ \Delta u_{N_{pred}-1} \end{bmatrix}$ and[35]

$$H = \begin{bmatrix} Q_y & 0 & \dots & & & \dots & 0 \\ 0 & \ddots & & & & & \vdots \\ \vdots & & Q_y & & & & \\ & & & Q_u & & & \\ & & & & \ddots & & \\ & & & & & P & \vdots \\ \vdots & & & & & \ddots & 0 \\ 0 & \dots & & & & 0 & P \end{bmatrix} \tag{51}$$

The block diagonal, symmetric, Hessian matrix H is desired to be to be positive definite, which can be achieved by choosing the weights appropriately. In addition, consider all the inequality constraints in (33) dropped, leaving only the cost function above and the linear equality constraint formed by a linear model $y = M(y, u, d, v)$. This model can also be expressed over the entire prediction horizon as

$$Az = b \tag{52}$$

By i.e. translating all the step response models to a discrete LTI state space model[36]. That is:

$$x_{k+1} = A_d x_k + B_d u_k\ , y_k = x_k \tag{53}$$

And transferring this state space model over to matrix form for the entire horizon as (using $N_{pred} = 3$ for brevity)

$$A = \begin{bmatrix} I & 0 & 0 & -B_d & 0 & 0 & 0 & 0 \\ -A_d & I & 0 & I & -(B_d + I) & 0 & I & 0 \\ 0 & -A_d & I & 0 & I & -(B_d + I) & 0 & I \end{bmatrix} \tag{54}$$

$$b = \begin{bmatrix} A_d x_0 \\ 0 \\ 0 \end{bmatrix} \tag{55}$$

[35]For a programmer, $H = blkdiag(Q_y, ..., Q_y, Q_u, ..., Q_u, P, ..., P)$ might be more descriptive.

[36]No disturbance included in the elaboration

This is now a QP with a strictly convex cost function and only linear equality constraints, which guarantees that the optimal solution, if found, to the problem is the global one[37]. This is a special case of a QP where a solution can be found by forming the KKT-matrix[Nocedal and Wright, 2006]

$$\begin{bmatrix} H & A^T \\ A & 0 \end{bmatrix} \begin{bmatrix} -p \\ \lambda^* \end{bmatrix} = \begin{bmatrix} g \\ h \end{bmatrix} \tag{56}$$

where λ^* is the Lagrange multipliers, $h = Az - b$, $g = Hz$ and $p = z^* - z$ is the desired step.

The problem now, which is the whole point of this elaboration, would be to invert the left hand matrix in eq. (56). For this matrix to be invertible, certain criteria must be met from A and H. As mentioned, it is desirable that H is formed as a positive definite matrix, which is helpful. The problem then lies with the matrix A which represents the models of the system. If A consists of models for each of the DHP's, it is in danger of having linearly dependant rows or columns since the step responses for each of them are so similar. This can cause the matrix to lose rank and make it difficult to invert, such that the matrix needs to be conditioned. This adds a risk of a less optimal solution. By adding a model for p_{diff}, it can become easier to invert.

A more direct approach is to imagine the gradients of the constraints formed by the model of step-responses. The gradient of the equality constraints must be linearly independent (and non-zero) for the linear independence constraint qualification (LICQ) to hold, which is part of the KKT first-order necessary optimality conditions. Adding p_{diff} can make the LICQ hold.

[37] The solution to a linear version of a non linear system is not necessarily the true solution.

Example The ability of PI and linear MPC to coordinate flow and choke is illustrated in Figures 22 and 21. The test scenario is a fairly simple one, with two set point changes on p_{mid}. The BHP, flow and choke is simulated using WeMod. Eq. (47) is used for p_{mid}, as in the previous section with q_p as q and the same friction parameter f_a.

SEPTIC is used as the MPC software. Both SEPTIC and WeMod is presented in Section 5.

Table 3: Manipulated and controlled variables for the gradient test scenario.

Mvr	Cvr
q_p	p_{mid}
z_c	p_{dh}
	p_{diff}

The PI controllers used can be found in eq. (58) in the PID appendix, Appendix B. The gains used for the BHP/choke controller were $K_p = -0.05$, $K_d = -0$ and $K_i = -0.01$, while the gains for the p_{mid}/pump controller were $K_{pp} = -0.0001$, $K_{pd} = -0.001$ and $K_{pi} = -0.00004$.

In the simulations, illustrated by Figure 22 and 21, the linear MPC has a lower BHP error and faster response than the PI controller. Also, the MPC decouples the effect of choke and pump significantly better than the PI result. For the PI result, the measured pressure for p_{mid} starts off the wrong way before turning towards its new set point. This is because no effort has been put into decoupling the two SISO PI controllers for choke/p_{dh} and pump/p_{mid}, other than trying to respect that the pump should have a lower gain than the choke. Wrt. Section 4.2.2, this an example of an "inverse response" that can occur in MIMO systems. The PI controller induces small spikes on the main mud pump q_p which is not good. The MPC has smooth curves for both the main mud pump and the choke. The PI controller had 4 parameters to tune, the linear MPC had several more. Since the more complex MPC performed much better than the simple PI controllers, it can be considered to be worth its complexity in the case of controlling more than one DHP. Therefore, the PI controller will not be given much attention in the following simulations in Section 5.

In [Breyholtz et al., 2009], where a non-linear model was used in a dual gradient MPD set up, the NMPC also proved able to control two DHP's. Linear MPC is simpler, so in a comparison limited to this one ability, (L)MPC is better than NMPC since it is less complex and achieves the same goal in this respect.

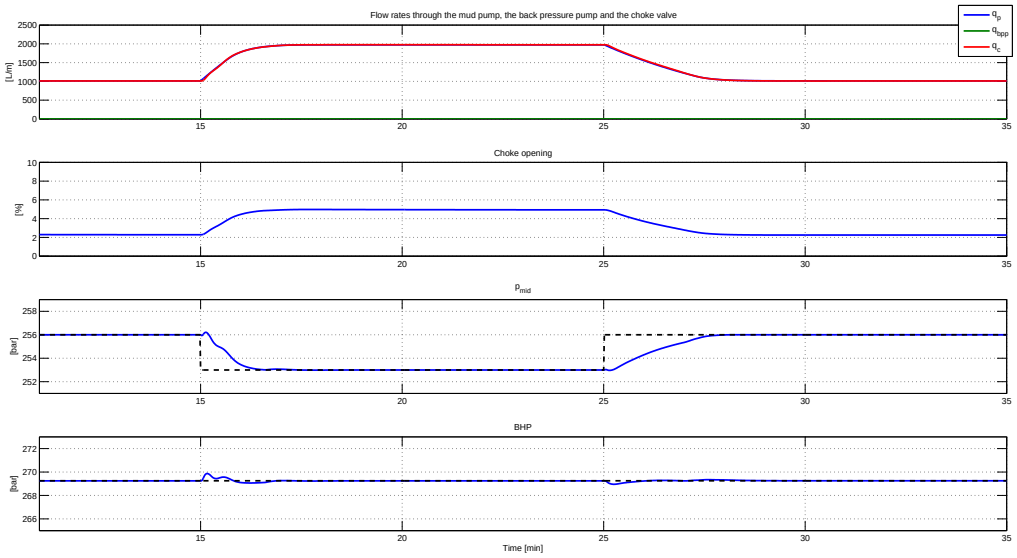

Figure 21: MPC. At $t = 15min$ and $t = 25min$ a set point change of 3 bars is forced on p_{mid}. The BHP is within $\pm 0.7bar$ of its set point. Choke and pump usage is not excessive.

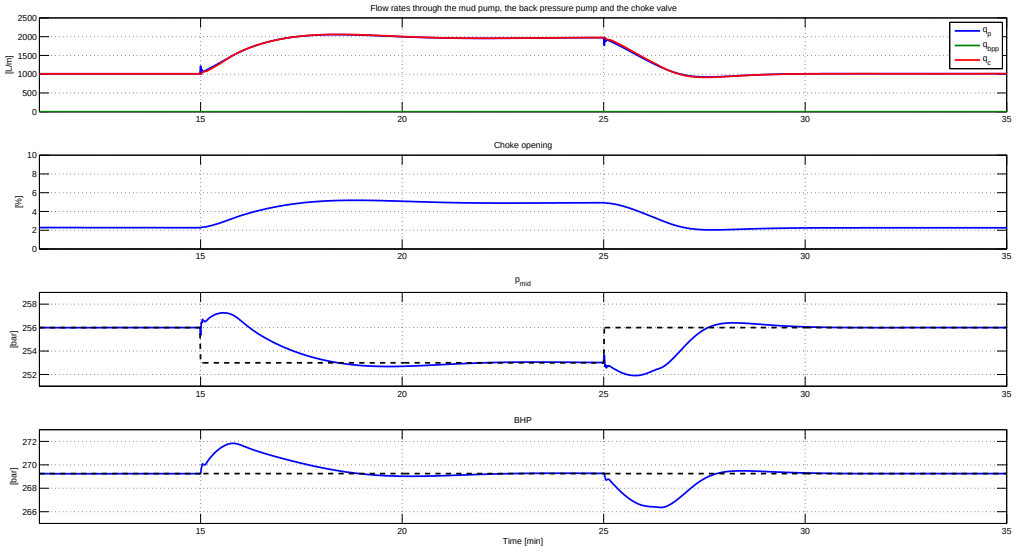

Figure 22: PI. At $t = 15min$ and $t = 25min$ a set point change of 3 bars is forced on p_{mid}. The BHP is within $\pm 3bar$ of its set point. Only the choke transients are smooth, all other measurements have unwanted spikes. The pressure readings overshoots their respective set points.

5 Simulation and Results

In this section the set up for the simulations will be stated and the results presented. In addition to the four cases from the problem description, a BHP/choke reference tracking scenario, with comparison to the results in [Breyholtz, 2008], has been added.

Overlapping control layers are presented as algorithms when needed. MPC variables Mvr, Cvr and Dvr are listed in tables for each simulation.

5.1 SEPTIC, OPC and WeMod

The simulation set up consist of three main components. First, the control and identification tool SEPTIC. Second, the simulated well itself, and finally the OPC server which allows communication between the simulated well and the controller.

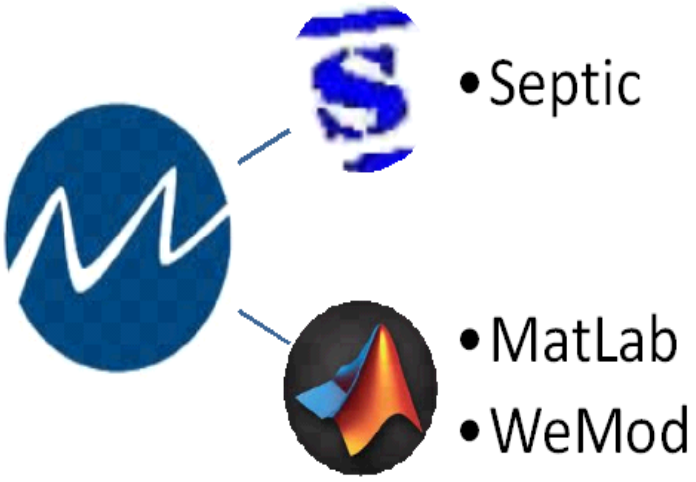

Figure 23: Simple illustration of the data flow between the MPC software SEPTIC and the well simulator in Matlab (WeMod), through a Matrikon OPC server.

The well simulator is a high fidelity simulator from IRIS called WeModNygård et al.. It has been in continuing development since the late 1990's and used in simulations connected to works such as [Breyholtz, 2008], [Breyholtz, 2007], [Breyholtz et al., 2009], [Breyholtz, 2011], [Breyholtz et al., 2011], [Zhou et al., 2010] and many more. The current version runs on Win7 with Matlab R2012b[38] and requires a license from IRIS[IRIS].

Any controller coded in Matlab[39] can be used in connection to WeMod. The simulator enables the user to set controller inputs to several drilling connected variables, and calculates the resulting outputs which can be used in a feedback loop. SEPTIC[Strand et al., 2003] was chosen to create the linear MPC. It enables the user to form step response models in a very intuitive manner, has a flexible user interface and is easily coded, but it lacks a good user support as any other proprietary software does[40]. That is, the public documentation is sparse, and there is no user forum such as for large commercial software's like Java or Matlab. Direct personal user support has been supplied by

[38] Matlab 32-bit version only.
[39] The PID controllers used are coded in Matlab.
[40] The author would like to again thank Statoil's Morten Fredriksen for his personal SEPTIC support.

Statoil for this thesis, which has been of great value. The advantages of SEPTIC outweighs its one big disadvantage. Constructing a new MPC framework in Matlab and Matlab's own MPC tool was considered less attractive than using SEPTIC.

OPC is an abbreviation for Object linking and embedding for Process Control. It is a way of sharing data (measurements/inputs) in process control, and was standardized in 1996[Wikipedia, 2013a]. This means that the Matlab box in Figure 23 can be replaced by a real well without altering the set up in SEPTIC or the OPC server, if the constructors of the well control systems chooses to. Likewise, the controller in SEPTIC can be adapted to fit a real well.

The OPC server software chosen for the simulations is the free MatrikonOPC server for simulation. Since OPC is standardized, the choice was merely based upon the graphical user interface of MatrikonOPC and, off course, the fact that it is free to download from their web site[41].

For Matlab to be able to communicate with the OPC server, the OPC toolbox is needed[42]. With all three components in place wrt. Figure 23, the way it all works is that SEPTIC and Matlab share what is called "Tags", which are updated in the OPC server. Measurements and input commands etc. are read/written to the tags in the OPC server which enables SEPTIC and Matlab to share variables.

Finally, a synchronizing time variable compensates for the fact that the measurements from WeMod is not in real time. Luckily, the simulations are much faster, that is, one real world hour of 60 minutes takes takes much less than an hour to simulate. The time variable synchronizes the time in SEPTIC and WeMod.

5.2 Well Description

The well for the following simulations is from IRIS[IRIS]. More specifically, it is the well used in the loss case from their user manual[Nygård et al.]. Changes made to this case are that the simulated loss has been removed, additional sensors have been placed in the annulus, pressure profiles are customized and optional drilling and back pressure pump has been added. The choke is somewhat oversized, and hence the operating range for the choke is below 10 %. The mud weight accounts for ca. 250 bar of the BHP.

TVD vs. MD

The well is mostly vertical, that is TVD=MD, for most of the well. The last section has a

[41] https://www.matrikonopc.com/downloads/178/index.aspx

[42] If you are a NTNU student it can be worth noting that this toolbox is included in the "employee" license only.

Table 4: Wellbore parameters

Parameter	Value
Initial MD	2300 m
Initial TVD	1720 m
Annulus inner diameter	0.2445 m
Drillstring inner diameter	0.1183 m
Drillstring outer diameter	0.1397 m
Fluid density	1.475 SG

bend to it as can be seen in Figure 24.

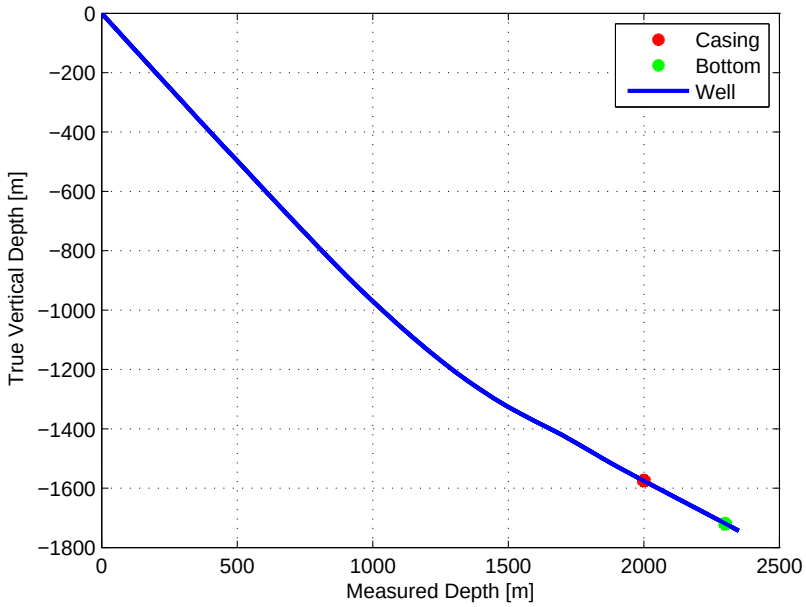

Figure 24: TVD vs. MD. in the well. The difference in MD and TVD between casing and bottom is 300m and 144m, respectively.

Down hole pressure profiles

The down hole pressure profiles for all the simulations have been drawn as an example of challenging, narrow pressure windows. Three measurements will be used, the pressure at the end of the last casing (p_{eoc}), the pressure at a narrow spot incidentally in the middle between EOC and the bottom named p_{mid} and the conventional BHP named p_{dh}. All three measurements are indicated as blue circles in Figure 25.

With reference to Figure 11 the allowable BHP set points have been planned before hand. These are indicated by the green polygon in Figure 25 which is formed by the steepest (cyan)

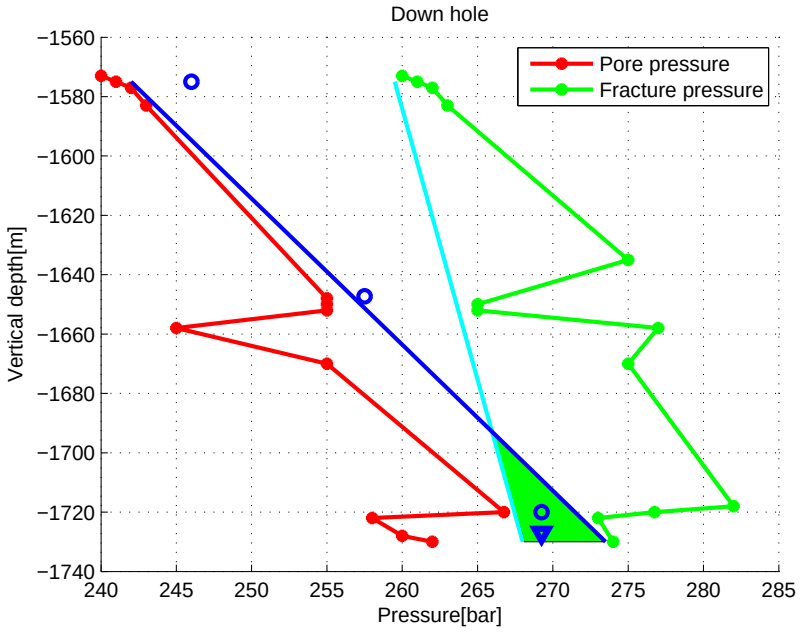

Figure 25: Pore and fracture pressures for the well. Pressure sensors are marked as blue circles. The green polygon indicates allowable set points for the BHP.

and the most moderate (blue) allowable pressure gradients. In the case of drilling, the set point and constraints for the BHP will have to be updated. One update is illustrated in Figure 25 by a blue triangle.

5.2.1 Effect of pump rate on DHP profile

This subsection illustrates the potential to manipulate more than one DHP in the simulator. In Section 4.3 the same was done while using eq. (47) to provide the pressure p_{mid}. In this section, only pressures provided directly from WeMod is used.

Figure 26 shows a simulation where the BHP is held relatively constant by the choke. Measurements of the pressure at the end of the last casing (p_{eoc}) for different flows is plotted to illustrate the potential to alter the pressure gradient in this short well.

By increasing the flow, the viscous pressure increases. The choke is then opened to reduce the pressure again. Equilibriums are found were the right choke opening gives the desired BHP for the given flow. Increasing the flow has a greater impact on the resulting pressure at the bottom, than further up the annulus. The pressure at the end of the casing then decreases as the flow and the choke opening is increased in balance to maintain the BHP. The result wrt. Figure 26 shows, again, that the pressure in the well can be regulated at two locations at once by controlling both the main mud pump and the choke.

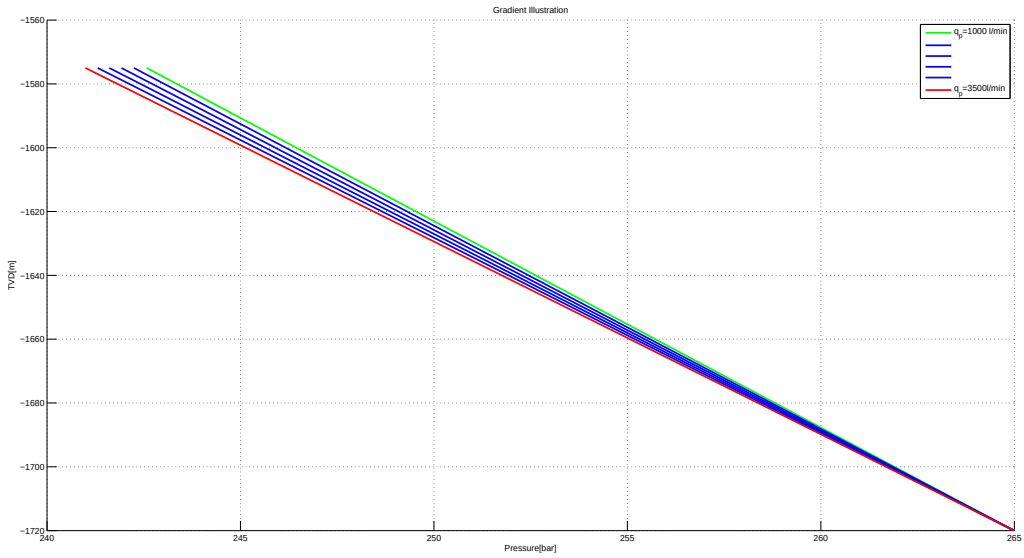

Figure 26: 5 step changes of 500 l/min each on the mud pump. From 1000 to 3500 l/min. The pressure at casing decreases by a total of 1.59 bar.

The well is fairly short and the open wellbore is no more than 300m. This limits the effect of changing the flow, since the sensors are not that far away from each other. However, since the EOC pressure could be manipulated 1.59 bar in the simulation presented by Figure 26, the following simulation was performed where p_{mid} receives three set point changes of +0.5, -1 and +0.5 bar. The MPC application then needs to adjust the choke and flow to achieve desired set points. The result can be seen in Figure 27.

Table 5: Manipulated, controlled and disturbance variables for the p_{mid} ref. tracking scenario.

Mvr	Cvr	Dvr
q_p	p_{eoc}	q_p
z_c	p_{mid}	
	p_{dh}	
	p_{diff}	

The main mud pump (q_p) was included as a Dvr in addition to being an Mvr. The reason for this is that it was desirable to control p_{diff} using only q_p and then control p_{dh} and p_{mid} using only z_c. Including q_p as, additionally, a Dvr allows the MPC application to estimate the effect of the pump on p_{dh} and p_{mid} without interfering with the control of p_{diff}, which can be considered an advantage. A disadvantage is that the predicted future behaviour of q_p is only available from the Mvr.

Figure 27 shows that the set point changes for p_{mid} are reached by automatically adjusting

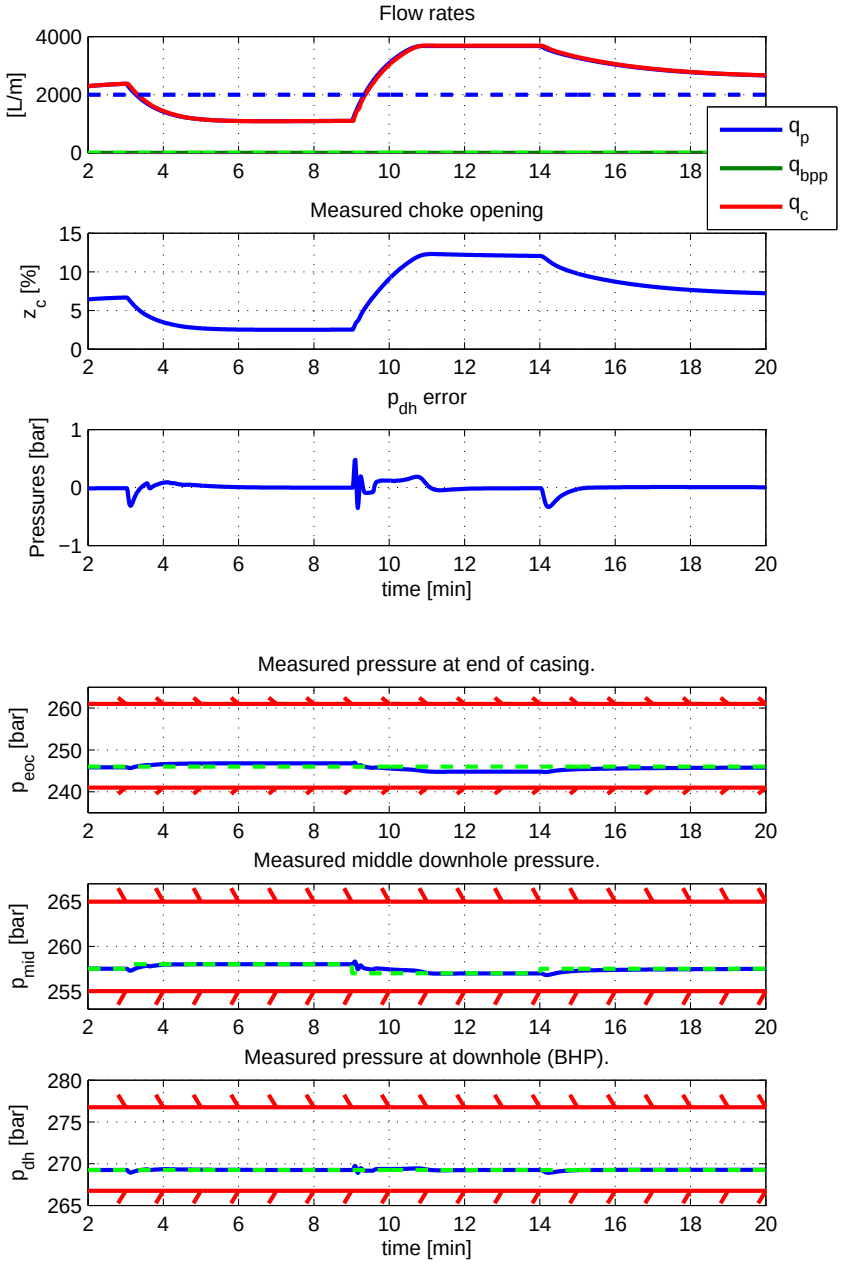

Figure 27: Reference tracking for p_{mid}. The BHP error is within 0.5 bar.

the flow and choke. This was achieved with the cost of a maximum BHP error of 0.5 bars.

5.3 Simulation Cases

For each of the 5 simulations in this section, short tables showing the Mvr, Cvr and Dvr for the simulation will be presented, as in the previous subsection. Algorithms will be used to show how procedures are planned before simulation. These fit on the top of pyramid in Figure 11.

For the scenarios normal drilling, connection, tripping and power loss, two figures will be given as the main results. These two figures illustrates the simulated flows, choke opening and BHP error, and the three DHPs with corresponding constraints and set points. In the figure Appendix D, plots of all pressures and all flows are stored. This includes the pump pressure p_p and choke pressure p_c.

Under normal conditions, it is expected that a regulator for MPD keeps the BHP error below $\pm 5 bars$ [Godhavn, 2009]. Additionally, all the DHPs must be within their constraints (pore and fracture pressures). Choke usage should not be excessive and, when possible, a minimum flow limit should be respected. Spikes of any kind is not desirable on any of the measurements.

For the reference tracking scenario, the main goal is to have the BHP follow its reference trajectory.

In all cases, a figure representing the mismatch between measured and predicted BHP will be presented. This will serve as an indication of the magnitude of modelling mismatch. These figures will compare the differentiated measured BHP with its differentiated predicted value. It is important to note that SEPTIC considers the change in predicted value, not its specific predicted value. That is, SEPTIC offers a history of the predicted BHP in a, more or less, random pressure area. It is the change that matters for SEPTIC, not the pressure area. Therefore, only the differentiated signals will be compared.

5.3.1 Normal Drilling

As the drillbit moves the constraints for the BHP is updated. The constraints for the end of casing and p_{mid} does not change, since these measurements/calculations refers to static points in the open well bore.

The measured depth (MD) is included as a disturbance variable. When drilling commences, a pressure increase will occur from both the ROP and the RPM of the drill string. In this scenario, ROP and RPM are set. The model of the resulting disturbance are from the DHP's to MD.

This is a large simplification. The ROP is not simply set, but a result of such variables as WOB, drill bit wear and so forth.

A minimum flow limit for hole cleaning is implemented. The specific procedure is presented in Algorithm 4, which is simply to drill a length of 10 meters. A table of Mvr's, Cvr's and Dvr's for the case where both the main mud pump and the choke is used can be found in Table 6. A figure of the measured depth can be found in Figure 64 in the figures appendix, Appendix D.

Table 6: Manipulated, controlled and disturbance variables for the normal drilling scenario.

Mvr	Cvr	Dvr
z_c	p_{eoc}	MD
q_p	p_{mid}	q_p
	p_{dh}	
	p_{diff}	

while $MD < 2310$ **do**
  ROP=25 [m/h] ;
  RPM=120 [rpm];
end
ROP=0 [m/h] ;
RPM=0 [rpm];

Algorithm 4: The ROP and RPM are simply set at t=5 minutes. After 10 meters of drilling, they are set back to zero.

Figure (29) and (28) show that the disturbance from drilling a short distance is not a challenge with this simulator, resulting in only 0.5 BHP error. The min. flow limit is pushed and respected.

The flow is decreased a considerable amount in order to maintain p_{diff}. It is pushed so far as to the min flow limit. During drilling, a high flow rate is desirable to insure sufficient hole cleaning. For comparison, the scenario was repeated with constant flow (2200 l/min). In this case, it is not possible to manipulate p_{diff}, hence wrt. Table 6 q_p is dropped as an Mvr and p_{diff} is dropped as a Cvr. This result can be seen in Figure 32 and 31.

Figure (32) and (31) show that there was not much to gain from including the mud pump as an Mvr. The control of p_{diff} is lost, but a higher flow rate is gained. The maximum BHP increased by around 0.4 bar to within 0.9 bar, which is still low. However, if the open well bore was considerably longer, there could possibly be more to gain from controlling p_{diff}.

The only challenge in the simulation is handling the pressure spikes occurring from starting and stopping the drilling. The models in Figure 30 and 33 gives the controller a heads up on the incoming pressure spikes, but the modelled spikes are simpler than actual ones.

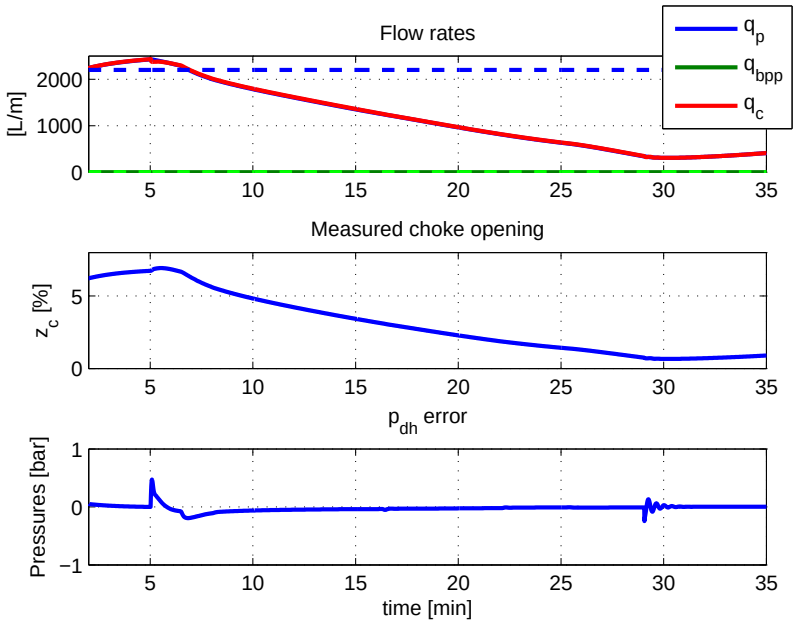

Figure 28: Pumps, choke and BHP error during drilling. The BHP set point is 269.25 bar for the entire scenario. The BHP error is within 0.5 bar. The ideal value set points for the pumps are also plotted in their respective color (dashed). The min. flow limit is 800 l/min. The back pressure pump is not used and is only plotted for continuity.

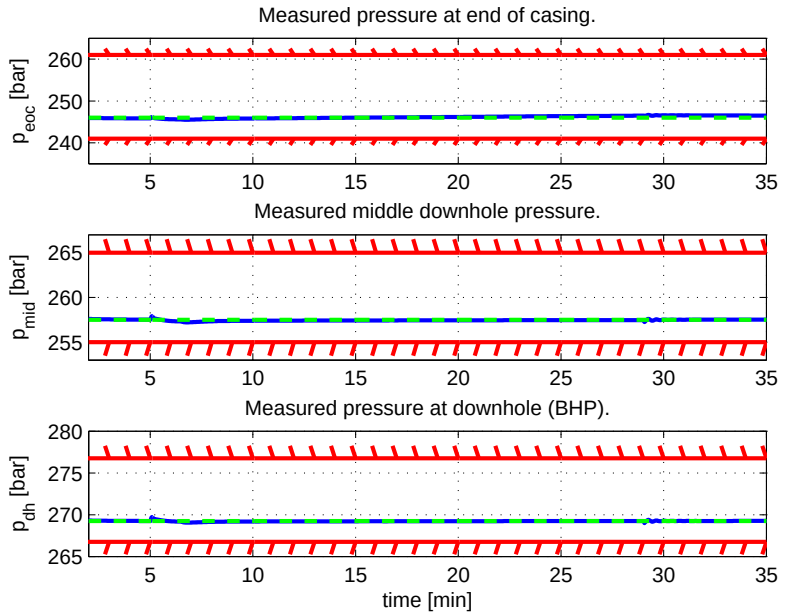

Figure 29: Pressure readings, constraints (Pore and Frac) and set point for all three down hole pressures.

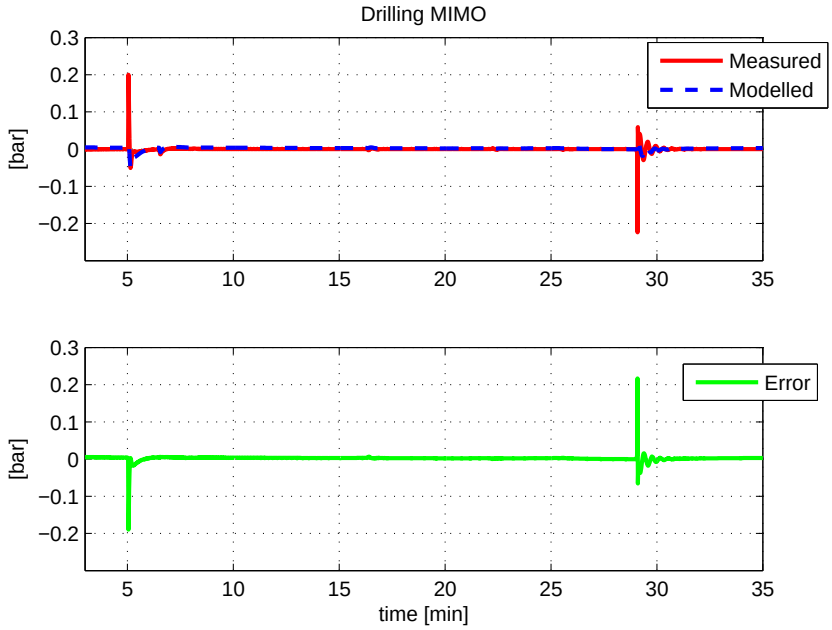

Figure 30: Comparison of differentiated predicted BHP (blue) vs. measured (red) for the MIMO drilling scenario. The model error (green) is low with two spikes where the drilling starts and stops.

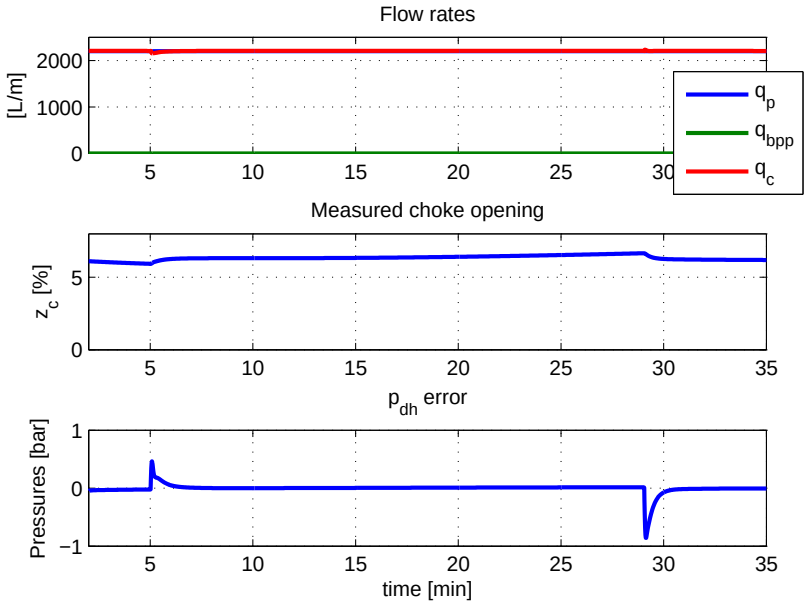

Figure 31: Pumps, choke and BHP error during drilling with constant flow. The BHP set point is 269.25 bar for the entire scenario. The BHP error is within 0.9 bar. The back pressure pump is not used and is only plotted for continuity.

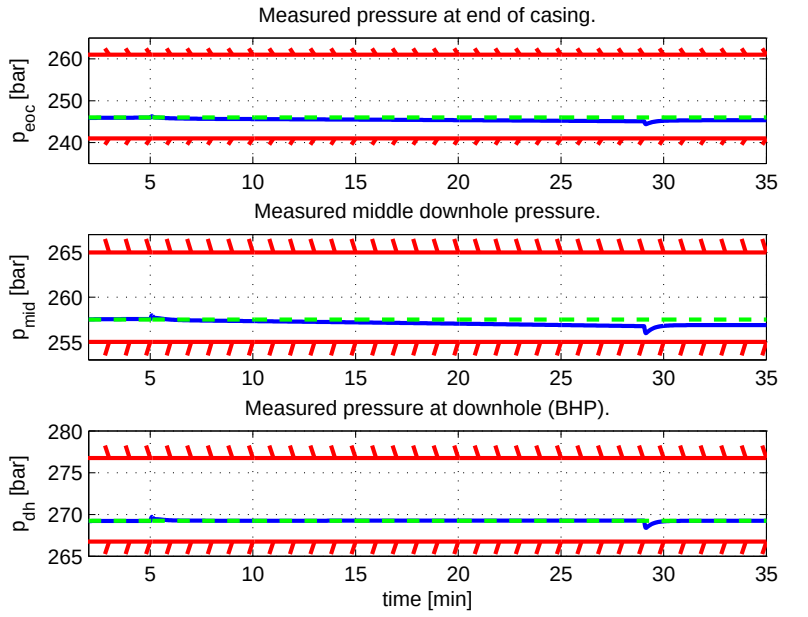

Figure 32: Pressure readings, constraints (Pore and Frac) and set point for all three down hole pressures while drilling with constant flow.

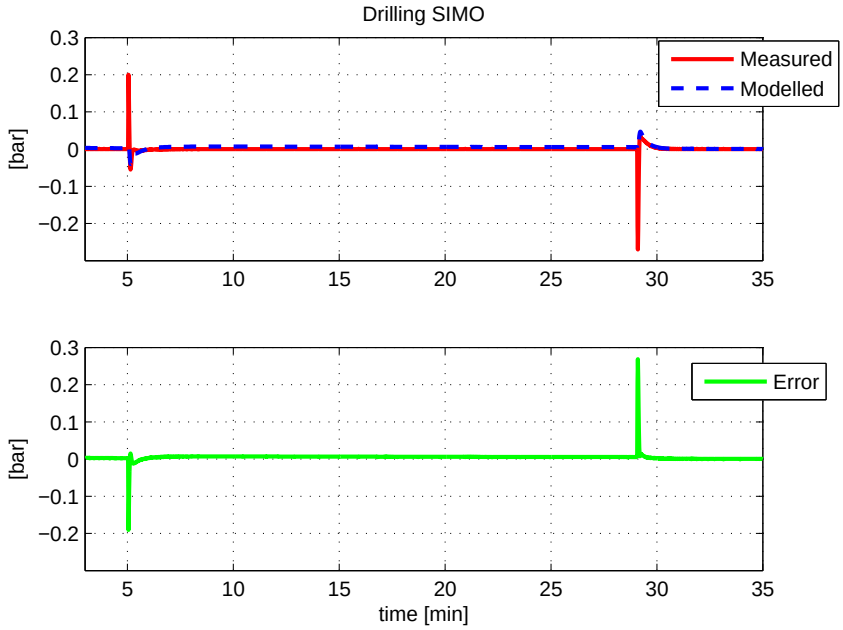

Figure 33: Comparison of the differentiated predicted BHP (blue) vs. measured (red) for the SIMO drilling scenario. The model error (green) is low and close to identical to the MIMO case.

The model error for the BHP in 30 and 33 are both low and flat, with spikes where drilling starts and stops.

If one would add "draw works" to the MPD set up, it could be possible to adjust the final WOB and possibly add the degree of freedom needed to help keep the flow rate high while using q_p as an Mvr, or at least achieve improved control over the pressure spikes from starting/stopping drilling.

5.3.2 Connection

Connection is the process of connecting additional lengths of pipe to the top of the drill string. In this case the mud pump is disconnected[43] from the top of the last pipe section. This is illustrated Figure 34. It is then necessary to ramp down the mud pump to zero. To maintain the DHP while the mud pump is reduced and when it is disconnected, a back pressure pump is used together with the choke valve. A NRV at the end of the drill string insures that mud does not move back up the drill string. Since this is not a simulation of an offshore floating rig, there will be no problems regarding heave motions[44]

A gelling model is included in this simulation. This means that the mud "thickens" when the flow is reduced. This sets up and additional challenge for the regulator when ramping the mud pump back up, since the mud then has a yield pressure that has needs to be considered. Gelling is an important property of a drilling mud as it adds the ability to suspend cuttings in the stationary mud. Without it, cuttings would fall rapidly to the bottom of the well causing the likely result of a stuck pipe.

Connection is a planned procedure. Therefore, it is assumed that tuning and modelling for the MPC can be fitted to the scenario.

Three Mvr's are used in this scenario. The main mud pump, the back pressure pump and the choke. All of which can be found listed in Table 7. As an overlapping layer, the proce-

Table 7: Manipulated and controlled variables for the connection scenario.

Mvr	Cvr	Dvr
q_p	p_{eoc}	q_p
q_{bpp}	p_{mid}	
z_c	p_{dh}	
	p_{diff}	

dures in algorithm 5 and 6 has been applied. At the start of the connection procedure, the

[43]This can be bypassed with a continuous circulation system (CCS).

[44]Heave motions is a significant disturbance on offshore floating rigs since the drill string is held firm during connection and consequently moves up and down with the oceans impact on the rig, resulting in pressure fluctuations down hole.

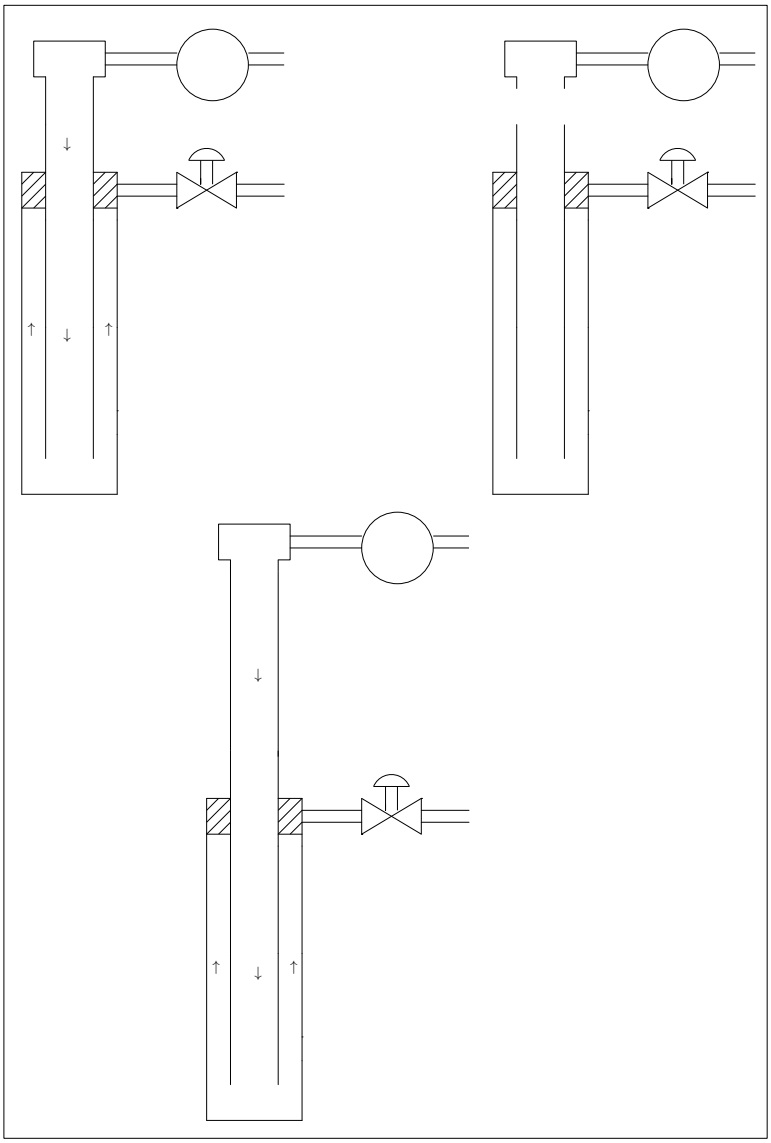

Figure 34: Illustration of the connection procedure. The mud pump needs to shut down in order to disconnect the top drive. Additional lengths of pipe is then connected together with the top drive. The back pressure pump and the NRV is not part of the illustration.

drillstring is rotating at a rate of 150 RPM. The ideal value for the main pump is set to 0, and its respective rate of change is set to 15 [l/min/s], and given a high priority. This starts the ramp down procedure. 5 seconds into the procedure, the back pressure pump is set to operate rather freely. This allows the regulator to calculate the best combination of choke and back pressure pump[45] to maintain the down hole pressures.

[45]The main pump is also available, but its priority is ramping down.

q_p.Iv=0;
q_p.IvPri=2;
q_p.IvRoc=15;
w=150 [RPM];
while q_p.*Measured* > *0* **do**
  timeCount = timeCount +1;
  if *timeCount* > *5* **then**
    q_{bpp}.Iv=800;
    q_{bpp}.IvPri=99;
  end
end
w=0 [RPM];
q_p.state=off;

Algorithm 5: Connection procedure, ramp down.

w=150 [RPM];
Wait(10s);
q_p.Iv=100;
q_p.IvPri=2;
timeCount=0;
while *timeCount* < *90* **do**
  if q_p.*Measured==100* **then**
    timeCount = timeCount +1;
  end
end
q_p.Iv=2500;
q_p.IvPri=99;
q_{bpp}.Iv=0;
q_{bpp}.IvPri=2;
while *Connection.end==false* **do**
  if q_{bpp}.*Measured==0* **then**
    q_{bpp}.state=off;
    Connection.end=true;
  end
end

Algorithm 6: Connection procedure, ramp up.

After the main mud pump is ramped down, the top drive is disconnected, additional length of pipe is connected, and the top drive connected again. During this, the pump must be off and the drill string can not be rotated. This allows the mud to gel.

With the additional length of pipe connected, the drill string is set to rotate again. This is the first step towards breaking up the gelling caused by the lack of flow. The next step is to ramp the main mud pump up to an intermediate, low, set point. This allows the yield pressure of the mud to be handled at a low flow rate, resulting in a significantly reduced pressure spike due to gel breaking. The last part of the procedure is to ramp the mud pump back up to its initial flow, and the back pressure pump down so that it can be turned off. The results can be seen in Figure 36 and 35.

For comparison, the scenario was also simulated without the use of the back pressure pump. These results can be seen in Figure 39 and 38.

Figure 40 and 37 show that the model error is not very "flat". Also, the model does not predict the un-modelled disturbance caused by gel breaking which causes the maximum error. This could suggest that one set of models is not sufficient when the operating area of the flow is both high and low, and that a model predicting the effects from gel-breaking should be considered.

When not using the back pressure pump, the error decreased by 1.1 bar to within 4 bars, which is a surprising improvement, albeit, higher spikes where induced on the choke flow, which is not good.

The collective result suggest that the models might be a poor fit. The use of the back pressure pump can be modified. The simulations presented in Figure 36 and 35 suggests that the back pressure pump is not really used, but rather ramped controlled. The use can be modified to focus on using the back pressure pump to specifically maintain a minimum choke opening.

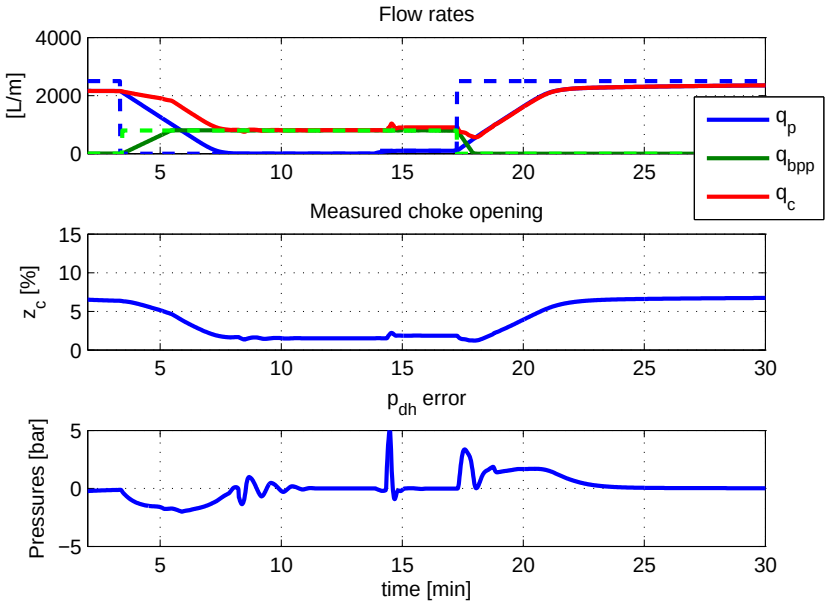

Figure 35: Pumps, choke and BHP error during connection with the use of the back pressure pump. The BHP set point is 269.25 bar. The BHP error is within 5.1 bar.

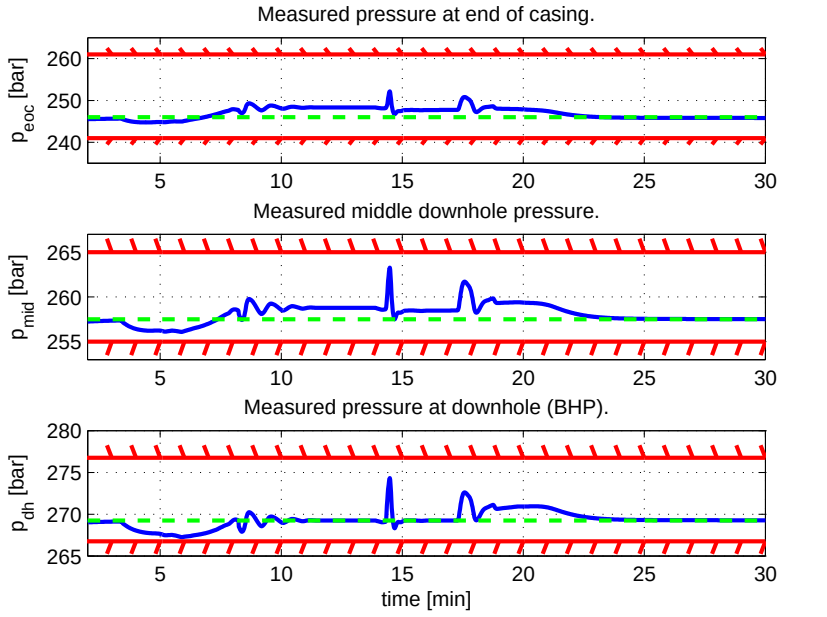

Figure 36: Pressure readings, constraints (Pore and Frac) and set point for all three down hole pressures during connection with back pressure pump.

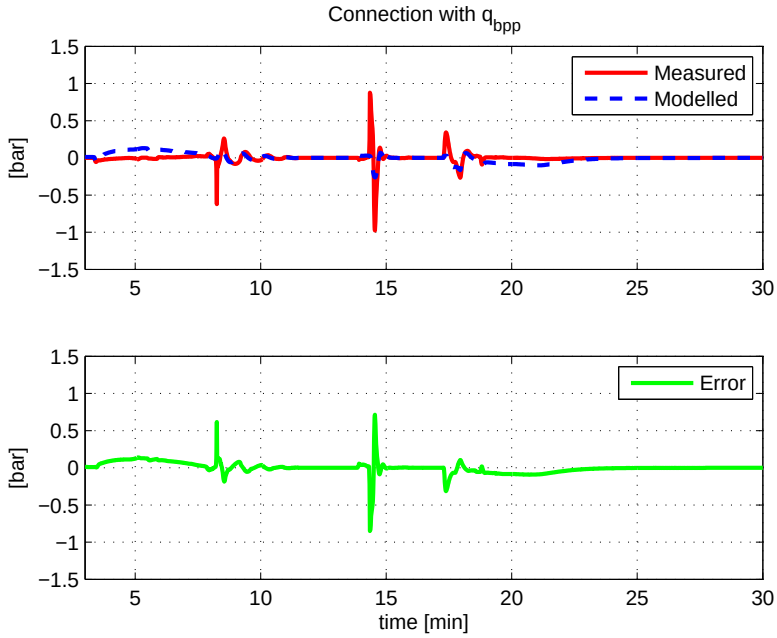

Figure 37: Comparison of differentiated predicted BHP (blue) vs. measured (red) for the connection scenario with back pressure pump. The model error (green) is not very flat. The model does not predict the un-modelled disturbance caused by gel breaking which causes the maximum error.

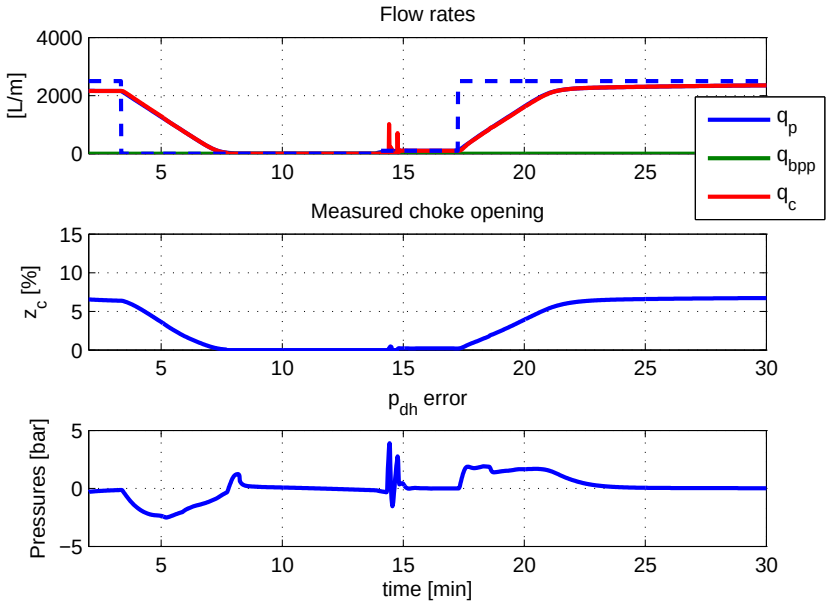

Figure 38: Pumps, choke and BHP error during connection without the use of the back pressure pump. The BHP set point is 269.25 bar. The BHP error is within 4 bar.

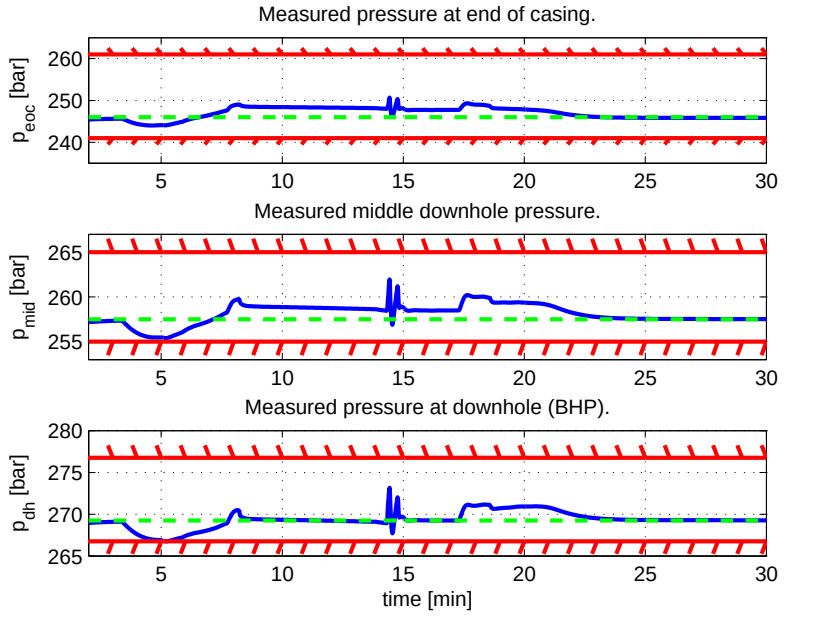

Figure 39: Pressure readings, constraints (Pore and Frac) and set point for all three down hole pressures during connection without back pressure pump.

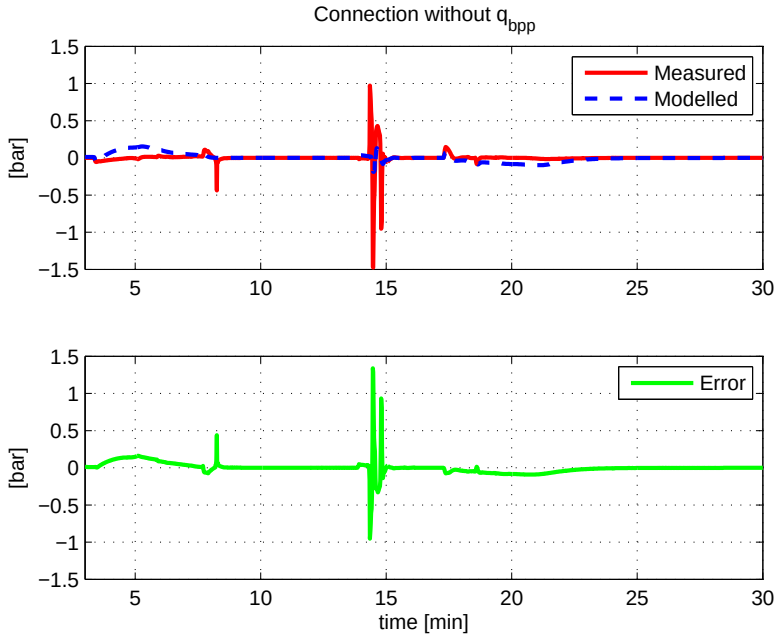

Figure 40: Comparison of differentiated predicted BHP (blue) vs. measured (red) for the connection scenario without back pressure pump. The model error (green) is not very flat. The model does not predict the un-modelled disturbance caused by gel breaking which causes the maximum error.

5.3.3 Tripping

Tripping is the process of pulling the entire drill string out and back in. That is, tripping in and tripping out. A round trip if you will. This causes surge and swab effects resulting in DHP changes.

Since the option of setting the drill string velocity is not available in the provided WeMod example, a modification has been added. This modification allows a crude simulation of the resulting tripping pressure from moving the drillstring. The deduction can be found in Appendix C.

In the following tripping scenario the drill string is first pulled out a short distance and then inserted back in. The drill string velocity is included as an Mvr. All Mvr's, Cvr's and Dvr are listed in Table 8.

Table 8: Manipulated and controlled variables for the tripping scenario.

Mvr	Cvr	Dvr
z_c	p_{eoc}	q_p
q_p	p_{mid}	
v_d	p_{dh}	
	p_{diff}	

A figure representing the tripping induced pressure together with the MD and v_d can be found in the Figures Appendix D Figure 65.

Figure 42 and 41 show the results from the tripping simulation. The BHP error is within 1.4 bars, all the DHP's constraints are respected, the choke usage is smooth and the pump usage is low. This is all good. Figure 43 show a "flat" model error with spikes wherever the drillstring accelerates. The model leaves something to be desired in regards to the model of the tripping induced pressure. The simulation of the tripping pressure has a very dominant acceleration term[46] which is hard to capture using a linear model, a step response model that is. The pressure spike due to acceleration is only handled when v_d is approaching its set Iv. When the Iv for v_d is changed, the initial pressure spike from acceleration is not handled, which is a significant weakness. To limit this, a maximum accelaration was set to 0.6 m/min/s for the drillstring. Specifically, the max./min. rate of change the Mvr v_d was set to ± 0.6 m/min/s in SEPTIC.

The tripping induced disturbance is handled. All constraints are respected and the BHP error is low.

[46]The deduction of this pressure can be found in Appendix C.

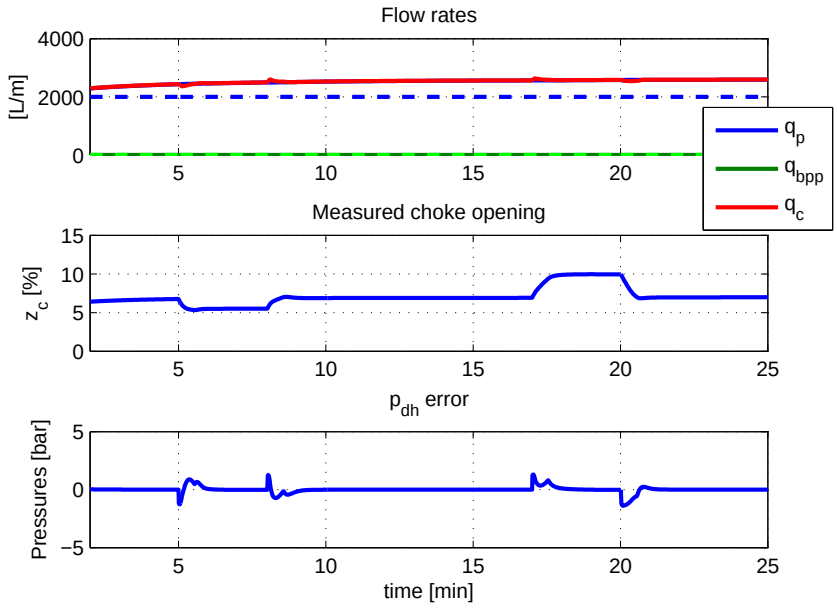

Figure 41: Pumps, choke and BHP error during tripping. Set point is 269.25 bar for the BHP. The BHP error is within 1.4 bar. The ideal value set points for the pumps are also plotted in their respective color (dashed). The ideal value for q_p has a low priority in this simulation and is consequently not reached. The back pressure pump is not used and is only plotted for continuity.

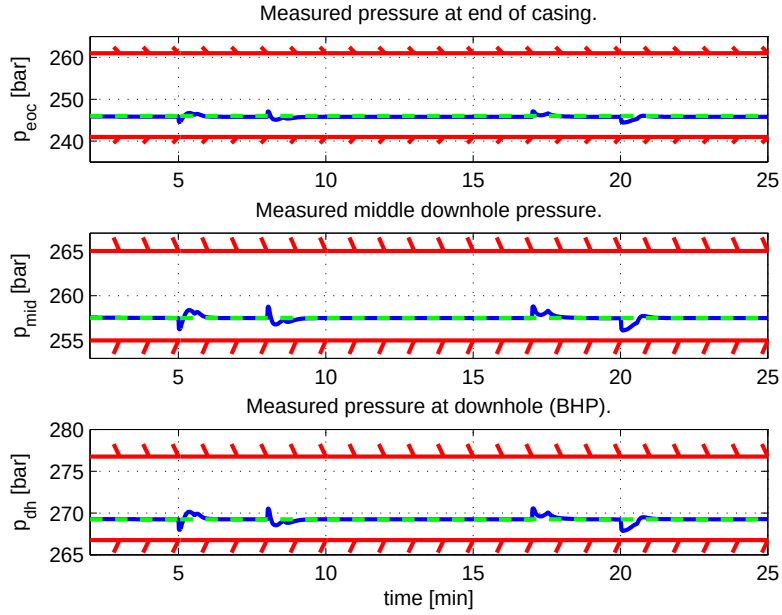

Figure 42: Pressure readings, constraints (Pore and Frac) and set point for all three down hole pressures.

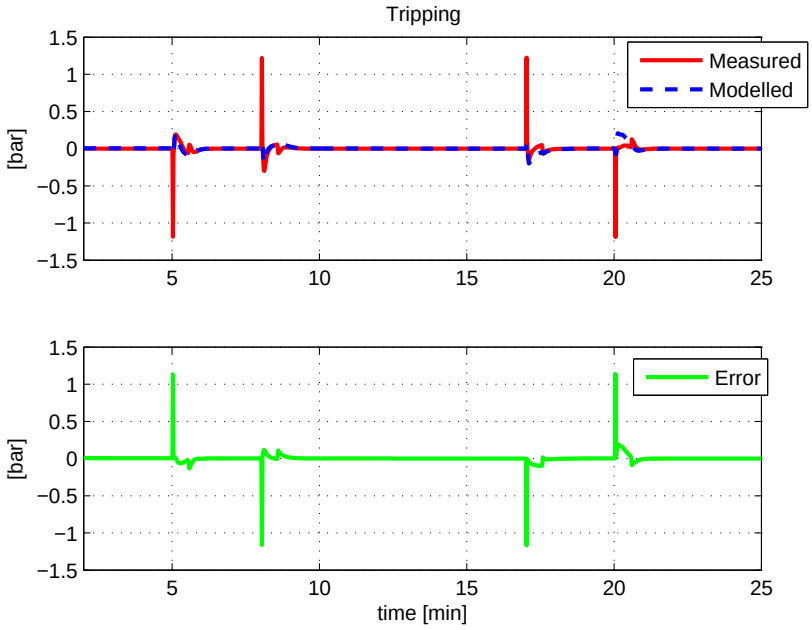

Figure 43: Comparison of differentiated predicted BHP (blue) vs. measured (red) for the tripping scenario. The model error (green) is flat with spikes wherever the drillstring accelerates.

One specific aspect of the tripping pressure that would be desirable to model in the simulator, is the fact that its influence differs throughout the well, with the greatest impact at the BHP. This is not included in the deduction in Appendix C which is the tripping pressure simulator used. Such an improvement would demand more of the pump usage to control several DHP's, since the disturbance from tripping would affect them differently.

The chosen ideal resting value for the mud pump was given a low priority and is not reached. Setting this priority high, would demand a compromise wrt. controlling more than one DHP. If the BHP was to be the only Cvr[47] on the other hand, the process would have a positive degree of freedom of 2, but one of them is already needed to reach the set points for v_d. The one remaing DOF could be used to balance the choke and pump to reach the ideal resting value for one of them.

5.3.4 Power Loss

In the case of a power loss, where all flow is lost, the choke must close quickly to minimize the reduction in the DHP. Without flow the viscous pressure is lost. Pressure resulting from mud weight is still present. When shutting the choke valve completely, the system is closed from choke valve to the NRV at the end of the drill string. It is possible to trap pressure within the annulus, as to maintain the DHP, if the valve is closed quickly. On the other hand, it is

[47] This would leave 3 Mvr's, 1 Cvr and 0 Dvr. Giving a positive DOF.

also possible to close to choke too fast, resulting in an unwanted pressure increase in the DHP.

The MPC tuning for this scenario is unique. It is assumed that a power loss is fairly easy to detect, and hence, the MPC can switch to the appropriate step response models and tuning parameters which are tuned for a power loss scenario, as is the case here.

Since power to the main mud pump is lost, it is no longer possible to control p_{diff}. The remaining Cvr's, Mvr and Dvr's are listed in Table 9.

Table 9: Manipulated, controlled and disturbance variables for the power loss scenario.

Mvr	Cvr	Dvr
z_c	p_{eoc}	q_p
	p_{mid}	q_{bpp}
	p_{dh}	

After the power loss has been detected, the procedure in Algorithm 7 is implemented. The ideal value set-point for the choke is set to 0 and its priority is placed second only to the DHP constraints. The application allows the choke to operate when it is nearly closed. This is avoided by redefining an input of less than 0.06 % as 0.

```
z_c.Iv=0;
z_c.IvPri=2;
while true do
    if z_c.input ≤ 0.06 then
        z_c.input=0;
    end
end
```

Algorithm 7: Power loss procedure

The results shown in Figure 45 and 51 indicates that the well is closed in time to trap a certain amount of pressure. After all flow is lost and the choke is completely closed, the pressure is decreasing at a considerable rate. The regulator cannot do any more at this point, since the flow is lost. The decrease in pressure can be caused by an increasing temperature[48]. Since there is no circulation, cool mud is not supplied and the stationary mud will be heated by the temperature of the earth at the specific depth[49]. The rate of which the pressure keeps decreasing will cause the pore pressure constraint for BHP, and p_{mid} to be broken within ten minutes.

[48]Density is connected to temperature. A change in density for a fluid in an enclosed environment will be reflected in the pressure.

[49]A normal geothermal gradient can be taken as approx. $25\frac{^\circ C}{km}$

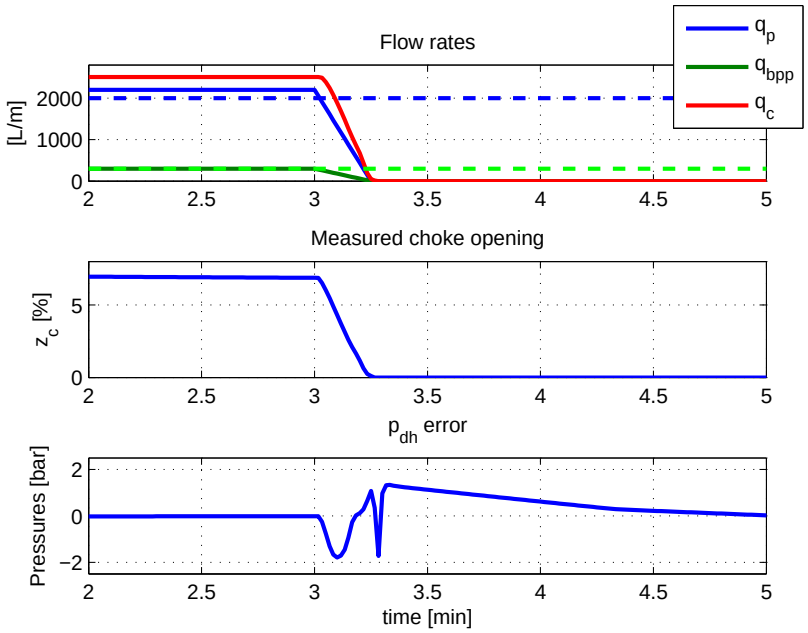

Figure 44: Pumps, choke and BHP error during power loss. Set point is 269.25 bar for the BHP. The BHP error is within 1.8 bar. Both pumps lose all their flow over 15 seconds. If the choke input is detected to be below 0.06%, the choke input is changed to 0. After the choke is closed completely, the BHP is decreasing at a considerable rate.

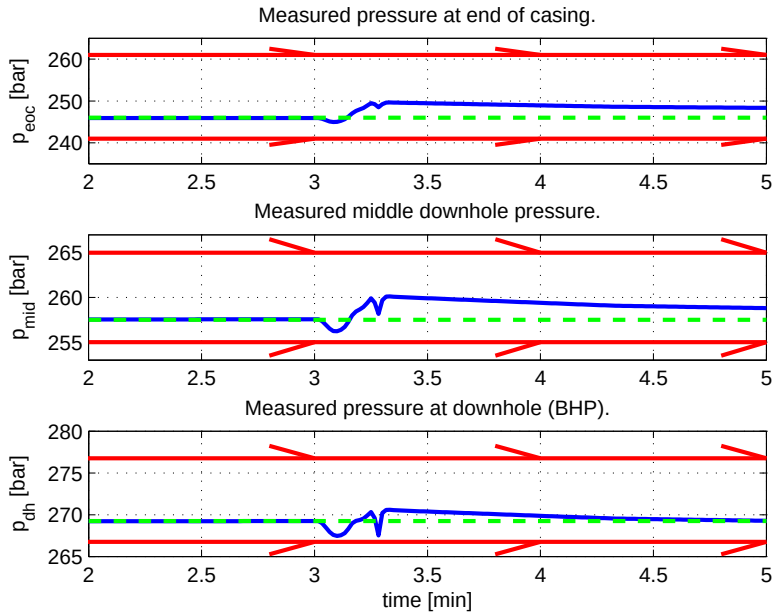

Figure 45: Pressure readings, constraints (Pore and Frac) and set point for all three down hole pressures.

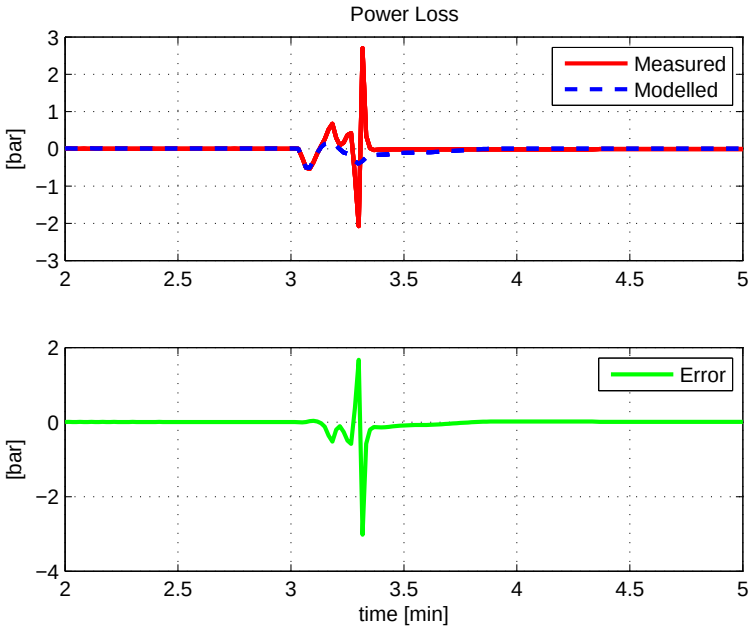

Figure 46: Comparison of differentiated predicted BHP (blue) vs. measured (red) for the power loss scenario. The model error (green) is high when the choke nearly closed.

Figure 46 shows that the model struggles when the choke is nearly closed and the flow is fading out. The model error is large, which can be caused by the fact that the choke closes and lets pressure build up, in a different manner than the step response models helps predict.

At the end of the simulation, the error is within 1.8 bars.

5.3.5 Reference Tracking

This simulation is aimed at replicating the result of the PI regulated reference tracking results in [Breyholtz, 2008] and further compare to linear MPC. Breyholtz used a PI-controller for comparison to his non-linear MPC (NMPC). Breyholtz's NMPC tracked every reference well, while his PI-controller had a small overshoot which increased with increasing pressure set point.

The reference for the BHP starts off at 270 bar and takes a 10 bar step every 500 seconds until it reaches 320 bar. The same steps are followed back down again to 270 bar. The main mud pump is set to run at 2500 l/min.

This PI-controller is based on eq. 58 from Appendix B with $K_p = -0.05$ and $K_i = -0.003$. The gains were chosen based on trial and error in the pressure range of 320 bar, which is the highest pressure in the reference tracking scenario. Training the PI-controller for the range with the fastest dynamics results in slower transients for lower pressures, but maximizes the performance in the most difficult high pressure range. Doing the opposite would lead to faster transients at the lower pressures, but poor performance at higher pressures.

When tuning the MPC, the same applies as for the PI-regulator in terms of pressure ranges. Therefore, the models for the MPC were made using step responses in the range of 320 bar. Furthermore, the MPC was tuned with regards to reference tracking with focus on parameters such as weighting of choke usage and set point deviance penalty. Mvr constraints were upheld, and Cvr constraints were removed. The remaining Mvr and Cvr is listed in Table 10.

Table 10: Manipulated and controlled variables for the reference tracking scenario.

Mvr	Cvr
z_c	p_{dh}

When comparing the results of the MPC reference tracking to that of the PI-regulator in Figure 47, they are fairly equal. Both follow the trajectory for the BHP well, with no overshoot. One very important difference is the choke usage. MPC achieved good tracking with less aggressive use of the choke.

When comparing *these* results from Figure 47 from this scenario for the MPC to that of the NMPC in [Breyholtz, 2008] with the same scenario, the linear MPC does not fade in comparison to the more complex NMPC. However, it is clear that only the NMPC in [Breyholtz, 2008] is invariant to the pressure range. Breyholtz did not include plots of the resulting choke flow.

Figure 48 shows that the model used in the MPC is a poor fit for the lower pressures. This is especially clear since the error spikes can be characterized as curves, rather than spikes. For the higher pressures on the other hand, the model error is very "flat".

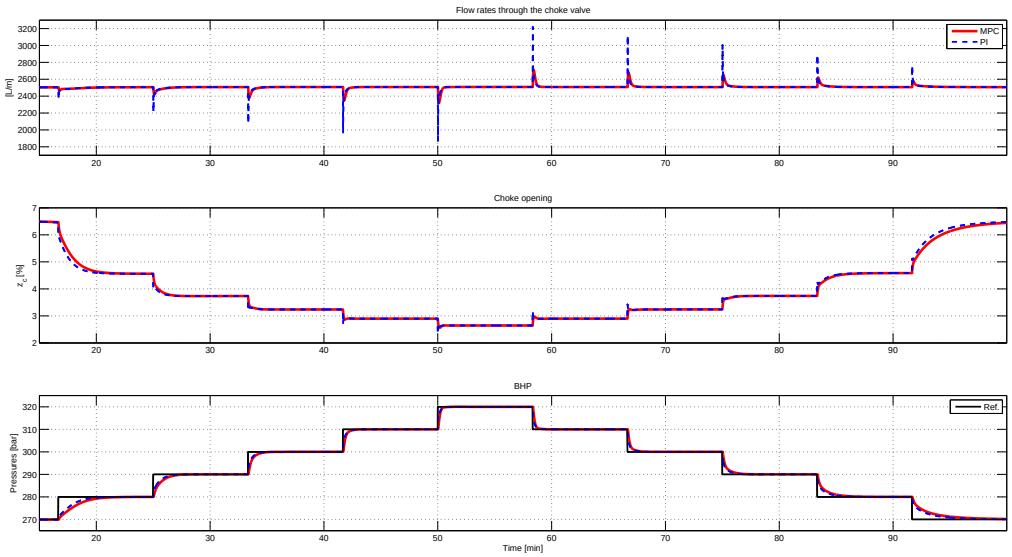

Figure 47: Comparison of MPC (red) and PI (blue dash). The perfomance in regards of reference tracking (bottom, black) is close to identical. However, the PI controller allows small spikes in the choke position which causes large unwanted spikes on the choke flow. The MPC regulator does not induce these spikes since the choke usage is weighted.

The results show that the performance of *this* PI-controller used in Figure 47 has smoother transients with nearly no overshoot at the cost of more aggressive use of the choke valve when compared to the results of PI-control in [Breyholtz, 2008].

The PI-controller can be greatly improved by implementing gain scheduling, as in [Breyholtz, 2007] or [Godhavn, 2009]. In a similar fashion, the models in the MPC application can be time varying. This will be illustrated in the following simulation. The model gain from BHP to choke will vary in the simplest manner. If the choke opening is larger than 3.5%, the model gain is scaled by a factor of 0.2. This allows a faster response when the BHP is far from the high pressure range where the step response models were created.

Figure 49 compares the MPC with and without varying gain. It shows that it is possible to

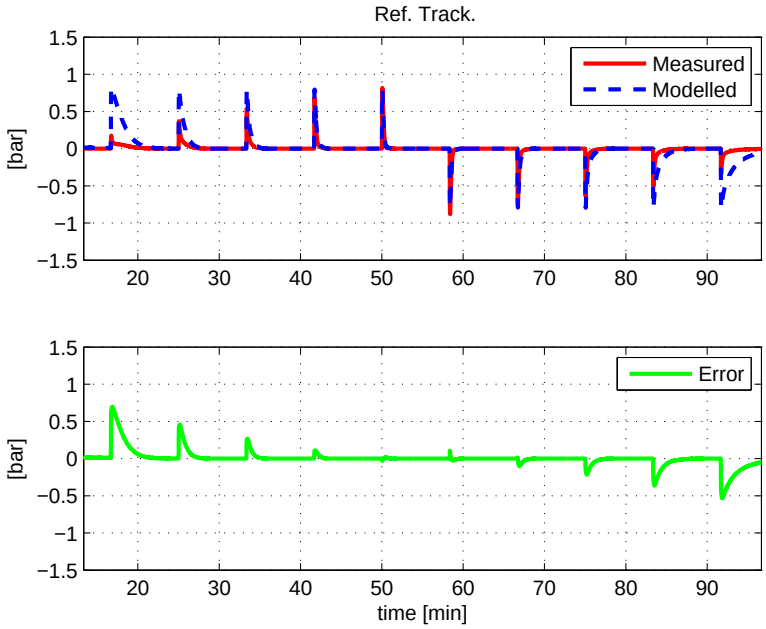

Figure 48: Comparison of differentiated predicted BHP (blue) vs. measured (red) for the ref. track. scenario with a constant model. The model error (green) is significantly larger in the lower pressure area. The model was created from a step response in the higher area.

manipulate the models during control. It should also be possible to implement time-varying model gains in such a way that the current pressure range can influence the model gain at all times, much like gain scheduling in PI control.

When comparing the model errors in Figure 50 and 48 it can be seen that the model error is significantly more ”flat” and the spikes are sharper. The predicted change in BHP is more accurate in the lower pressure area when a varying model is used.

By using this varying model, a discontinuity is introduced. This technically renders the MPC a NMPC, but a simple one at that.

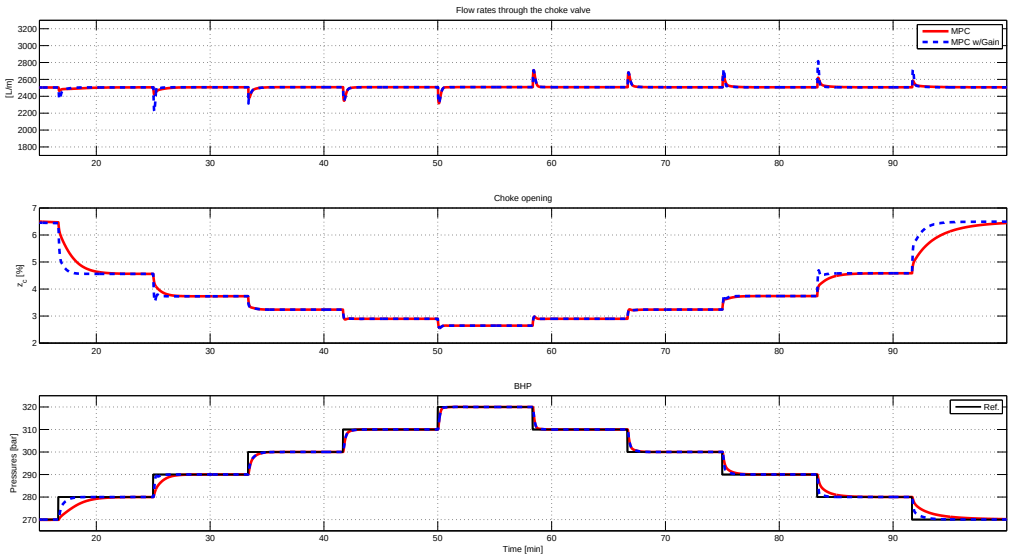

Figure 49: Comparison of MPC (red) and MPC with varying model gain (blue dash). The perfomance in regards of reference tracking (bottom, black) is greatly improved for the lower pressures. The high pressures are identical. The spikes on the choke flow are increased, but still low. The model gain is scaled with a factor of 0.2 when the choke opening is larger than 3.5%.

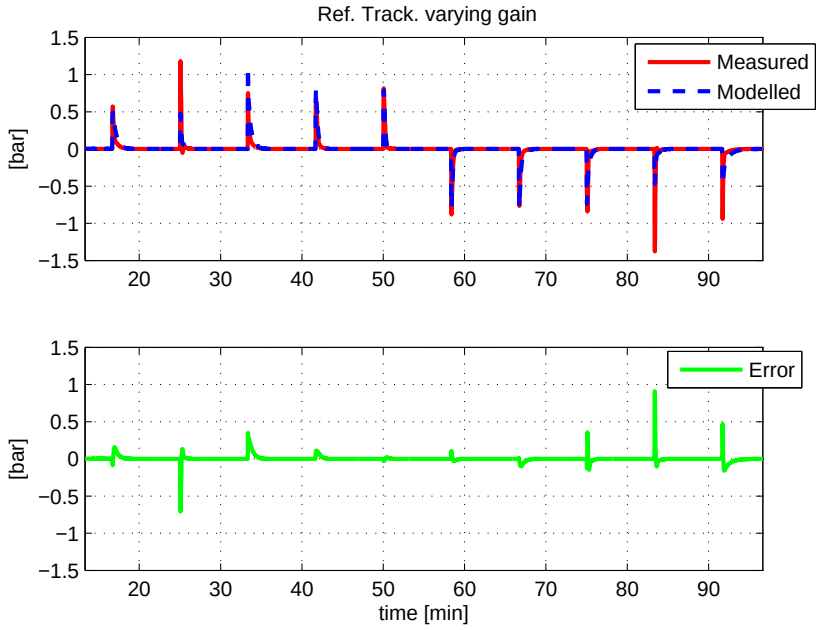

Figure 50: Comparison of differentiated predicted BHP (blue) vs. measured (red) for the ref. track. scenario with a varying model. The model error (green) is significantly improved.

6 Discussion

The results from Section 5 shows some of the potential of (L)MPC for MPD. By tuning the large number of MPC parameters as in Section 4, the BHP error is kept low and the usage of Mvr's is weighted[50]. By including more than one DHP and the main mud pump in the MPC, the level of automation is increased. This does however set demands to the resolution of the pump. The mud pump needs to be precise in a range of around 50 l/min. All Cvr constraints were respected.

All the simulation cases were executed by the push of a button. For the drilling case, the desired MD was set and the controller handled the rest. Likewise, for the connection case the mud pump was shut off for a specified time period to allow additional lengths of pipe to be connected. After connection, the pump was ramped back up. For the tripping case, the drillstring velocity set point was the only user input. The power loss simulations suggest that the controller is able to close the choke properly by it self in the case of a power failure for the pumps. This gives an indication of the level of automation for the MPC used.

During normal drilling it can be an advantage to include the main mud pump as an Mvr. This is where the linear MPC can take advantage of adjusting the flow to keep control of more than one DHP as the well is drilled longer. In Section 5.3.1 the minimum flow limit was respected. At this point it could be time to circulate in a lighter mud so the flow can be increased again. This would in essence be manipulation of the density in eq. (48). Such a manipulation has a much slower effect than manipulating the flow, since the lighter mud has to be circulated through the system for the simple density parameter in (48) to be truly changed. Mud mixing is not included in the MPC.

The connection case was the most difficult to tune, with the highest BHP error. The back pressure pump and choke needed to be coordinated when the mud pump was shut down. Since the simulation without back pressure pump gave a lower BHP error, it can be expected that the coordination was poor. More effort could be put into some form of mid-range controller to coordinate the choke and back pressure pump better. The largest BHP error was caused by gel breaking on ramp up. This effect was not part of the model in the MPC, meaning it is an unmeasured disturbance. The procedure used to handle this improved the BHP error, but more effort could be put in here. It should be possible to predict the effect of gelling and include it in a NMPC scheme. For (L)MPC it is probably not that easy to include gelling. When comparing these results from the connection case to [Breyholtz, 2008] and [Breyholtz, 2007], it should be noted that those simulations does not seem to include gelling.

In the tripping simulations, the resulting tripping pressure was simulated using the deriva-

[50]The SEPTIC, OPC and Matlab files used in this thesis is not included. Given the tuning elaboration in Section 4, the software introduction in Section 5 and well description in Section 5.2, including every file was considered too much and not necessary.

tion in Appendix C. This was constructed to resemble a true effect of tripping, but also to challenge the MPC. The MPC handled this modelled disturbance with a BHP error of 1.4 bars, which is not bad.

Section 5.3.5 showed a further comparison of the current MPD regulator schemes, PI, (L)MPC and NMPC to follow a reference trajectory for the BHP. This was continued from the work done in [Breyholtz, 2008]. The comparison showed that (L)MPC does not fade in comparison to the more complex NMPC in this scenario. In a comparison, the simpler controller should always be preferred. This is the case in this one specific scenario. This does not state that (L)MPC is a better choice than NMPC in all cases. This section also showed the clearest example of model errors by comparing Figures 50 and 48, where simple gain scheduling improved the model error considerably.

PI control was considered in Section 4.3 for controlling both choke and pump to control two DHP's. (L)MPC proved superior in this respect and worth its added complexity. The PI controller used had only 4 parameters. PID control can be expanded to be much more advanced, with possibility for decoupling, feed forward etc. A comparison of a more advanced PI controller could be of interest, as to see if the MPC is actually not that complex compared to a more worthy comparison.

The (L)MPC was able to control more than one DHP when including p_{diff} (the difference between two DHP's) as a Cvr. This was not achieved without it. The reason why p_{diff} makes it possible to control more than one DHP was discussed in Section 4.3. All the DHPs measured by WDP can be included as Cvr's. By using the priority hierarchy as discussed in Section 3.3, the constraints of all the DHPs can be prioritized before the set-points and ideal values. This way, all the DHPs are monitored and ensured to be within their constraints, while two DHPs set-points can be prioritized after the constraints. Only two DHP set points can be controlled with the Mvr's main mud pump and choke.

With reference to the Problem Description, an MPC solution has been developed to control three DHP's with pore and fracture pressures as constraints. By utilizing the main mud pump as an Mvr, it is possible to manipulate the downhole gradient, and consequently more than one DHP, while using *linear* MPC as shown in the simulations, which corresponds to the theory in Subsection 4.3. To attain the DHPs, WDP is desirable. With several downhole sensors the pressure at specific depths can be calculated using the nearest pressure sensor and e.g. the calculations and estimation presented in Subsection 2.3. A measure of how exact the calculated pressure at the chosen depth is, depends on the distance to the nearest pressure sensor and the friction model used. By using linear MPC, there can be enough time to try and solve the QP at each iteration several times per second. This allows much flexibility in using a priority hierarchy as presented in Subsection 3.3. Modelling, weighting, filtering and input blocking for the MPC problem can be done as elaborated in Section 3 and 4. By weighting the choke usage and filtering the Cvr error, wear and tear

can be expected to decrease when compared to using PI control. An example was shown in Figure 47 where MPC choke usage was compared to PI control in a simple simulation. The cases; Normal drilling, Connection, Tripping and Power loss where simulated where the MPC automated the use of both the main mud pump and back pressure pump, as well as the choke, to control the DHP's. This shows how MIMO control, such as MPC, offers to automate much more than simple SISO PID control. That is, not only the BHP by means of the choke. The well used in the simulations, as described in Subsection 5.2, was short and consequently the ability to manipulate the downhole gradient was small, but possible as shown.

As mentioned in Section 2.2, a choke pressure controller can be used as an inner controller. The reference for such a choke pressure would then be calculated from the the desired BHP and a measure for MW and friction, by e.g. using eq. (6). Instead of using the choke (position) as an Mvr in the MPC, the choke pressure reference could take its place. This would to some degree rely on the accuracy of eq. (6), or the step-response models from choke pressure to DHP's. The advantage of not including such an advanced inner controller, is that SEPTIC can weight the choke usage more directly. The non-linear characteristics of the choke can be handled by SEPTIC, as shown in Section 5.3.5.

7 Conclusions and Future Work

- Linear MPC can control the DHP gradient by controlling the difference between two DHP's by means of the main mud pump.
- Gel breaking in the connection case caused the greatest BHP error.
- MPC is able to automate pumps and choke and increases the level of automation.
- WDP and the calculations shown can supply pressure readings of several DHP's.
- The constraints of all the DHPs can be prioritized before the set-points of the two chosen DHPs for set-point control.
- Linear MPC was able to keep the BHP error within $\pm$ 5 bars for all given cases.
- Automatic control of pumps does not necessarily improve the BHP error.

For future work, it can be recommended to test the linear MPC on a longer well with the possibility of drilling more than 10 meters to explore the benefits of including the pore and fracture pressures as moving constraints for the BHP and how the calculations of the pressures at static points of depth in the open well bore, e.g. the EOC pressure, works when drilling a longer distance.

Model scheduling could be of interest. Gain scheduled PI control is known to offer large improvements to a simple PI controller. The simplest form of model scheduling was presented in Subsection 5.3.5, and proved a large improvement for the MPC. Some work could be put into developing a varying model gain, i.e. dependant on the choke pressure, for the step response models from choke to DHP's.

References

Trygve Birkeland. Automated well control using mpd approach. Master thesis, UiS, 2009.

Øyvind Breyholtz. Linear model predictive control during drilling operations. Student Project, 2007.

Øyvind Breyholtz. Nonlinear model predictive pressure control during drilling operations. Master thesis, NTNU, 2008.

Øyvind Breyholtz. *Managed Pressure Drilling: Improved Pressure Control through Model Predictive Control*. Ph.d. thesis, UiS, 2011.

Øyvind Breyholtz et al. Deep water drilling: Full pressure profile control in open hole section using model predictive control. 2009.

Øyvind Breyholtz et al. Managed pressure drilling: Using model predictive control during dual-gradient drilling. 2011.

Eric Cayeux. Wired pipe and closed loop control, workshop on automated drilling, stavanger, 2009.

Yunus A. Çengel and John M. Cimbala. *Fluid Mechanics Fundementals and Applications (2. edition)*. 2010. ISBN 978-007-128421-9.

Chi-Tsong Chen. *Linear System Theory and Design (3. edition)*. 2009. ISBN 978-0-19-539207-4.

Panos M. Pardalos Christodoulos A. Floudas. *Encyclopedia of Optimization (2. edition)*. 2009. ISBN 978-0-387-74759-0.

John Morten Godhavn. Control requirements for high-end automatic mpd operations. 2009.

John Morten Godhavn et al. Drilling seeking automatic control solutions. 2011.

Svein Olav Hauger. Lecture, ttk4135 optimization and control, 2012.

Lars Imsland. Introduction to model predictive control. Unpublished note, 2007.

Petros A. Ioannou and Jing Sun. *Robust Adaptive Control*. Tapir akademiske forlag, 2003.

International Research Institue of Stavanger IRIS. URL `http://www.iris.no`.

Glenn O. Kaasa. Lecture, tk17 system identification, 2012.

Glenn O. Kaasa et al. Simplified hydraulics model used for intelligent estimation of downhole pressure for a managed-pressure-drilling control system. 2012.

Ingar Landet et al. Modelling for mpd operations with experimental validation. 2012.

Jan Marian Maciejowski. *Predictive Control with Constraints*. 2002. ISBN 0-201-39823-0.

Norman S. Nise. *Control Systems Engineering (5. edition)*. 2008. ISBN 978-0-470-16997-1.

Jorge Nocedal and Stephen J. Wright. *Numerical Optimization (2. edition)*. 2006. ISBN 978-0387-30303-1.

National Oilwell Varco NOV, February 2013. URL `http://www.nov.com/intelliserv/`.

Gerhard Nygård et al. *IRISDrillForMatlab Win7 User's Guide*.

sir. Isaac Newton. *Philosophiæ Naturalis Principia Mathematica*. 1687. URL `http://www.ntnu.no/ub/spesialsamlingene/ebok/02a019654.html`.

Pål Skalle. *Pressure Control During Oil Well Drilling (3. edition)*. 2012. ISBN 978-87-403-0252-3.

Stig Strand et al. Mpc in statoil - advantages with in-house technology. 2003.

Varodom Toochinda, February 2013. URL `http://www.controlsystemslab.com/doc/b4/pid.pdf`.

Wikipedia, April 2013a. URL `http://en.wikipedia.org/wiki/OLE_for_process_control`.

Wikipedia, April 2013b. URL `http://en.wikipedia.org/wiki/Trapezoidal_rule`.

Jing Zhou et al. Adaptive observer for kick detection and switched control for bottomhole pressure regulation and kick attenuation during managed pressure drilling. 2010.

A Example of SEPTIC .mdf file

```
//      File=  models//p_dh_m_q_p_m.mdf
       Text1=  ""
       Text2=  ""
       Atext=  "Wed Mar 13 12:58:46 2013 Generert som last-step modell av Septic "
       Nsecs=  1
       Amodl=  95
 -5.7515e-006   0.00095356    0.0031707    0.0054929    0.0070371
    0.0078156    0.0081927    0.0084582    0.0087417    0.0090612
    0.0093863    0.0096824      0.00993     0.010126     0.010278
     0.010396     0.010488      0.01056     0.010618     0.010665
     0.010701      0.01073     0.010752     0.010768      0.01078
     0.010789     0.010794     0.010797     0.010799     0.010799
     0.010797     0.010795     0.010792     0.010788     0.010784
      0.01078     0.010775      0.01077     0.010764     0.010759
     0.010753     0.010748     0.010742     0.010736      0.01073
     0.010724     0.010718     0.010713     0.010707     0.010701
     0.010695     0.010689     0.010683     0.010677     0.010672
     0.010666      0.01066     0.010654     0.010648     0.010643
     0.010637     0.010631     0.010625      0.01062     0.010614
     0.010608     0.010603     0.010597     0.010591     0.010586
      0.01058     0.010574     0.010569     0.010563     0.010558
     0.010552     0.010547     0.010541     0.010536      0.01053
     0.010525     0.010519     0.010514     0.010508     0.010503
     0.010498     0.010492     0.010487     0.010481     0.010476
     0.010471     0.010465      0.01046     0.010455      0.01045
```

B P,PI,PID Control

PID controllers are widely known and constructed in several ways. The following derivation is taken from [Toochinda, 2013].

A PID controller in parallel form is expressed as

$$u(t) = K_p e(t) + K_i \int_0^t e(\tau)d\tau + K_d \frac{d}{dt} e(t) \tag{57}$$

where $e(t)$ is the output error, i.e $e(t) = p_{dh}^{ref} - p_{dh}(t)$

Its Laplace transform

$$G(s) = K_p + \frac{K_i}{s} + K_d s$$

The connection from parallel form to the more standard form used in Ziegler-Nichols is $K_p = K$, $K_d = KT_d$, $K_i = K/T_i$.

The z-transform of 57 is

$$u(z) = \frac{(K_p + K_i + K_d) + (-K_p - 2K_d)z^{-1} + K_d z^{-2}}{1 - z^{-1}} E(z)$$

which can be rewritten with $K_1 = K_p + K_i + K_d$, $K_2 = -K_p - 2K_d$, $K_3 = K_d$ as

$$U(z) - z^{-1}U(z) = (K_1 + K_2 z^{-1} + K_3 z^{-2})E(z)$$

and converted back to the very implementable difference equation

$$u(k) = u(k-1) + K_1 e(k) + K_2 e(k-1) + K_3 e(k-2) \tag{58}$$

The gains needs to be tuned. Raw tuning relies heavily on experience and knowledge of the system at hand. Some help can be found, for example, in the Ziegler-Nichols method, but as this method demands making the systems output oscillate it is often not recommended for physical systems were damage can be done. There are adaptive approaches, as well as gain scheduling, which can make a simple PID controller much more sophisticated.

Eq. 58 can act as a P,PI or a PID by choosing the gains in an appropriate manner.

When tuning eq. 58 there is often a trade off between noise rejection and robustness. That is, an aggressively tuned PID-controller will reject noise within a limited range of set points, but might not operate very well when the set point travels beyond said limits. A more cautiously tuned PID will have less noise rejection, but a wider range of set point to within it will perform evenly.

C Adding Tripping to the Simulator

Adding tripping induced pressure to the simulator
Since the option of setting the drill string velocity is not available in the WeMod example, a modification has been added with inspiration from eq. (5),(6) and [Breyholtz et al., 2011].

The resulting pressure from tripping can be found as the change in annulus volume as expressed in eq. (5), that is

$$\frac{V_a}{\beta_a}\frac{dp_c}{dt} = q + q_{bpp}(u_{bpp}) - q_c(p_c, z_c) - \dot{V}_a$$

The term of interest is that which can be subtracted from the choke pressure to account for tripping. That is

$$\int \frac{\beta_a}{V_a}\dot{V}_a \, dt \tag{59}$$

Manipulating the drill string velocity causes changes in the annulus volume when tripping. There is no drilling when tripping, so the annulus volume will only increase if the drill string is moved upwards. Likewise, the annulus volume will be at its smallest when the drill string is fully inserted at TD.

The change in annulus volume can then be expressed as

$$\dot{V}_a = v_d A_d \tag{60}$$

Where A_d is the cross sectional area formed by the outer diameter of the drill pipe.

As mentioned, the annulus volume will be at its smallest when the drill string is at TD (MD=TD). When the drill string is moved upwards, MD will decrease and the annulus volume will then increase.

$$V_a = TDA_a + (TD - MD)A_d \tag{61}$$

While the cross sectional area of the drill string is easily determined, and most likely constant since it its set from the choice of drill pipe, the same can not be said for the annulus A_a. Each time a new casing is inserted, the drill bit is tripped out and replaced by a smaller bit as to fit through the new casing. This means that the annulus cross sectional area decreases further down the well, and is in no way constant. Also, the annulus volume is not easily determined since casings are not necessarily placed throughout the well if it is not needed.

The purpose in this thesis of adding a tripping induced pressure to the WeMod simulator is to simulate the challenging dynamics it offers, not to create a valuable contribution to the simulator itself. Therefore, simplification will be done and simple dynamics added.

Specifically, since tripping is done one stand at a time, around 30m-100m, the change in the initially 2300m deep MD is between 1.3% and 4.3%. Therefore, the simplification of constant MD (MD=TD) for calculating the tripping pressure will be forced:

$$V_a = TDA_a \tag{62}$$

Furthermore, the cross sectional areas will be simplified to be equal, giving

$$\dot{V}_a = v_d A_a \tag{63}$$

Inserting (62) and (63) into eq. (59) consequently cancels out the cross sectional areas.

$$\int \frac{\beta_a}{TDA_a} v_d A_a \tag{64}$$

These simplifications leaves the following equation

$$\frac{\beta_a}{TD} \int v_d \, dt \tag{65}$$

Using the trapezoidal rule[Wikipedia, 2013b] and a time step of one second, the implementable tripping pressure can finally be formed as

$$\frac{\beta_a}{TD} \frac{v_d(k-1) + v_d(k)}{2} \, dt \tag{66}$$

where k is the increment and $dt = 1$ is the time step.

Eq. (66) does not offer any challenging dynamics as to offer any new insight to the performance of the regulator. Therefore, an additional acceleration term will be added, resulting in the implemented tripping pressure

$$trip = c_1 \frac{v_d(k-1) + v_d(k)}{2} + c_2 a_d(k) \tag{67}$$

Where a_d is the drill string acceleration, $c_1 = 10\frac{\beta_a}{TD}$ and $c_2 = 2.5c_1$. c_1 and c_2 are tuned to offer a considerable disturbance. Adding an acceleration term adds pressure spikes to the tripping pressure. Modelling the tripping pressure as an expression of velocity and acceleration was inspired by the controller model in [Breyholtz et al., 2011].

Since the change in choke pressure is not available for manipulation in the WeMod simulator, the tripping pressure is implemented by adding[51] the pressure resulting from eq. (67) to the BHP. From eq. (6) it can be seen that this is comparable to adding to the choke pressure. The same is done for the EOC pressure and p_{mid}. In this way, tripping induced pressure is included as a challenge to the regulator.

The tripping induced pressure will impact the three DHPs differently. This is not reflected in this simple modelling of the tripping pressure.

[51] The pressure is *added* since the drill string velocity v_d is chosen to be positive tripping into the well.

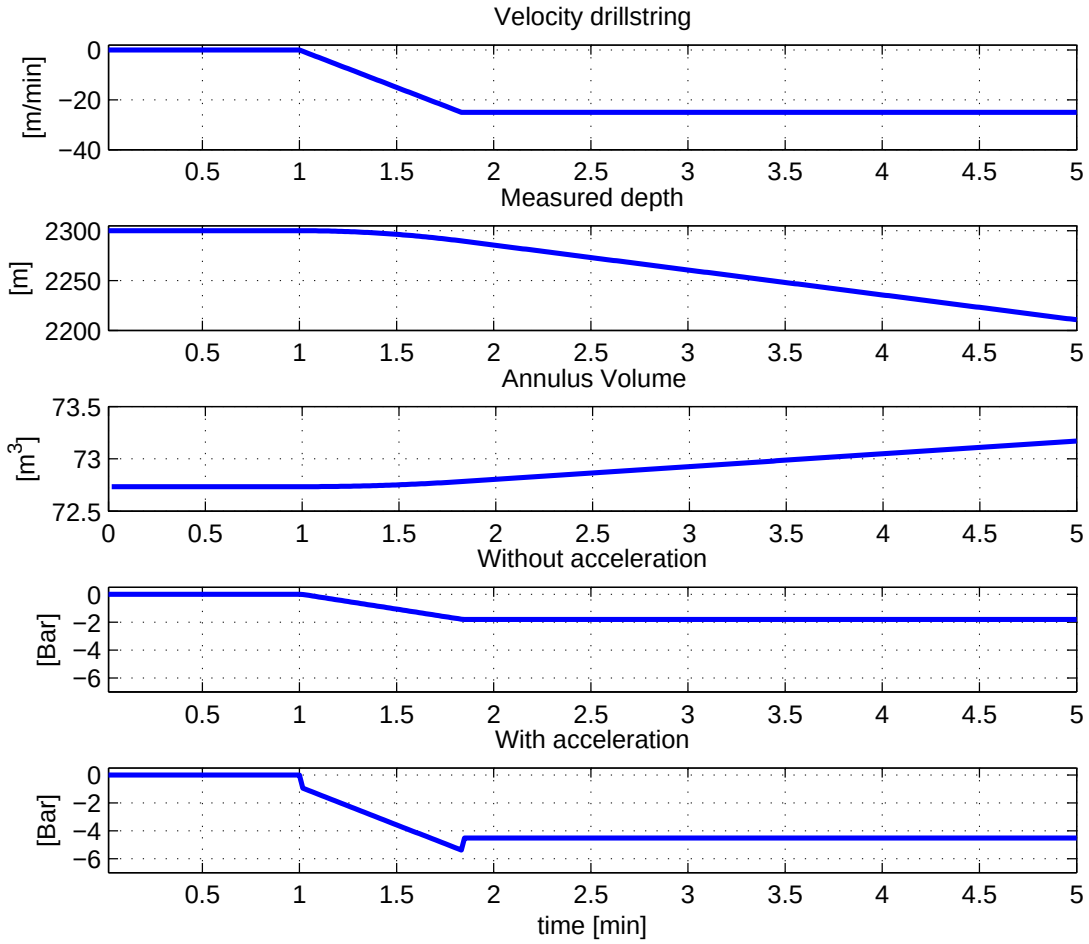

Figure 51: Illustration of the added tripping pressure eq. (67) (bottom). The drill string velocity (top) is ramped up, positive direction is into the well. Measured depth and annulus volume changes are also plotted. The alternative tripping pressure from eq. (66) is also plotted. It can be seen that eq. (67) offers a challenging disturbance, while eq. (66) does not.

D Figures

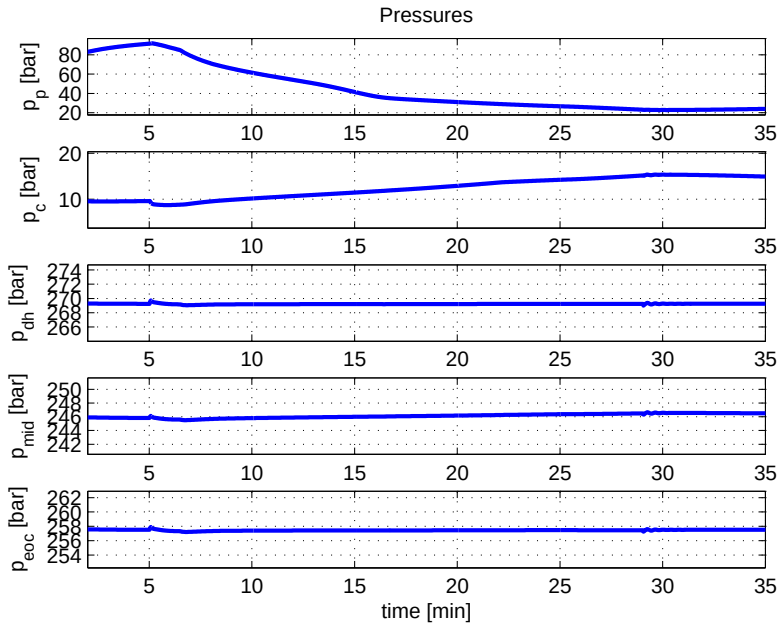

Figure 52: Pressure measurements during MIMO drilling in Section 5.3.1.

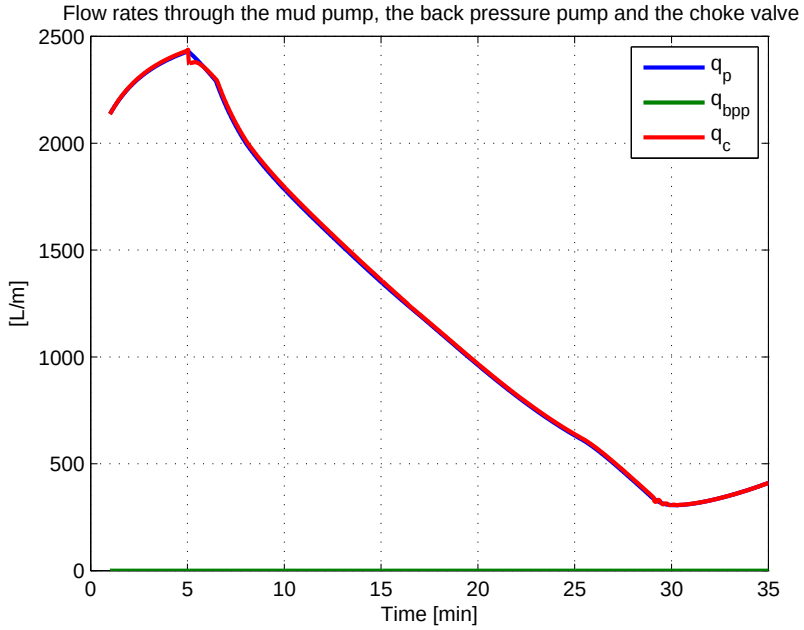

Figure 53: Flow measurements during MIMO drilling in Section 5.3.1.

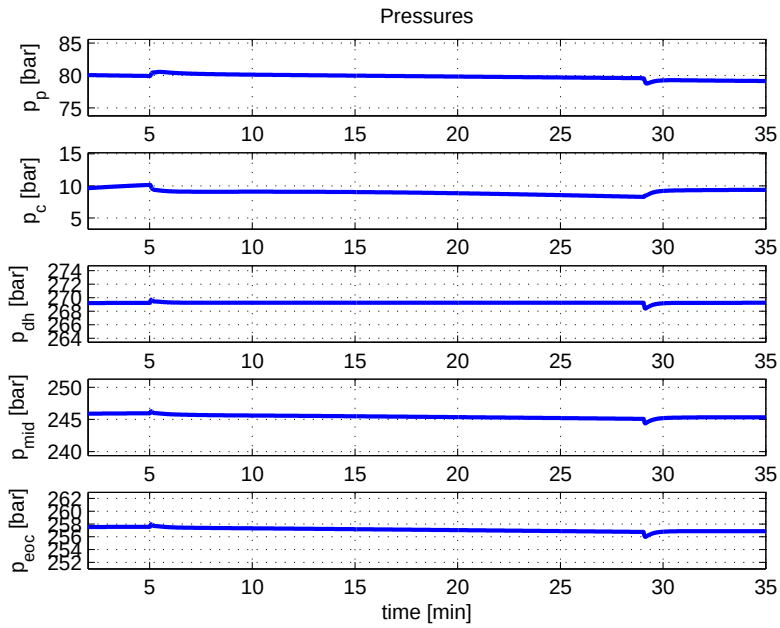

Figure 54: Pressure measurements during SIMO drilling in Section 5.3.1.

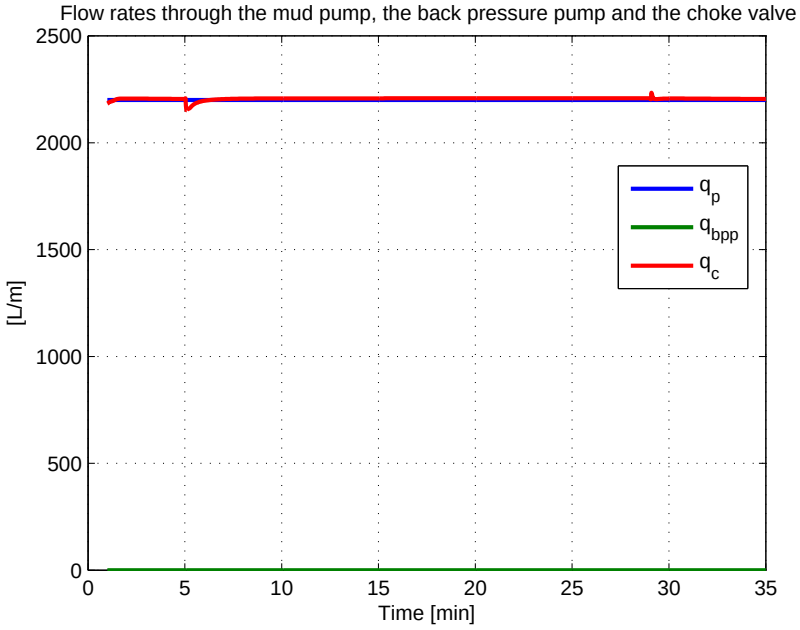

Figure 55: Flow measurements during SIMO drilling in Section 5.3.1.

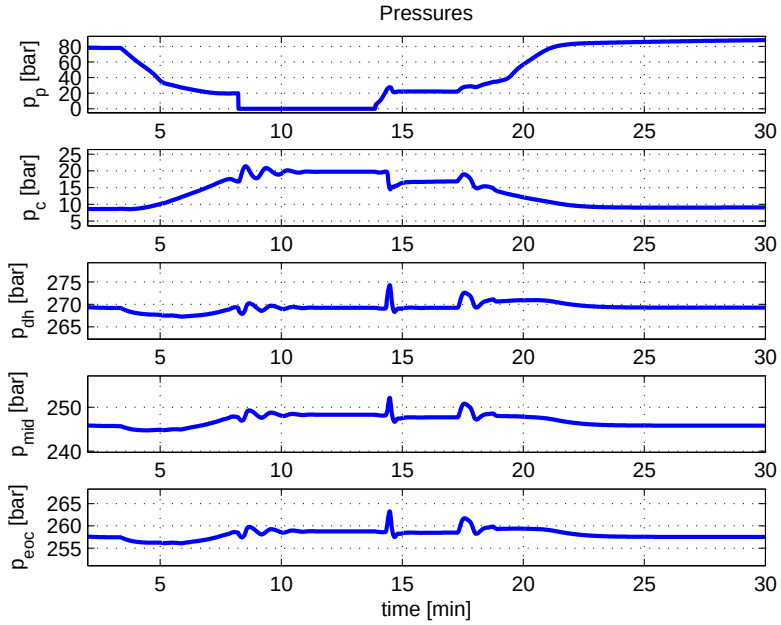

Figure 56: Pressure measurements during connection with use of back pressure pump in Section 5.3.2.

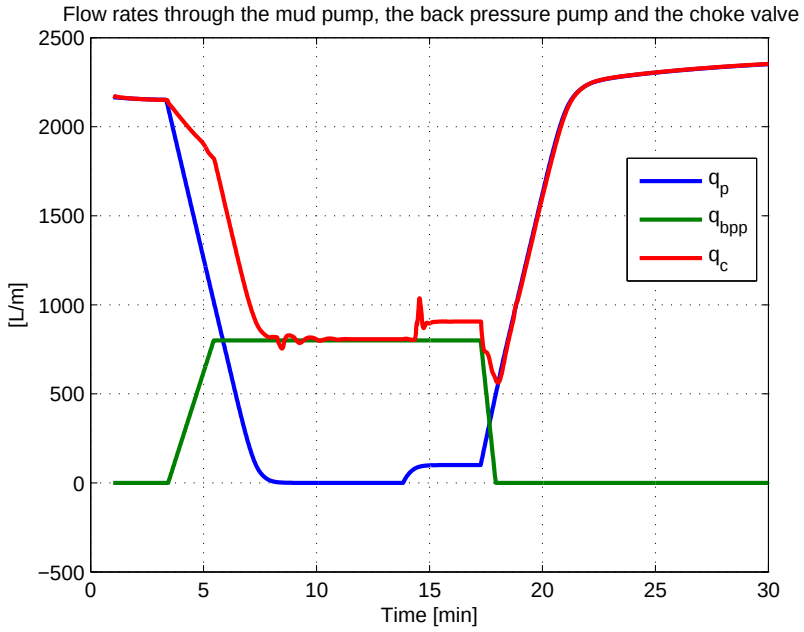

Figure 57: Flow measurements during connection with use of back pressure pump in Section 5.3.2.

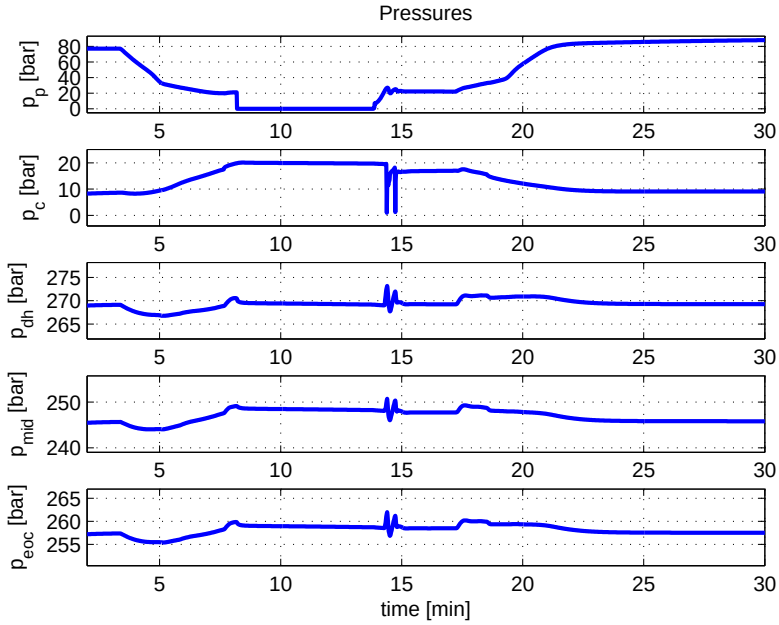

Figure 58: Pressure measurements during connection without use of back pressure pump in Section 5.3.2.

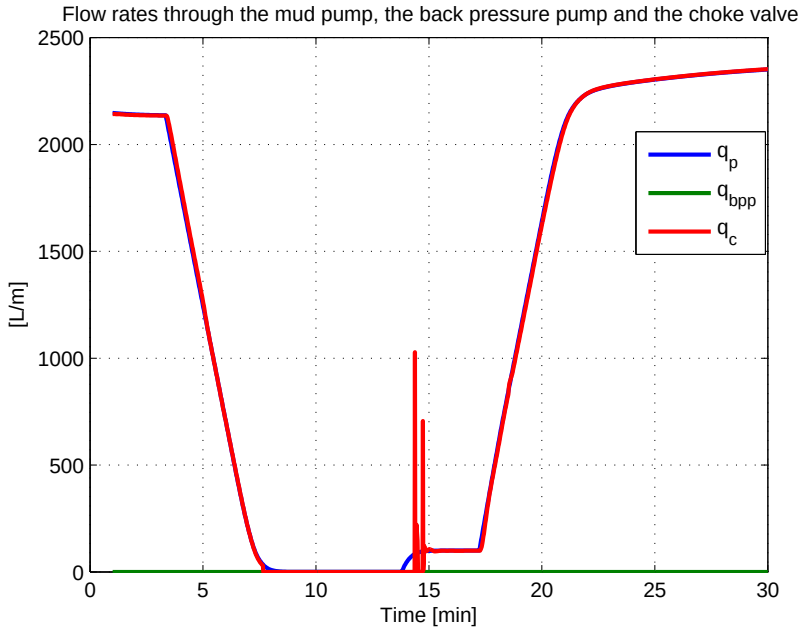

Figure 59: Flow measurements during connection without use of back pressure pump in Section 5.3.2.

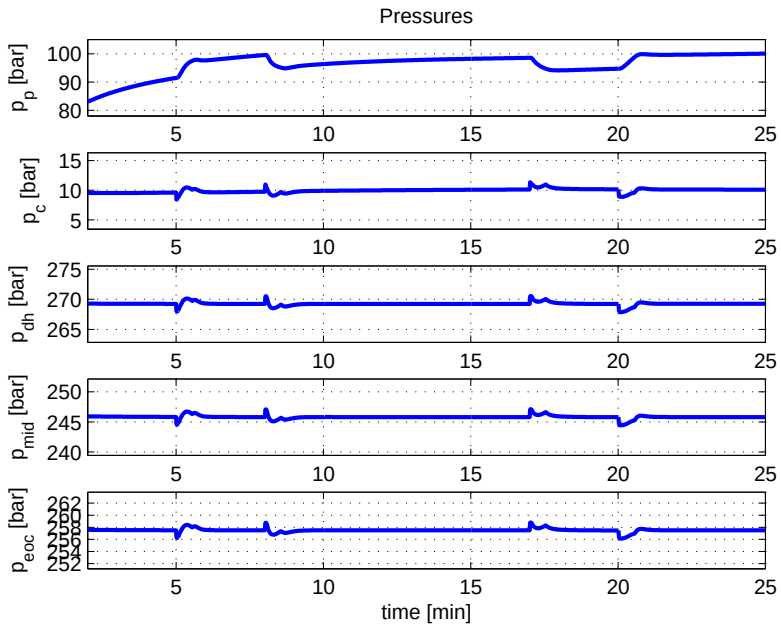

Figure 60: Pressure measurements during tripping in Section 5.3.3.

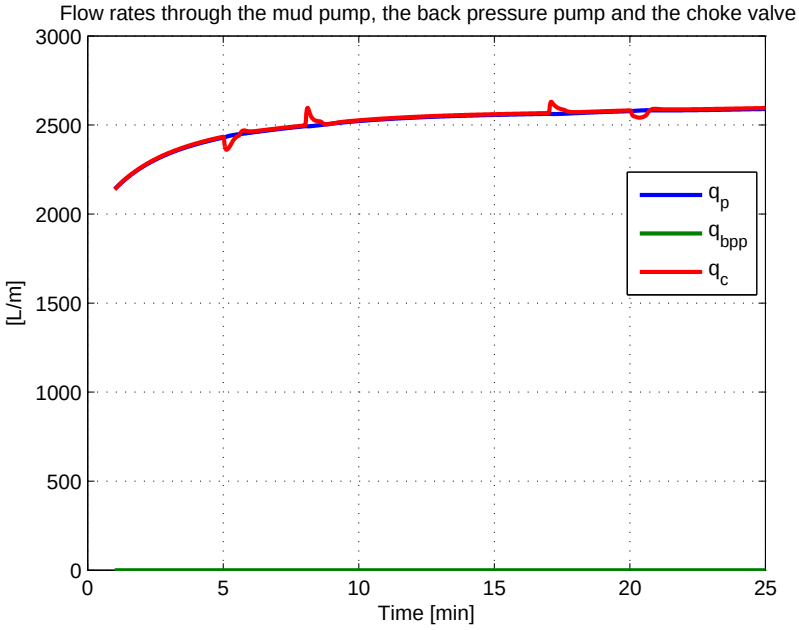

Figure 61: Flow measurements during tripping in Section 5.3.3.

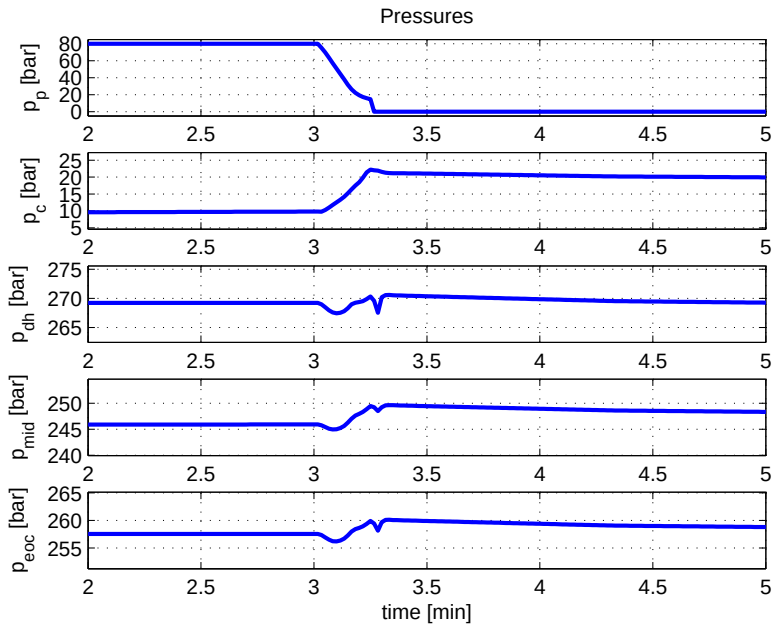

Figure 62: Pressure measurements during power loss in Section 5.3.4.

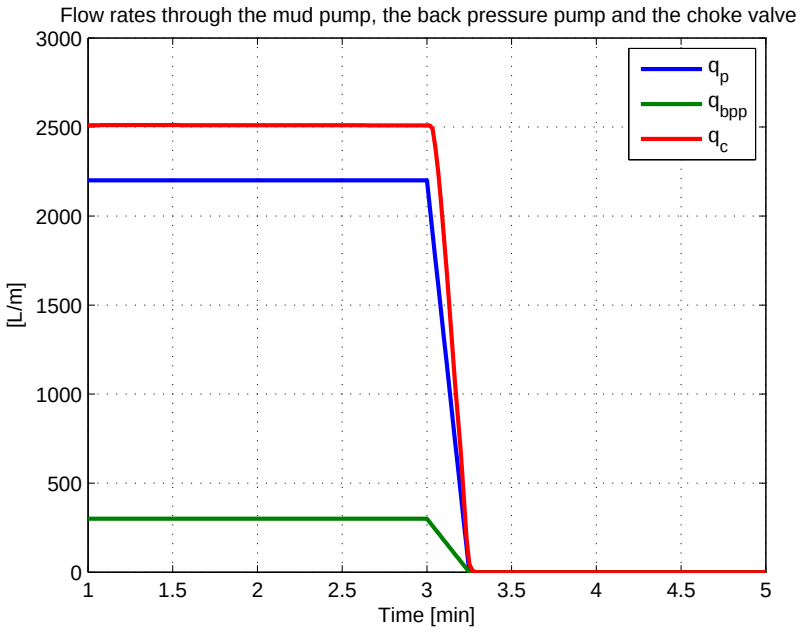

Figure 63: Flow measurements during power loss in Section 5.3.4.

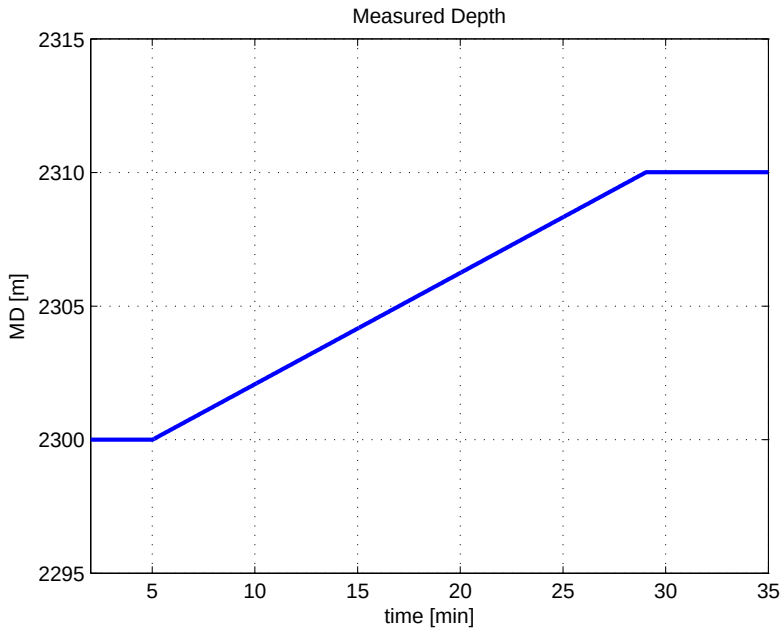

Figure 64: Measured depth during drilling scenario in Section 5.3.1.

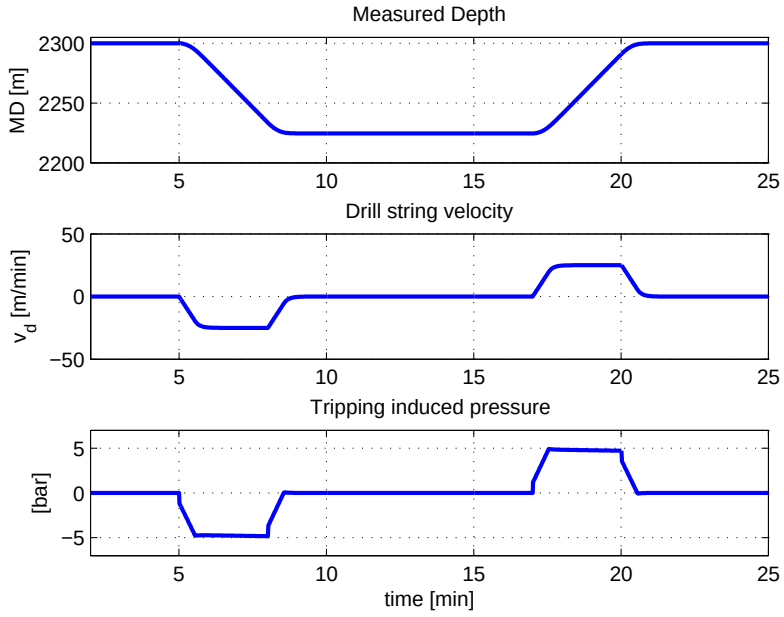

Figure 65: Measured depth, drill string velocity and tripping induced pressure for the tripping scenario in Section 5.3.3. The drill string velocity is included as an Mvr. The pressure spike due to acceleration is only handled when v_d is approaching its set Iv. When the Iv for v_d is changed, the initial pressure spike from acceleration is not handled, which is a significant weakness. Max. accel. was set to 0.6 m/min/s.